

3 4456 0360222 4

CENTRAL RESEARCH LIBRARY
DOCUMENT COLLECTION

ORNL 2
REACTORS

cy-220

DECLASSIFIED

CLASSIFICATION CHANGE TO: _____
BY: *TID-1150*
EVL: *W. Morrison 7/3/57*

LABORATORY RECORDS
1954

PHYSICS DIVISION

AN ELECTRICALLY DRIVEN SERVO FOR THE HIGH FLUX PILE

H. A. STRAUS

CENTRAL RESEARCH LIBRARY
DOCUMENT COLLECTION
LIBRARY LOAN COPY
DO NOT TRANSFER TO ANOTHER PERSON
If you wish someone else to see this document, send in name with document and the library will arrange a loan.

OAK RIDGE NATIONAL LABORATORY

OPERATED BY
CARBIDE AND CARBON CHEMICALS CORPORATION
FOR THE
ATOMIC ENERGY COMMISSION
POST OFFICE BOX #
OAK RIDGE, TENNESSEE

TRANSMITTAL DATE *12-17-58*



ORNL # 2

This document consists of 86
pages.

Copy 24 of 14, Series A.

ISSUED: *A. M. Weinberg*

Contract No. W-7405, eng 26

PHYSICS DIVISION

AN ELECTRICALLY DRIVEN SERVO FOR THE HIGH FLUX PILE

Work done by:

H. A. Straus
T. E. Cole
D. W. Cardwell

Written by:

H. A. Straus

DATE ISSUED: DEC 17 1948

OAK RIDGE NATIONAL LABORATORY
OPERATED BY
Carbide and Carbon Chemicals Corporation
for the
Atomic Energy Commission
Post Office Box P
Oak Ridge, Tennessee



3 4456 0360222 4

DISTRIBUTION:

1. G. T. Felbeck (C&CCC N.Y.-N.Y.)
- 2-4. 706-A Library
5. 706-B Library
6. Biology Library
7. Health Physics Library
8. Training School Library
- 9-12. Central Files
13. D. C. Bardwell
14. C. D. Cagle
15. A. S. Householder
16. A. H. Hooper
17. J. H. Ely, Jr.
18. E. J. Murphy
19. M. D. Peterson
20. C. N. Ruster
21. J. C. Stewart
22. A. M. Weinberg
23. S. McLain
24. J. A. Lane
25. H. A. Straus
26. S. R. Sapir (AEC-Townsite)
27. H. M. Roth (AEC-Townsite)
- 28-35. Argonne National Laboratory
- 36-37. Atomic Energy Commission, Washington
38. Battelle Memorial Institute
- 39-44. Brookhaven National Laboratory
45. Bureau of Ships
46. Chicago Operations Office
- 47-50. General Electric Company, Richland
51. Hanford Operations Office
52. Iowa State College
- 53-56. Knolls Atomic Power Laboratory
- 57-59. Los Alamos
60. Massachusetts Institute of Technology (Kaufmann)
61. NEPA Project
- 62-63. New York Operations Office
64. North American Aviation, Inc.
65. Patent Advisor, Washington
- 66-80. Technical Information Division, ORCO
- 81-84. University of California Radiation Laboratory

I.	Introduction	1
II.	a) An Example---A Simple Servomechanism and Some Properties of Servomechanisms	1
	b) Analysis of a Simple Servomechanism	10
	c) Steady State Analysis---The Nyquist and Bode Diagrams	13
III.	The Pile Regulation Problem	21
	a) Components Used in the Velocity Servomechanism	26
	b) Steady State Analysis of the Linearized System	34
	c) Experimental System's Performance	42
	d) Suggested Modifications of the Velocity Servomechanism	52
IV.	Performance	57
	a) Notes on Performance of the Isolated Servomechanism	57
	b) The Servo System as a Regulator of the Simulator	62
V.	Appendixes	66
	a) Experimental Methods	66
	b) Elementary Theory of the Amplidyne	67
	c) Some Mathematical Results	72

I. Introduction

There are many conditions under which it is either necessary or desirable that some quantity be controlled by a device at a distance from the site at which the controlled quantity exists. Examples of such situations are (1) the manipulation of a strong radioactive sample, (2) the steering of a ship, and (3) transmission of a shaft position, such as that of a temperature controlling device on a furnace. Devices to perform such functions fall under the general classification of remote control units.

Those special remote control units which function in such a manner that the controlled quantity's variation with time approximates the function of time according to which the input signal varies are called servo systems, provided they satisfy two further conditions. The system must not draw from the input signal the power which it supplies to the output, but must have an independent power supply. The system must function in some manner depending upon the comparison of the input signal with some function of the output quantity. In the special case that the output quantity is a mechanical one, the servo system is termed a servo mechanism. The class of commonly used servo mechanisms can be further broken down into three classifications according to the mode of operation: (1) The relay type servo mechanism in which full motor power is developed when the error signal becomes large enough to operate the motor. (2) Systems in which the correction is applied on a definite time interval schedule. (3) Continuous control systems in which the motor is controlled continuously by some function of the error. The first system has the advantage of ruggedness and simplicity but usually yields relatively crude control. The second is used in industrial control instruments. The discussion to follow will deal with the continuous control type of system.

An open cycle system (one in which there is no internal comparison of the input signal with any function of the output) must necessarily be a calibrated unit if performance is to be reliable. This means that the amplifier characteristic must be independent of aging of components and fluctuations in the power supply. The motor torque characteristic must be independent of temperature. The system must be insensitive to load variations. Unfortunately, these conditions are not in general attainable.

IIa. An Example—A Simple Servomechanism and Some Properties of Servomechanisms

In a differential analyser it is desired to multiply together two functions of time, $G(t)$ and $H(t)$, each of which is available in the form of a

voltage from a source of negligible impedance. Suppose $H(t)$ and $-H(t)$ are applied to the terminals of a linear potentiometer, whose arm has a range \mathbb{H} . If now it is possible to move the arm of the potentiometer in such a way that its departure, θ , from the center of the winding $= k G(t)$ and so that $k G_{\max.}(t) \leq \frac{\mathbb{H}}{2}$, then at any instant the voltage at the potentiometer contact will represent, to its scale, the quantity $G(t) \cdot H(t)$. Figure 1 indicates a possible scheme for mechanizing the system.

In this case a system has been chosen in which the angular position of a shaft is the output quantity which is to approximate, in its time dependence, the function $G(t)$ which is supplied as a voltage.

Consider this servomechanism in the steady state when each of the variables shows a time dependence of the form e^{pt} , where p is, in general, complex (see Fig. 2).

The output shaft positions the arm of a potentiometer. The voltage at the potentiometer arm is $k \cdot$ (instantaneous departure of the arm from the mid point on the winding). This voltage is the function of the controlled quantity mentioned in the definition of a servo system. The differential has an input impedance so high compared to the source of voltage $G(t)$ that the latter is unaffected by the presence of the differential.

$$\text{Then: } \epsilon_o e^{pt} = V_i e^{pt} - k \theta_o e^{pt}$$

$$\text{The amplifier output is } V e^{pt} = Y_a(p) \epsilon_o e^{pt}$$

$Y_a(p)$ is the transfer characteristic of the amplifier, the ratio of its output to its input—which depends on the details of its construction and can be calculated by the methods of circuit theory.

The motor transfer characteristic will be derived for a simple type of motor: d.c., separately excited, neglecting winding inductance. Then the differential equation of the motor is

$$M \ddot{\theta}_o + R \dot{\theta}_o = K_T \frac{V - K_g \dot{\theta}_o}{R_a}$$

where M = effective moment of inertia of motor armature and driven system

R = viscous damping coefficient of mechanical system

K_T = torque const = torque/armature current

V = applied voltage

K_g = voltage generated in armature/unit angular velocity

$\dot{\theta}_o$ = angular velocity of armature

R_a = total resistance in motor armature circuit

FIG. 1

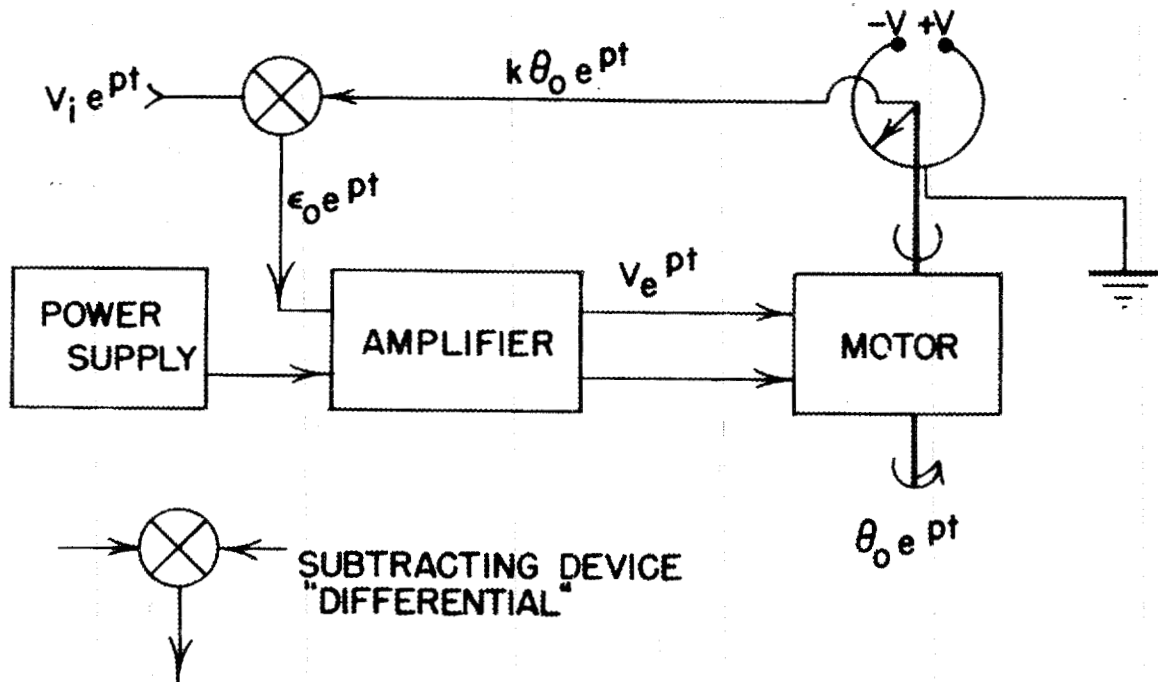
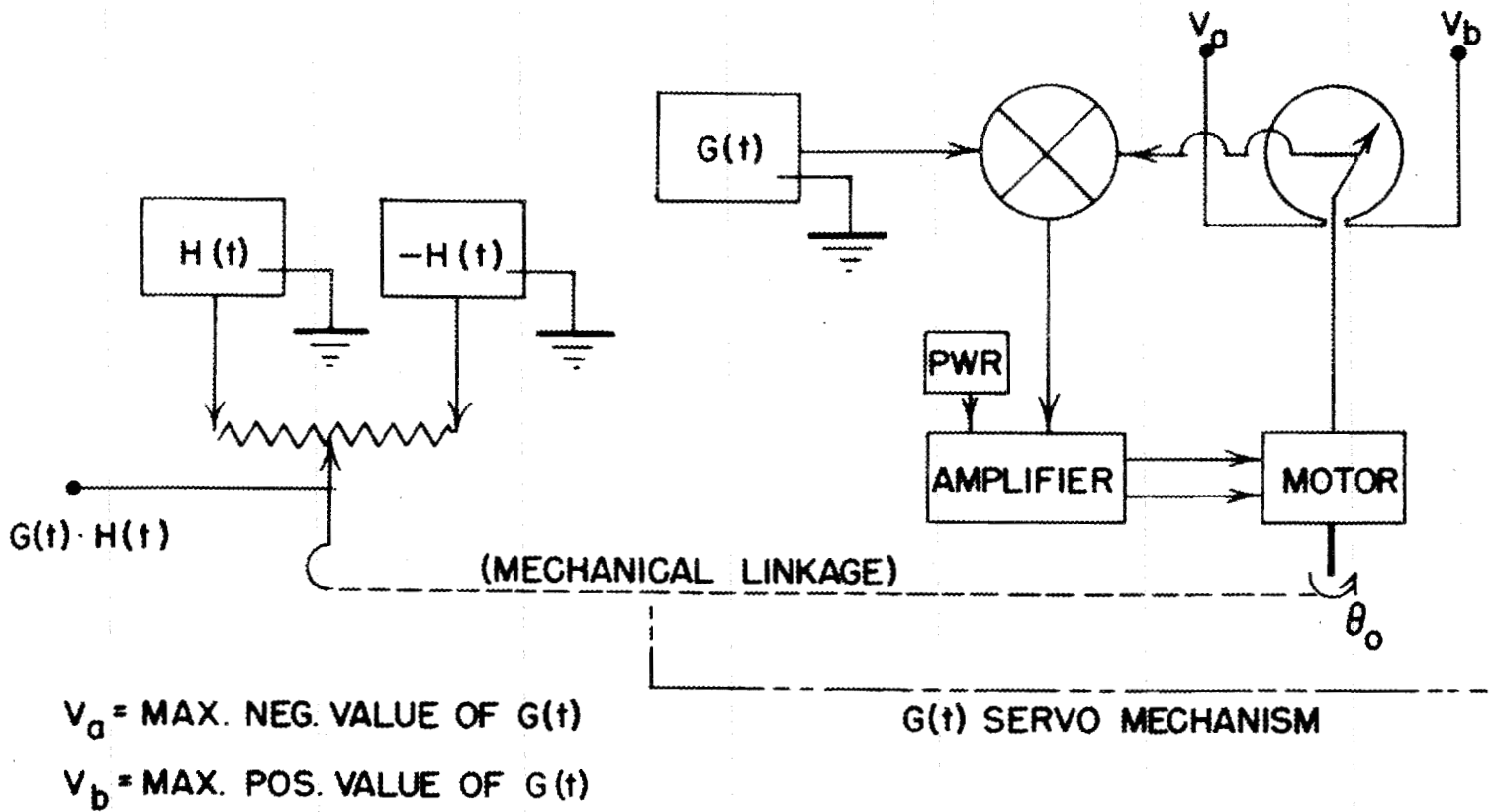


FIG. 2

This equation can be rewritten:

$$M\ddot{\theta}_o + \left(R + \frac{K_T K_G}{R_a}\right)\dot{\theta}_o = \frac{K_T}{R_a} V$$

Setting

$$R + \frac{K_T K_G}{R_a} = \rho, \text{ a new effective viscous damping coefficient,}$$

$$M\ddot{\theta} + \rho\dot{\theta} = GV, \text{ where } G = \frac{K_T}{R_a}. \text{ Then, in the steady state,}$$

$$(Mp^2 + \rho p)\theta_o = GV,$$

$$\theta_o = \frac{GV}{p(Mp + \rho)}$$

$$\text{Set } \frac{M}{\rho} = \tau = \text{motor time const.}$$

$$\text{Then } Y_{\text{motor}}(p) = \frac{\theta_o}{V} = \frac{G/\rho}{p(\tau p + 1)}$$

The potentiometer, neglecting contact noise, granularity of output due to finite size of the wire used, and non-linearities due to non-uniform winding and varying resistance per unit length of the wire, supplies a voltage instantaneously proportional to the departure of the contact arm from the (grounded) center point of the winding:

$$Y_{\text{pot}} = k(\text{volts/radian})$$

The system is connected in such a manner that the output of the differential is the algebraic difference of the input and the potentiometer arm voltage.

In the steady state then

$$\epsilon = \epsilon_0 e^{pt} = V_i e^{pt} - k\theta_0 e^{pt}$$

The quantity θ_0 can be expressed in terms of ϵ .
The amplifier output (steady state) is

$$V e^{pt} = Y_a(p) \epsilon = Y_a(p) \epsilon_0 e^{pt}$$

This is, however, the input to the motor, so

$$\theta_0 e^{pt} = \frac{GY_a(p)}{\rho p(p\tau + 1)} \epsilon_0 e^{pt}$$

divide by $\epsilon_0(p) e^{pt}$ and multiply by k to obtain the ratio of the voltage fed back to the differential to the output from the differential:

$$\frac{k\theta_0}{\epsilon_0} = \frac{kGY_a(p)}{\rho p(p\tau + 1)}$$

Then since $\epsilon_0 = V_i - k\theta_0$,

$$\theta_0 = \frac{\frac{kGY_a(p)}{\rho p(p\tau + 1)}}{1 + \frac{kGY_a(p)}{\rho p(p\tau + 1)}} \cdot k^{-1} V_i$$

or

$$\theta_0 = \frac{1}{1 + \frac{\rho p(p\tau + 1)}{kGY_a(p)}} \cdot k^{-1} V_i$$

In many practical cases it is possible to make $Y_a(p)$ approximate a large positive constant A . Then:

$$(B) \quad \theta_0 = \frac{1}{1 + \frac{\rho p(p\tau + 1)}{kGA}} \cdot k^{-1} V_i$$

Consider the case $p = j\omega$; when p is small the output is thus proportional to V_i . When p becomes large, the second term in the denominator $\rightarrow \infty$ and the output vanishes. Thus the system behaves in general like a low pass filter. The servo mechanism will reproduce $G(t)$ satisfactorily as long as the important Fourier components of $G(t)$ are in the frequency range in which $kGA \gg \rho p(p\tau + 1)$.

To see another feature of the simple servo mechanism which is common to the class, set

$$\frac{kGY_a(p)}{\rho p(p\tau + 1)} = Y_n(p). \quad \text{Then Equation B becomes}$$

$$\theta_o = \frac{Y_n(p)}{1 + Y_n(p)} k^{-1}V_i.$$

$Y_n(p)$ here is the transfer function from the amplifier input around the loop to the differential. We have directly

$$\frac{\theta_o}{k^{-1}V_i} = \frac{Y_n(p)}{1 + Y_n(p)} = 1 - \frac{1}{1 + Y_n(p)}$$

Thus for any value of p for which $Y_n(p) \gg 1$, θ_o departs from its proportionality to V_i by a fractional amount $\sim |1/Y_n(p)|$. Thus we need not make $Y_n(p)$ any special function to approach the ideal condition. Also, consider the sensitivity of the system to variations in $Y_n(p)$:

$$\frac{d}{dY_n(p)} \left[\frac{\theta_o}{k^{-1}V_i} \right] = \frac{1}{[1 + Y_n(p)]^2}$$

Thus, as long as $Y_n(p)$ is large, slight variations in the amplifier due to tube and component aging and small changes in motor torque due to heating of windings will not affect the system performance appreciably. Contrast the difficulties in an open cycle system.

IIb. Analysis of a Simple Servo-Mechanism

We here treat the $G(t)$ servo mechanism in the differential analyser. The motor used in this example is a Bodine NCO-12 compound wound motor reconnected to be used with separate field excitation with its armature driven from the plate of one half of a 6AS7 and the cathode of another. The relevant data are:

$$\begin{aligned}
 K_T &= 1.10 \times 10^4 \text{ dyne cm/ma.} && \text{-Torque constant} \\
 K_{\text{gen}} &= 8.37 \times 10^{-2} \text{ volts/rpm} && \text{Generated voltage const.} \\
 M_{\text{armature}} &= 584 \text{ gm cm}^2 && \text{Armature moment of inertia} \\
 R_a &= 860 \Omega = \text{armature circuit equiv. resistance} \\
 \tau_m &= .08 \text{ sec} = \text{measured motor time constant}
 \end{aligned}$$

(See Fig. 3) The gear reduction is used to make possible the precise positioning of the potentiometer arm in spite of the tendency of the motor to slot-lock at 12 positions per rotation. This tendency would be greatly reduced in a motor designed for servo applications by skewing the armature slots. The reflected inertia of the gear train and potentiometer arm will be assumed negligible. We assume the voltage at the potentiometer arm to vary in an ideally linear manner with motor armature rotation—perfect couplings, zero backlash in the gear train, and linear resistance vs. rotation characteristic for the potentiometer.

The differential equation of the system can be written at once:

$$M\ddot{\theta} + R\dot{\theta} = K_T \frac{(V - K_{\text{gen}}\dot{\theta})}{R_a} \quad \text{for the motor}$$

$$V = A\epsilon$$

or,

$$M\ddot{\theta} + \left[R + \frac{K_T K_G}{R_a} \right] \dot{\theta} = \frac{K_T V}{R_a} \quad R = \text{viscous damping coef.}$$

But from Fig. 3

$$V = A [V_i(t) - k\theta]$$

$$M\ddot{\theta} + \rho\dot{\theta} = \frac{K_T A}{R_a} [V_i(t) - k\theta]$$

$$\ddot{\theta} + \tau_m^{-1}\dot{\theta} + \frac{K_T A k}{R_a M} \theta = \frac{K_T A}{M R_a} V_i(t) \quad \text{or}$$

$$\ddot{\theta} + \alpha\dot{\theta} + \beta\theta = \gamma V_i(t)$$

NOT CLASSIFIED

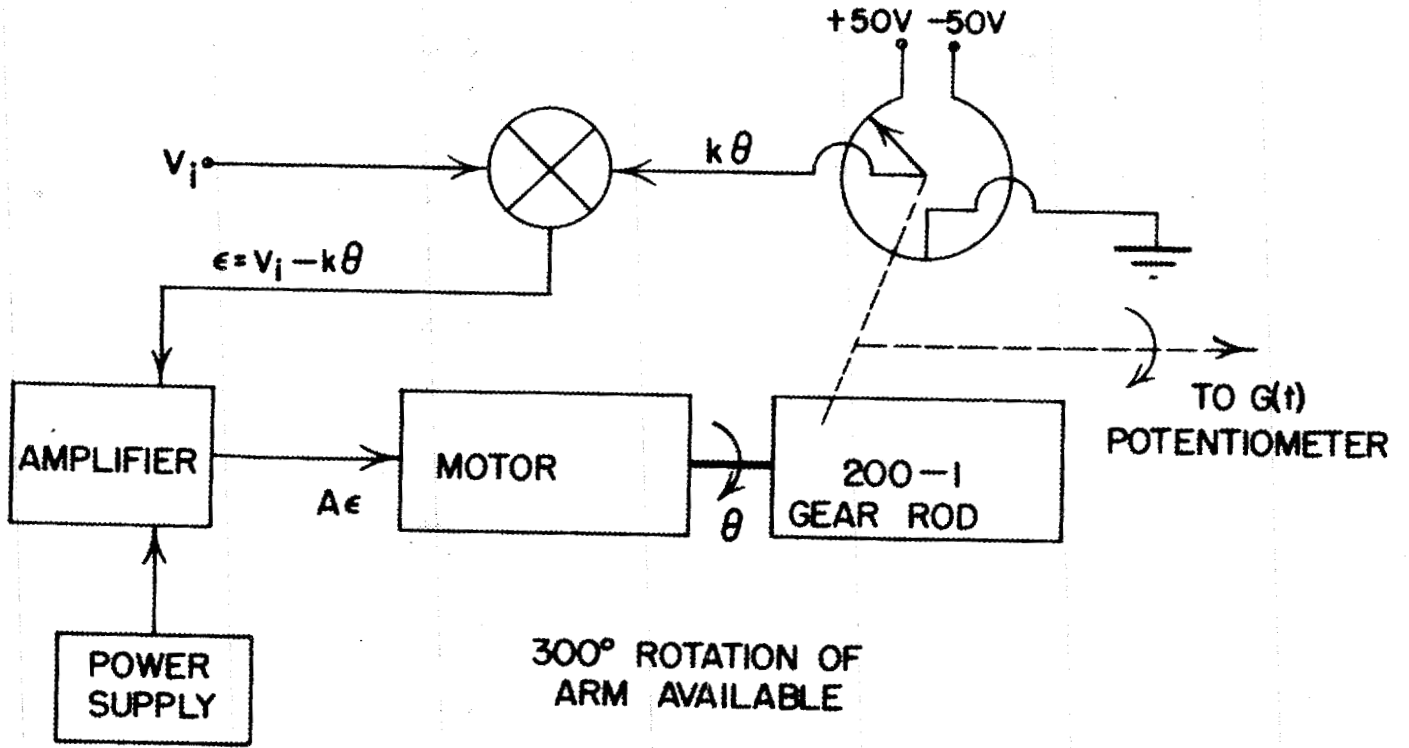


FIG. 3

It must be recalled at all times that the information to be obtained by solving the differential equation is no better than the information put into the equation. The equation should describe the system as used as accurately as one can manage without making the equation useless by producing one that is not accessible to solution.

1. Try a step input $25 S(t)$. The output will be of the form:

$$K \frac{B e^{-\frac{A}{2}t} (\frac{A}{2} \sin Bt + B \cos Bt)}{B(\frac{A}{2}^2 + B^2)}$$

Set the amplifier gain at 63.4. With the gear reduction above and the indicated angle of rotation of the potentiometer, $k = .191$ volt/radian at the motor.

$$B = \frac{1}{2} \sqrt{\alpha^2 - 4\beta}$$

$$\frac{A}{2} = \frac{1}{2}\alpha$$

$$\alpha = \frac{1}{m}$$

$$\beta = \frac{K_T A k}{R_a M}$$

$$25 \frac{K_T A}{R_a M} = 25 \times 1410$$

The transient is damped with a time constant twice that of the motor. The angular frequency of the oscillatory component of the output is 15.2 radians/sec or 2.42 cps—pretty slow. After the transient has finally died, the motor shaft will have rotated through 130.5 radians and the potentiometer arm through 0.652 radians or 75° . The constants of the system are so thoroughly mixed up in the solution that, although this solution tells all one can hope to find out about the response to the given input, the differential equation gives little help in an attempt to improve the system.

Suppose we increase the amplifier gain to 280 instead of 63.4. $|B|$ now becomes 34 radians/sec. The damping constant remains unchanged. So does the steady state response, but now the transient oscillation is truly

horrifying. This was hardly a profitable way to improve the situation. The transients are plotted in Fig. 9, parts one and two.

IIC. Steady State Analysis—The Nyquist and Bode Diagrams

The theoretical results in this section logically belong in the section on mathematical results but are presented here because the meaning is very simply seen when applied to a concrete example.

Consider a system being subjected to a harmonically varying input signal of constant amplitude and angular frequency ω . In the steady state, the quantities of interest will all vary harmonically. One can then write:

$$V_i(t) = V_e e^{j\omega t}$$

$$\theta_o(t) = \theta_o e^{j\omega t}$$

Substituting in the differential equation:

$$-\omega^2 \theta_o + \tau_m^{-1} j\omega \theta_o + \frac{K_T A k}{R_a M} \theta_o = \frac{K_T A}{R_a M} V$$

or, in terms of the error voltage ($V - k\theta_o$)

$$-\omega^2 \theta_o + \tau_m^{-1} j\omega \theta_o = \frac{K_T A}{R_a M} \epsilon$$

So that,

$$\frac{\theta_o}{\epsilon} = \frac{K_T A}{R_a M} \cdot \frac{1}{j\omega(\tau_m^{-1} + j\omega)} = \frac{\tau_m K_T A}{R_a M} \cdot \frac{1}{j\omega(1 + j\omega\tau_m)}$$

In the above expression we have a relation between the steady state amplitude of the oscillations of the motor shaft position and the error signal amplitude in terms of constants of the differential equation and the angular frequency of the oscillation. Here is a simple case for the application of the Nyquist test for stability. In the Nyquist diagram Fig. 4 this complex function is plotted on the Argand diagram. The circles on the

FIG. 4
 NYQUIST DIAGRAM
 INSTRUMENT SERVOMECHANISM

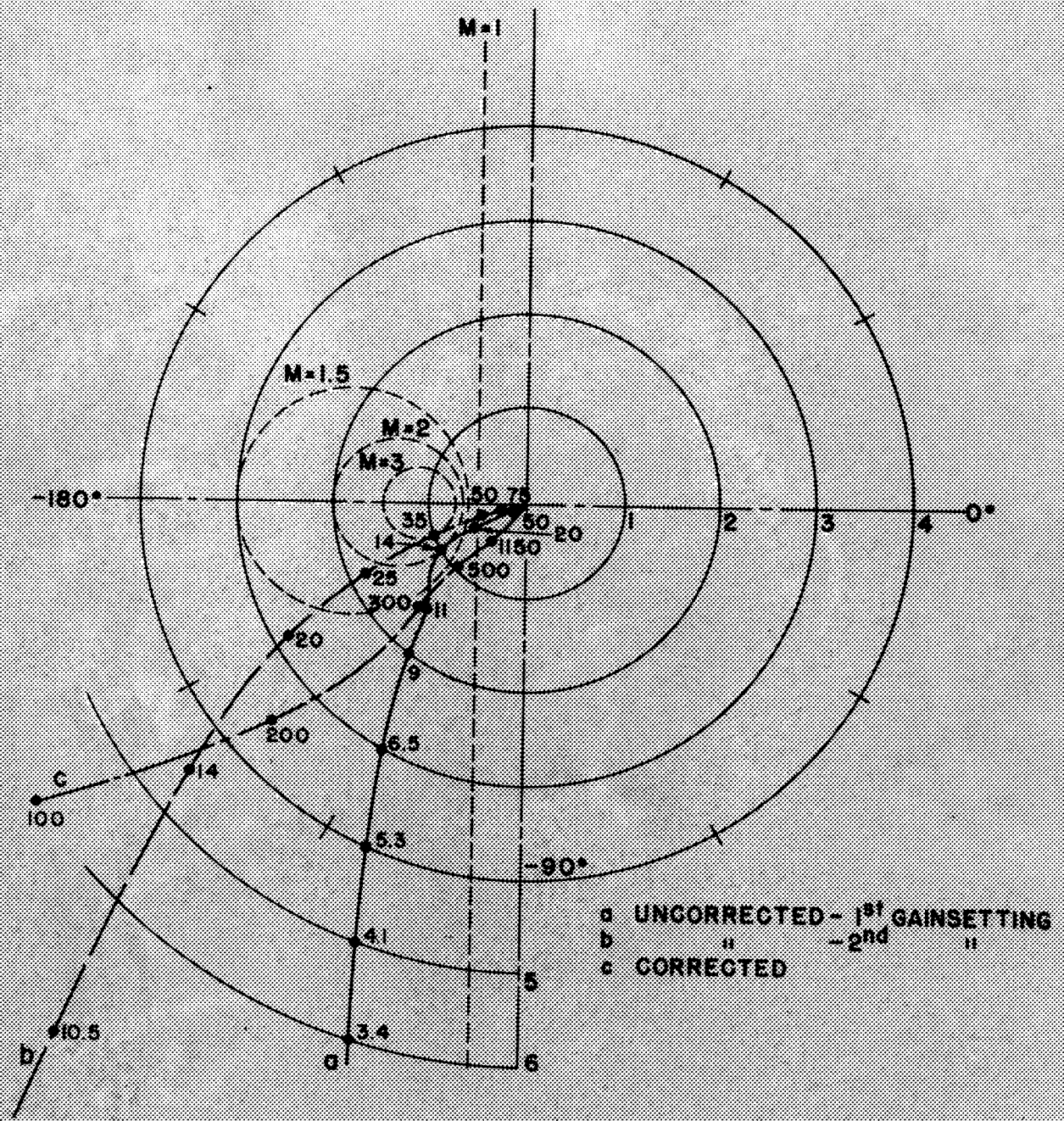


diagram centered at the origin are curves of constant loop gain (ratio of voltage fed back to the error detecting device to the error voltage). The locus of $Y_{12}(p)$ —the loop gain—is plotted with $p=j\omega$. The numbers associated with points on the locus are the values of the angular frequency at which $Y_{12}(j\omega)$ takes on the plotted values. Curves a and b are to be studied and compared with the transients plotted in Fig. 9. Curve C corresponds to a situation which will be discussed later. The dotted lines associated with M values are curves of constant over-all system gain which is the ratio of output voltage (a measure of controlled shaft position) applied to the differential to the input voltage amplitude. The magnification by the system becomes infinite as the locus of $Y_{12}(-1,0)$ as is indicated clearly by the contour map of system gain. Physically, the system maintains oscillations at zero input. It will be noted that in both cases, a and b, the angular frequency of the oscillatory component of the transient is in the frequency region at which the transfer locus cuts its highest valued M contour. Also, the curve cutting the higher M contour corresponds to the case of the greater overshoot and poorer damping of the transient. If the amplifier gain were further increased, the oscillation would grow worse for systems of this type. Evidently, it would be a sound idea to keep the locus of $Y_{12}(j\omega)$ as well away from the -180° phase region as feasible in the neighborhood of the frequency at which it crosses the circle of loop-gain unity (feed-back cross-over). The angle measured from the negative real axis to the vector joining the origin to a point on the locus is called the phase margin corresponding to that point on the locus. The phase margin is positive if the phase is less negative than -180° .

The Nyquist criterion is stated in terms of the magic point, $-1,0$. If the point is enclosed by the locus, the system is unstable. Otherwise the system is stable. This is true in the mathematical sense but is of limited practical interest. The plot, including the contours of system amplification, shows clearly the manner in which the design approaches the unacceptable as it is changed to bring the locus of the loop transfer characteristic closer to the Nyquist critical point.

H. W. Bode is responsible for a highly perspicuous mode of presentation of that information included in the Nyquist diagram. Consider now the loop transfer characteristic obtained for our instrument servo:

$$Y_{12}(j\omega) = \text{Const.} \times \frac{1}{j\omega(1 + j.08\omega)}$$

Take the logarithm

$$\ln Y_m(j\omega) = \ln |Y_m(j\omega)| + j \arg Y_m(j\omega)$$

These may be plotted separately against a logarithmic frequency scale. The real part is the log of the magnitude of Y_m and the imaginary part is the phase. The quantity usually plotted is $20 \log_{10} |Y_m(j\omega)|$ —the loop attenuation (or gain) in decibels. Recall that for the minimum phase class of transfer functions the attenuation is completely determined by the phase characteristic and vice versa. This fact can be used to reduce the labor of constructing a db-log frequency and phase-log frequency plot, especially for complex systems since the attenuation curves can be very simply constructed. The saving is less impressive for a single loop system like this but is still useful. We have

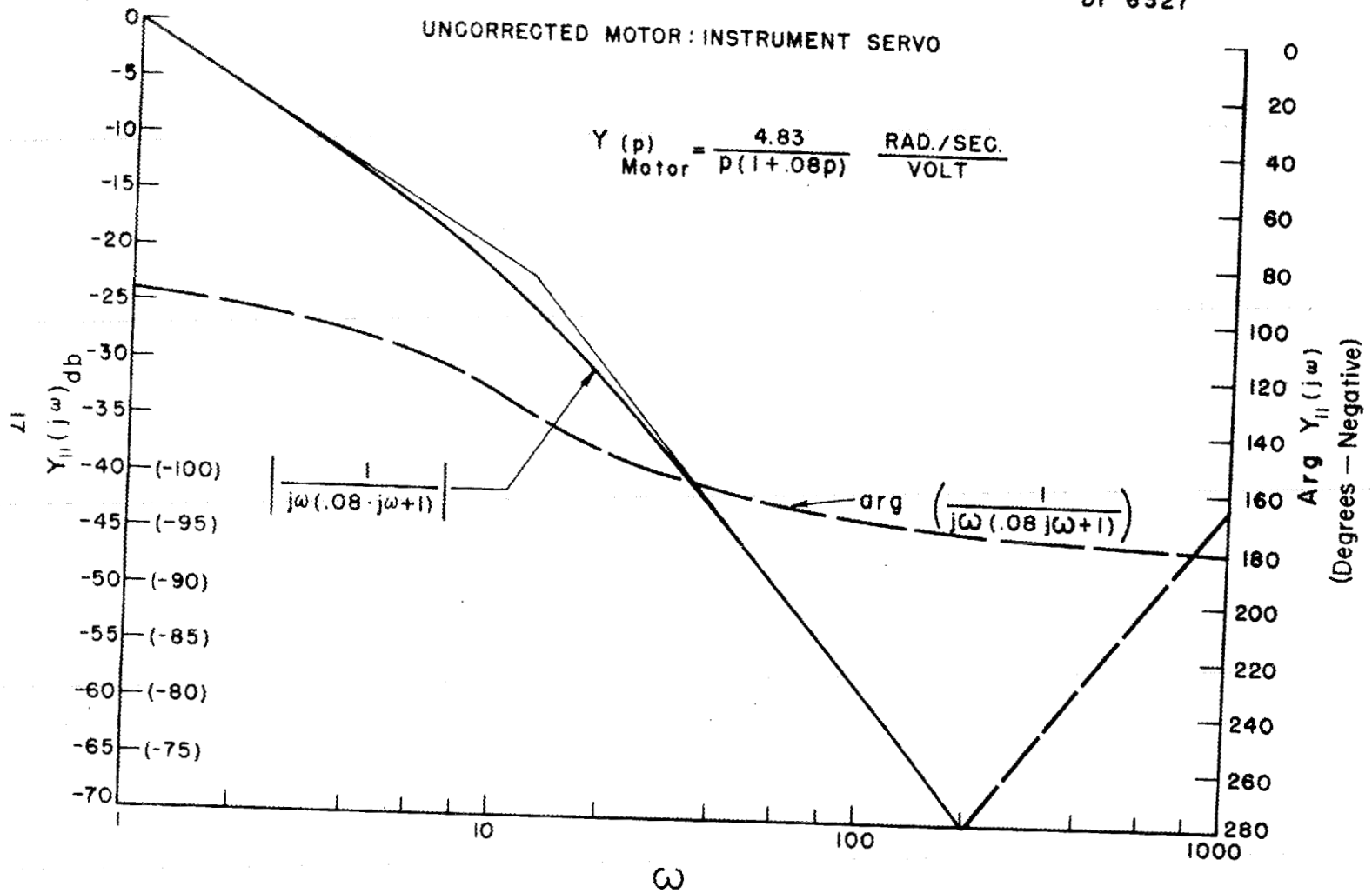
$$A = K + 20 \log_{10} \left| \frac{1}{j\omega(1 + j \cdot 08\omega)} \right| = K - 20 \log_{10} |j\omega| - 20 \log_{10} |1 + j \cdot 08\omega|$$

A is the loop gain in db.

The first contribution, K, represents a vertical displacement of the whole curve and is here omitted. $-20 \log_{10} |j\omega|$ passes through 0 at $\omega = 1$. It has a slope of -6 db/octave. The other contribution, $-20 \log_{10} |1 + j \cdot 08\omega|$ is zero at $\omega \ll 1$. When $\omega \gg 1$, it too has a slope of -6 db/octave. This quantity is approximated by $-20 \log_{10} |j \cdot 08\omega|$ at large ω . This asymptotic form goes to zero at $0.08\omega = 1$. Thus the asymptotic representation of the type quantity $-20 \log_{10} |1 + j \cdot 08\omega|$ is a line of zero slope intersecting a -6 db/octave line at the radian frequency $= \tau_m^{-1}$, where τ_m is the associated (motor) time constant in this case. The true attenuation characteristic departs only 3 db at the break point from the asymptotic curve and the departure is reduced to 1 db at one octave to either side of the break frequency. The phase of a type factor $(1 + jx)$ is evidently $\tan^{-1}x$ and is positive or negative as the factor appears in numerator or denominator. Fig. 5 shows $Y_{db}(j\omega)$ and $\arg Y_m(j\omega)$ for the instrument servo-mechanism. The $Y_{db}(j\omega)$ curve is reflected in the -70 db line at $\omega \geq 200$. If one sets the phase margin at feedback cross-over at 40° , one sees that the coefficient of $1/(1 + j \cdot 08\omega)j\omega$ must be such that the loop gain is 27 db at $\omega = 1$, since the curve has fallen 27 db from its value at $\omega = 1$ by the time the loop phase margin has fallen to 40° . If one chooses to reduce the phase margin at feedback cross-over to 20° , the coefficient must bring the loop gain at $\omega = 1$ to 40 db.

NOT CLASSIFIED

Dr 6327

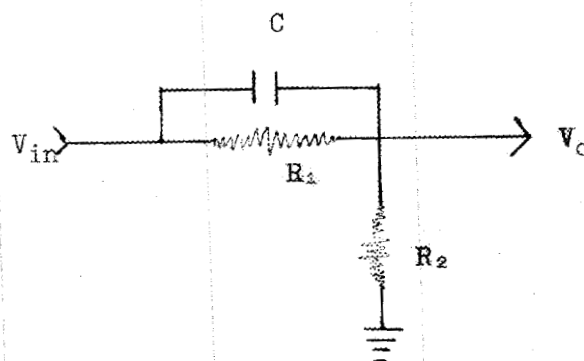


The effect of these gain settings on the over-all frequency response of the system can be found far more readily by graphical means than by analytical evaluation of $Y_n(j\omega)/1 + Y_n(j\omega)$. A convenient method of doing this is to find the contours of constant over-all system gain and system phase on a coordinate system of loop gain as ordinate and loop phase or phase margin as abscissa.* By this means the frequency responses shown in Fig. 6 were obtained. By some coincidence they show resonances at the frequencies indicated on the Nyquist diagram and in the transient responses.

The lead circuit (so called, strangely enough, because it produces a phase lead) has the transfer characteristic

$$Y(p) = K_1 \frac{1 + \tau_1 p}{1 + K_1 \tau_1 p}$$

where $\tau_1 = R_1 C$



$K_1 = R_2 (R_1 + R_2)$, which becomes in the steady harmonic-oscillation state

$$Y(j\omega) = K_1 \frac{1 + j\omega\tau_1}{1 + jK_1\tau_1\omega}$$

The filter constants that were chosen to improve the system performance are $K_1 = 1/10$, $\tau_1 = .005$. In Fig. 7 are shown the attenuation and phase characteristics of the filter with the attenuation curve at an arbitrary level. These curves were added to the respective attenuation and phase

*The contours of constant system scalar magnification M are given by

$$|Y_n|_{db} = 20 \log_{10} \frac{\cos \phi \sqrt{\cos^2 \phi + M^{-2} - 1}}{M^{-2} - 1}$$

and phase

$$|Y_n|_{db} = 20 \log_{10} (\sin [\phi - \psi] / \sin \psi)$$

ϕ and ψ are respectively $\text{Arg } Y_n$ and $\text{Arg } Y_o$.

NOT CLASSIFIED

Dr 6328

INSTRUMENT SERVO: OVERALL UNCORRECTED LOOP

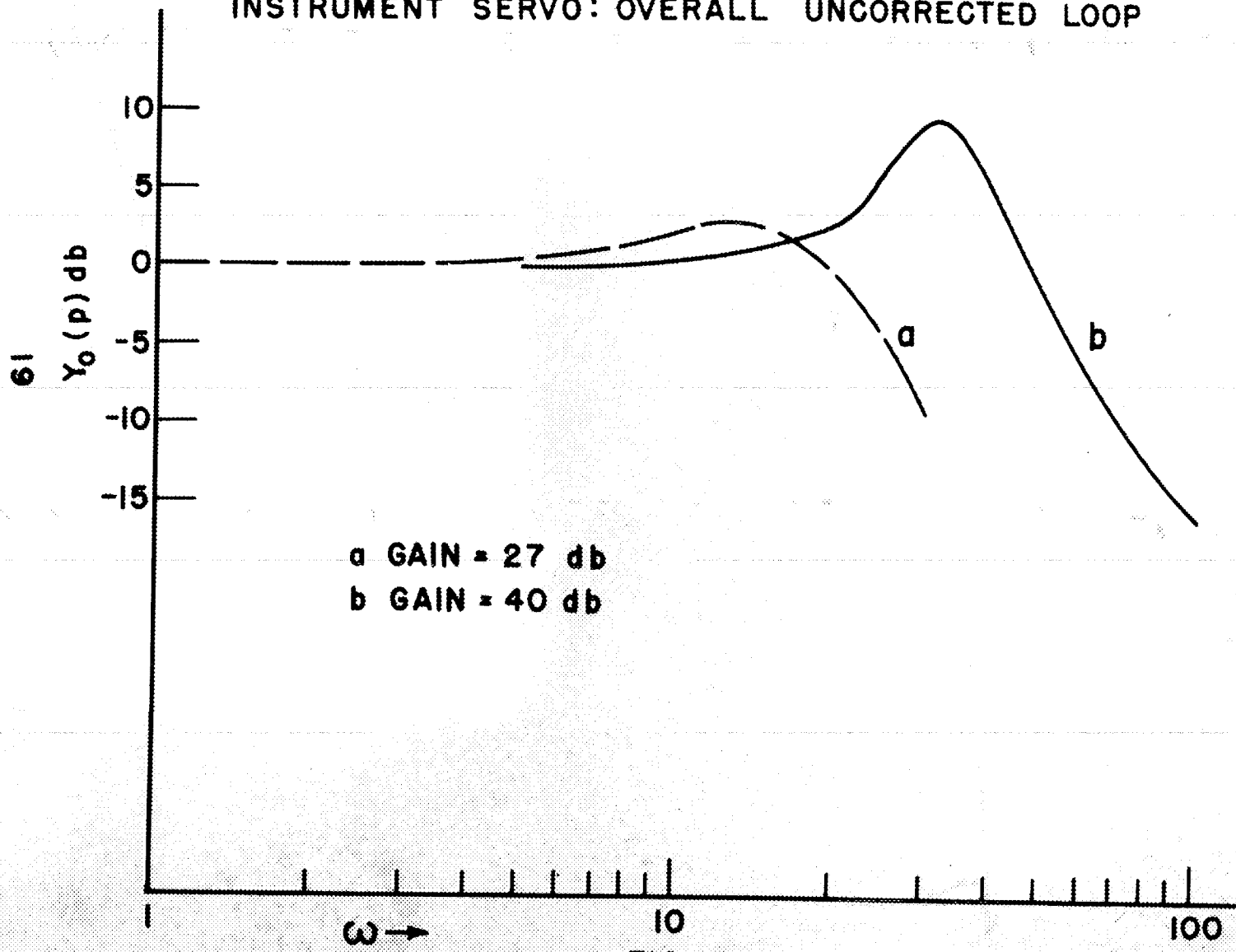


FIG. 6

NOT CLASSIFIED

Dr 6320

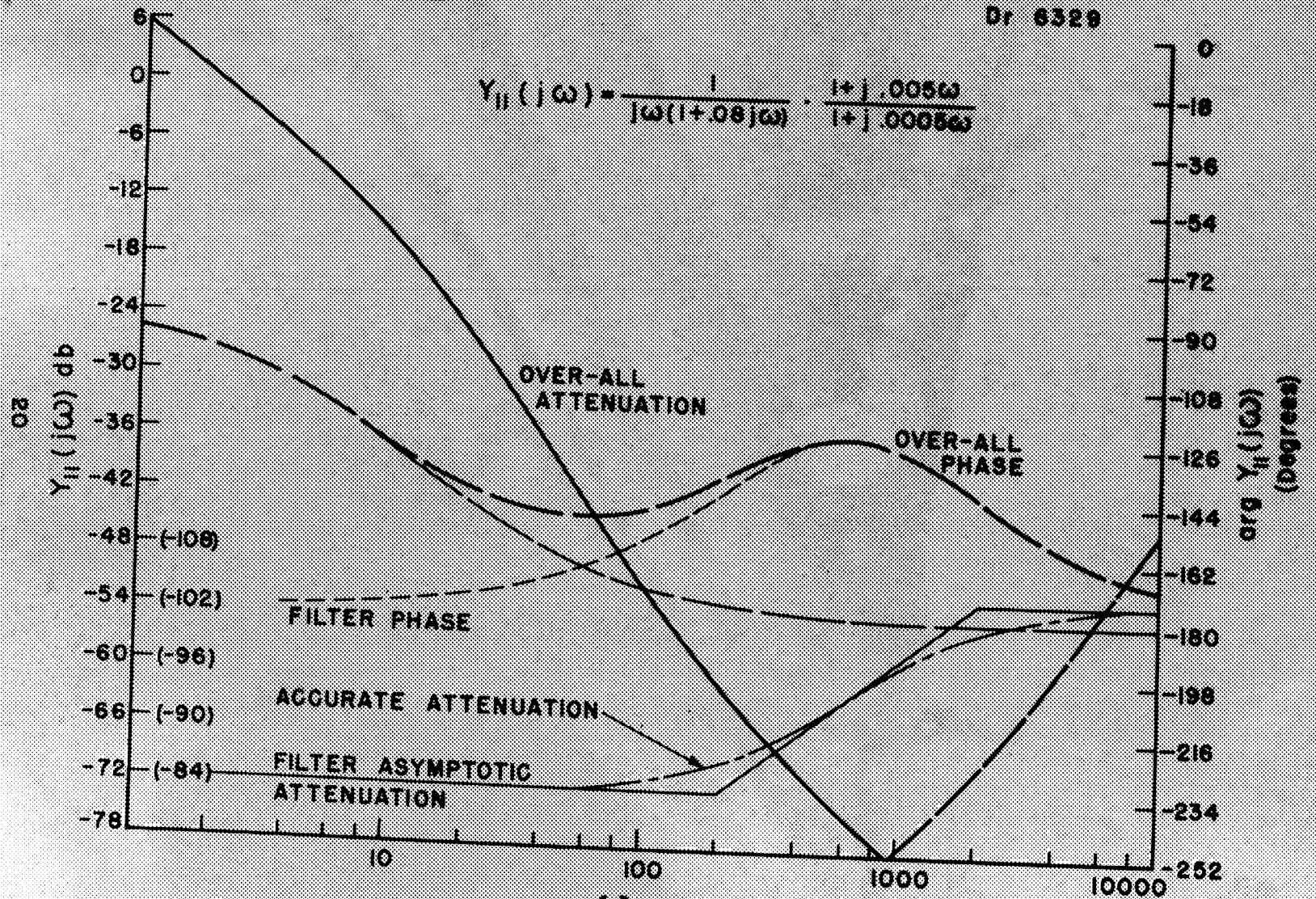


FIG. 7

curves of the unequalized system to yield the loop characteristics plotted on the figure. We now choose gain cross-over at the point of local maximum phase margin. This places feedback cross-over at $\omega = 600$ radians/sec and makes loop gain at $\omega = 1$ about 80 db. In Fig. 8 is shown the effect of increasing the frequency of feedback cross-over to a point at which phase margin is reduced to 40° instead of 55° , and of decreasing system gain to a point at which the phase margin at feedback cross-over is 33° . In both cases there is a definite increase in the height of the resonance response. But the system is still stable over this wide range of amplifier gain. Note that the system speed has been increased by a factor of approximately 58 by this simple filter. The curve C on the Nyquist diagram is for this equalized system. The response to a step input for the equalized system is shown in Fig. 9, (3).

The above example is not to be taken as an example of how readily one can triumph over a recalcitrant servo. In the first place, we have neglected non-linearities due to Coulomb friction, backlash, saturation of the amplifier and motor. There will be time delays also in the amplifier and usually equivalent time delays in the motor will show up at higher frequencies. Some of these problems will be indicated in the discussion of the large system which is described later in the report. In any case, this example was chosen to show rather graphically what one would like to do to a system and how one goes about doing it.

III. The Pile Regulation Problem

In report Mon P-271 by H. W. Newson, it is shown that the pile will return to level in a well damped manner following a disturbance, provided that a regulating rod is moved at a rate proportional to a linear combination of the instantaneous departure of the power from the desired operating level and the logarithmic time derivative of the pile flux. This consideration dictated the type of control whose development is described in this section.

The quantity whose variation is to be controlled is in principle dk/dt , where k is the reactivity represented by the absorption in a rod referred to the absorption when the rod is at an arbitrarily defined zero position. The quantity actually controlled by the servo system is the speed of vertical translation of a rod which is inserted into the reflector at the edge of the active lattice. Since the statistical weight varies as \cos^2 across the height of the pile, the effectiveness of a given increment of absorber varies with the distance from the median plane at which the absorber is placed. This fact causes

OVER-ALL RESPONSE OF INSTRUMENT
SERVO WITH EQUALIZATION

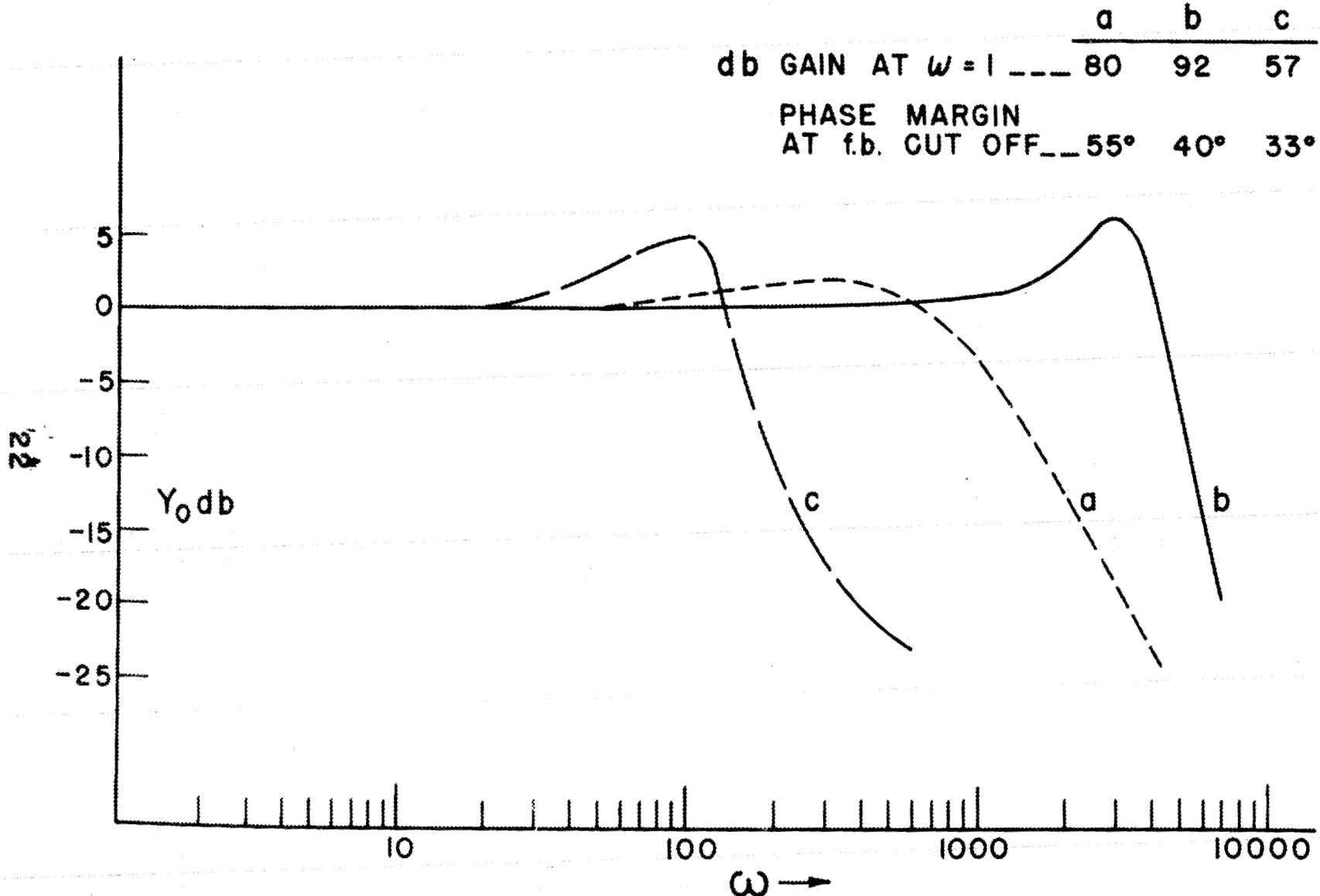
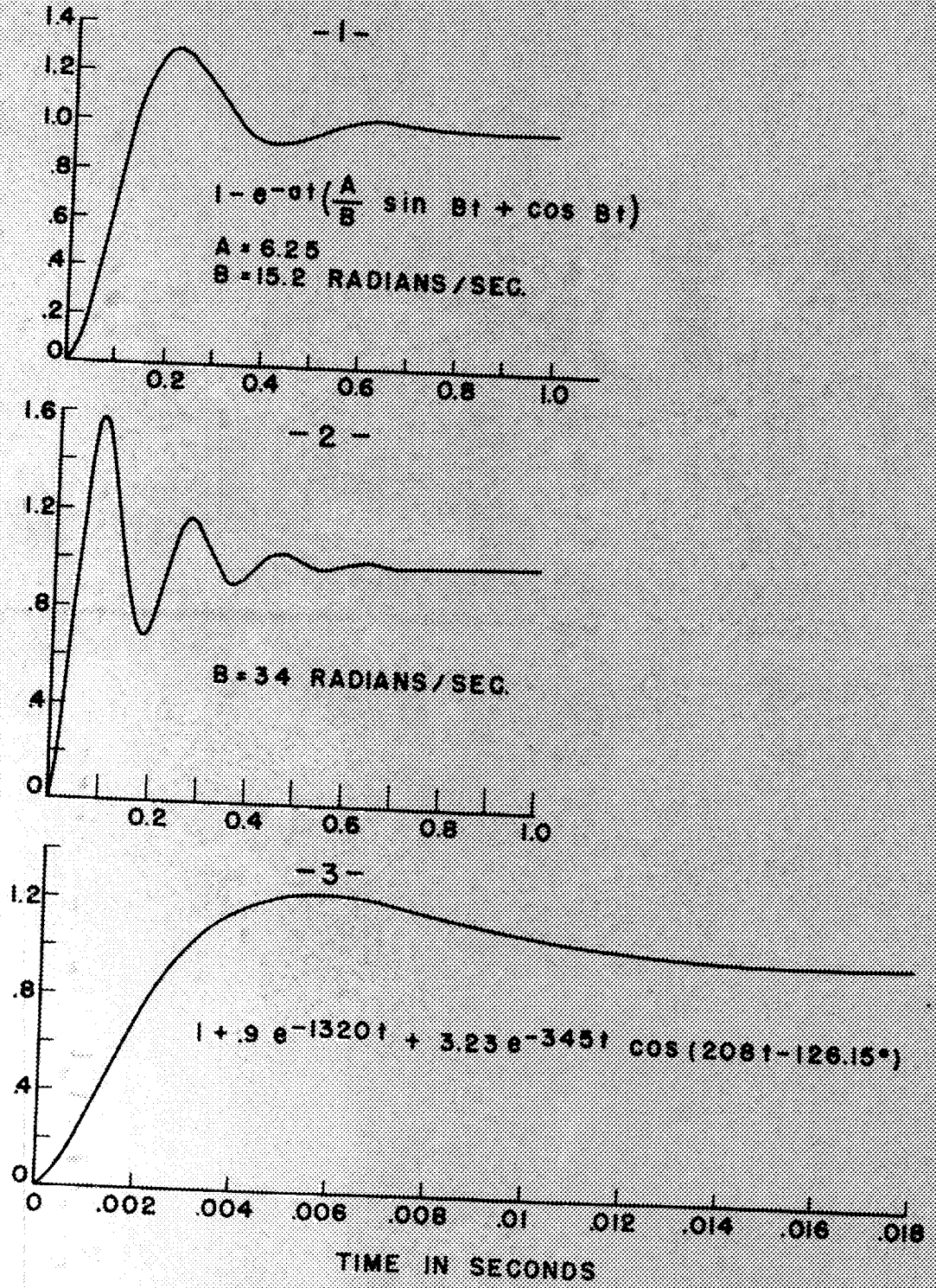


FIG. 8

FIG. 9



the sensitivity of the regulating rod to vary with the position of the rod in its stroke along the pile height. In normal operation the tip of the regulating rod never departs from the region limited by the points $\frac{1}{4}h$ below the top of the lattice and $\frac{1}{4}h$ above the bottom of the lattice where h is the lattice height. In this region the rod sensitivity changes only by a factor of two. This variation of sensitivity does not affect the system performance appreciably. The servo continues to operate in a manner such that it reduces toward zero the departure of pile level from the prescribed level even though the sensitivity of the system varies steadily with rod position.

First consider the general nature of a system which will produce a velocity at the output member which is closely proportional to a voltage signal applied (see Fig. 10). This figure will be shown to represent a system which in principle will produce a rate of rotation of the output shaft ($\dot{\theta}_o$) proportional to the input signal V_i .

The forward loop includes an amplifier with corrective filters which operate on the error signal, ϵ , which is the difference between the input V_i and the signal fed back by the tachometer, a generator whose voltage output is proportional to the angular rate of the output shaft. The amplifier output is applied to the motor, producing an angular rate of its shaft, $\dot{\theta}_o$. The meaning of the transfer functions associated with various blocks in the diagram will be recalled from section II of this report.

In the steady state:

$$\dot{\theta}_o = Y_{AM}(p)\epsilon$$

$$\epsilon = V_i - \alpha\dot{\theta}_o$$

Substituting:

$$\dot{\theta}_o = Y_{AM}(p)(V_i - \alpha\dot{\theta}_o)$$

$$\dot{\theta}_o[1 + \alpha Y_{AM}(p)] = Y_{AM}(p)V_i$$

$$\dot{\theta}_o = \frac{\alpha Y_{AM}(p)}{1 + \alpha Y_{AM}(p)} \alpha^{-1} V_i = \frac{V_i}{\frac{1}{Y_{AM}}(p) + \alpha}$$

Thus for signals, V_i , whose important frequency components lie in the range in which $Y_{AM}(p) \gg 1$, we have the approximate relation:

NOT CLASSIFIED

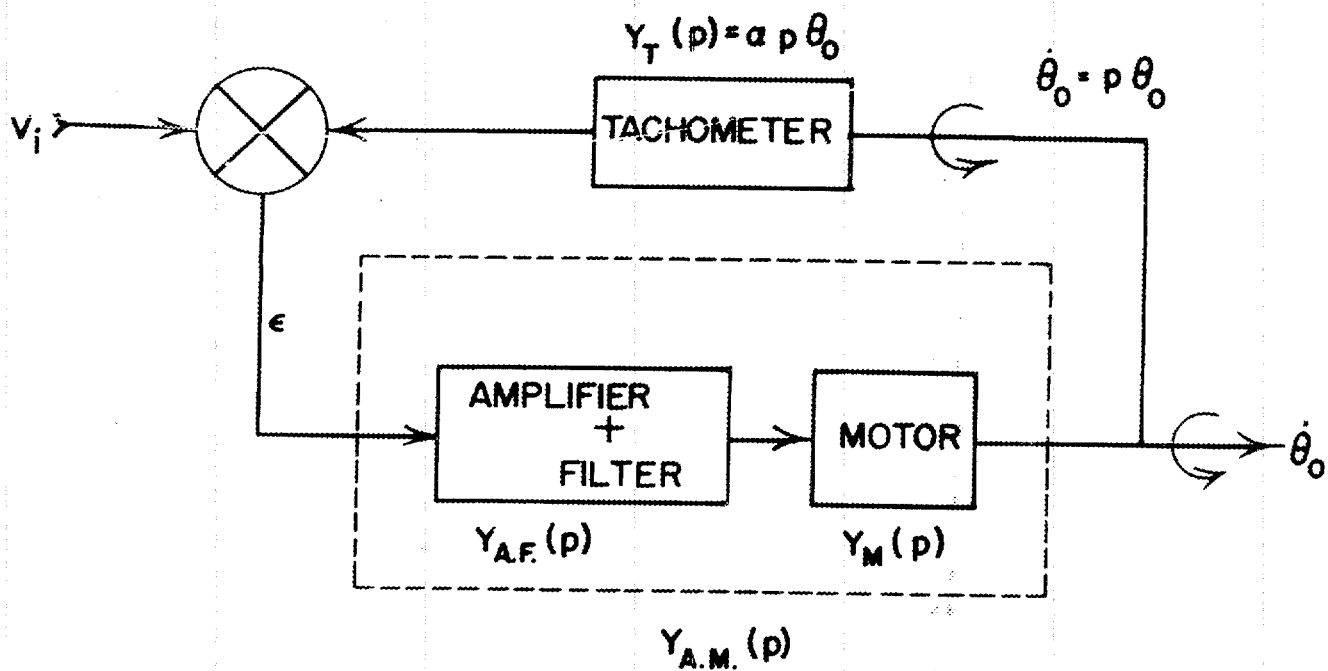


FIG. 10

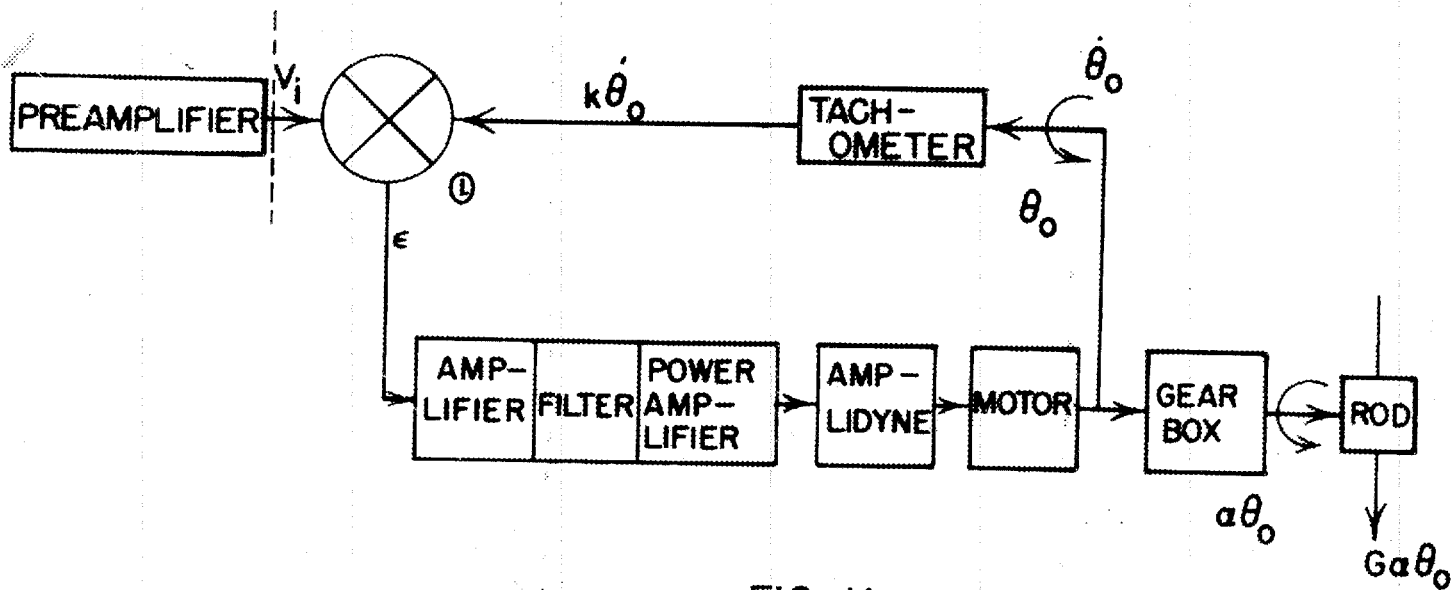


FIG. II

$$\dot{\theta}_o = \frac{1}{a} V_i$$

This is the desired functional relation between output rate and input signal.

The actual application of a regulating rod to the proposed pile represents an operation on the engineering scale. It is necessary to control a motor which is capable of developing approximately one horsepower. The motors in this power range will not "mix" well with hard thermionic tubes with comparable power handling capabilities. Since it has been implicitly indicated above that the most rapid possible response is desired, 60 cycle A.C. motor control was rejected. If an electric motor is to be used, it is necessary to use a direct current amplifier with larger power capacity and lower output impedance than vacuum tube amplifiers will conveniently yield. One such device that is available is the amplidyne; manufactured by the G.E. Company. The elementary theory of the amplidyne is given in the appendix with that title.

IIIa. Components Used in the Velocity Servo Mechanism

The equipment used in this system is indicated in Fig. 11.

Amplidyne—Model 5AM78AB78 }
Motor—Model 5BBY79AB7 } On loan from U.S.N.
Tachometer Elinco FB-B4C

The amplidyne is rated 1500 W at 250 volts. The drive motor is a 3 phase 440 V 3.6A induction motor which affords excellent speed regulation. The zero load hysteresis curve of the amplidyne is shown in Fig. 12. Fig. 13 is for a resistive load equal, at rated terminal voltage, to the machine's rating. Figures 14 and 15 show the voltage amplitude vs. angular frequency of output for sine inputs to the power amplifier which drives the amplidyne fields with no load and rated resistive load applied to the amplidyne terminals, respectively.

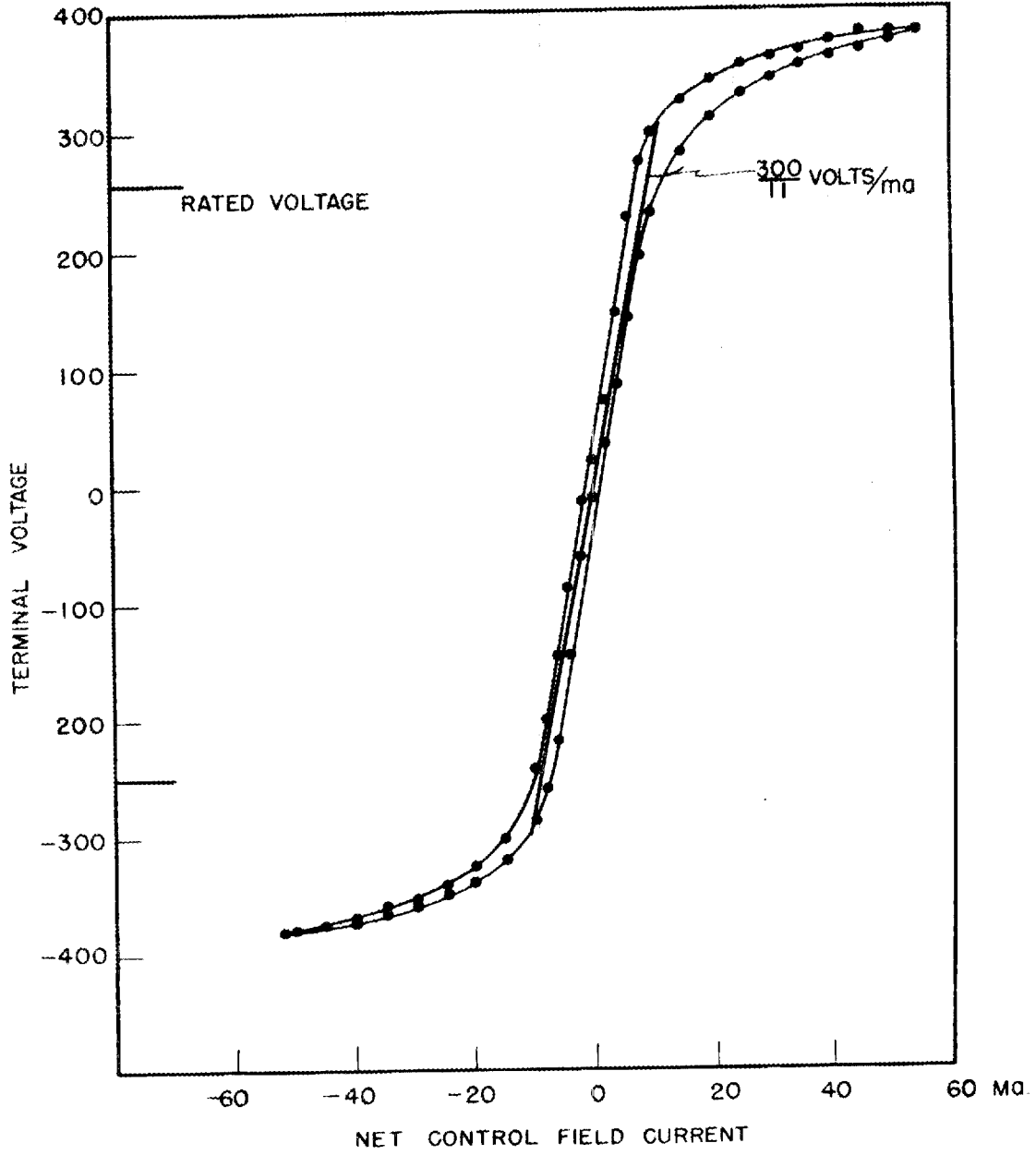
Figures 16 and 17 show the torque characteristic, the speed-voltage characteristic, and the speed-power characteristic for the 1 horsepower motor with no external load. The excellent linearity of the motor torque characteristic is due to the heavy compensating fields required by the use of a permanent magnet field. The tachometer has a nominal rating of 7.5 volts per 100 rpm.

Fig. 11 is evidently a more detailed example of Fig. 10, a velocity servo-mechanism.

NOT CLASSIFIED

—FIG. 12—

AMPLIDYNE 5AM78AB78
1 JULY 47
OPEN CIRCUIT HYSTERESIS



—FIG. 13—

AMPLIDYNE 5AM78AB78 HYSTERESIS UNDER LOAD

$R_{LOAD} = 41.6 \Omega$

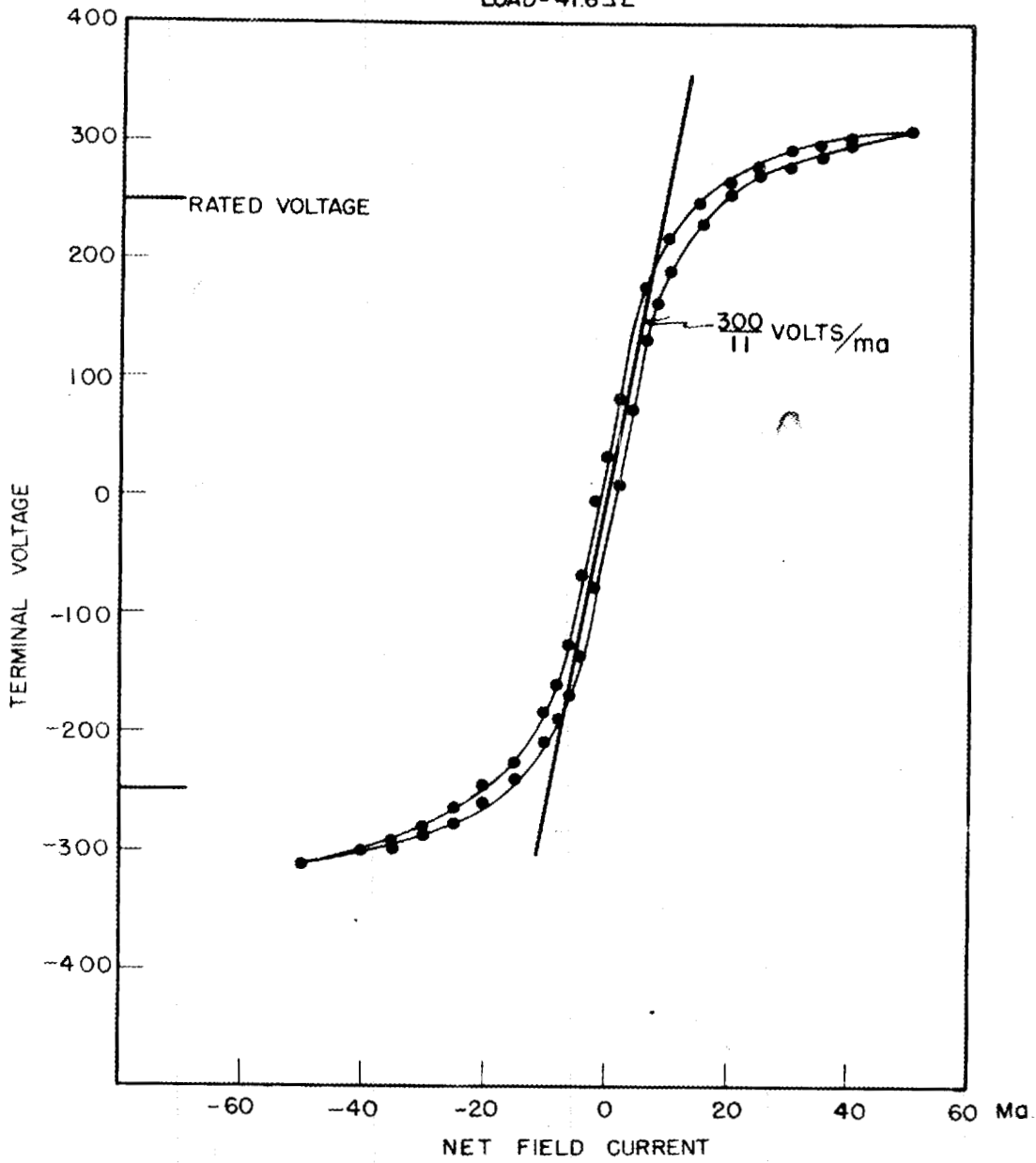


FIG. 14

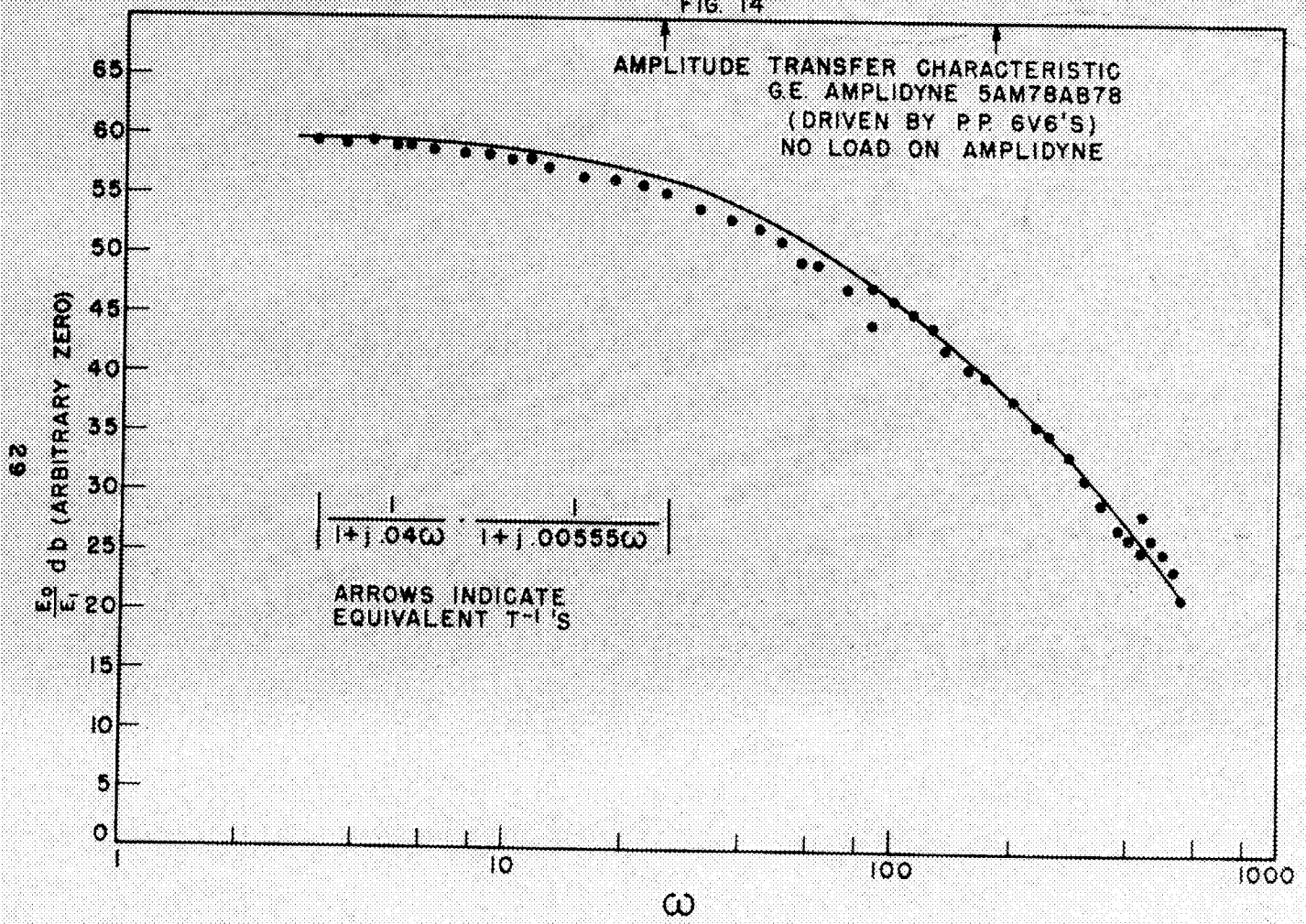


FIG. 15

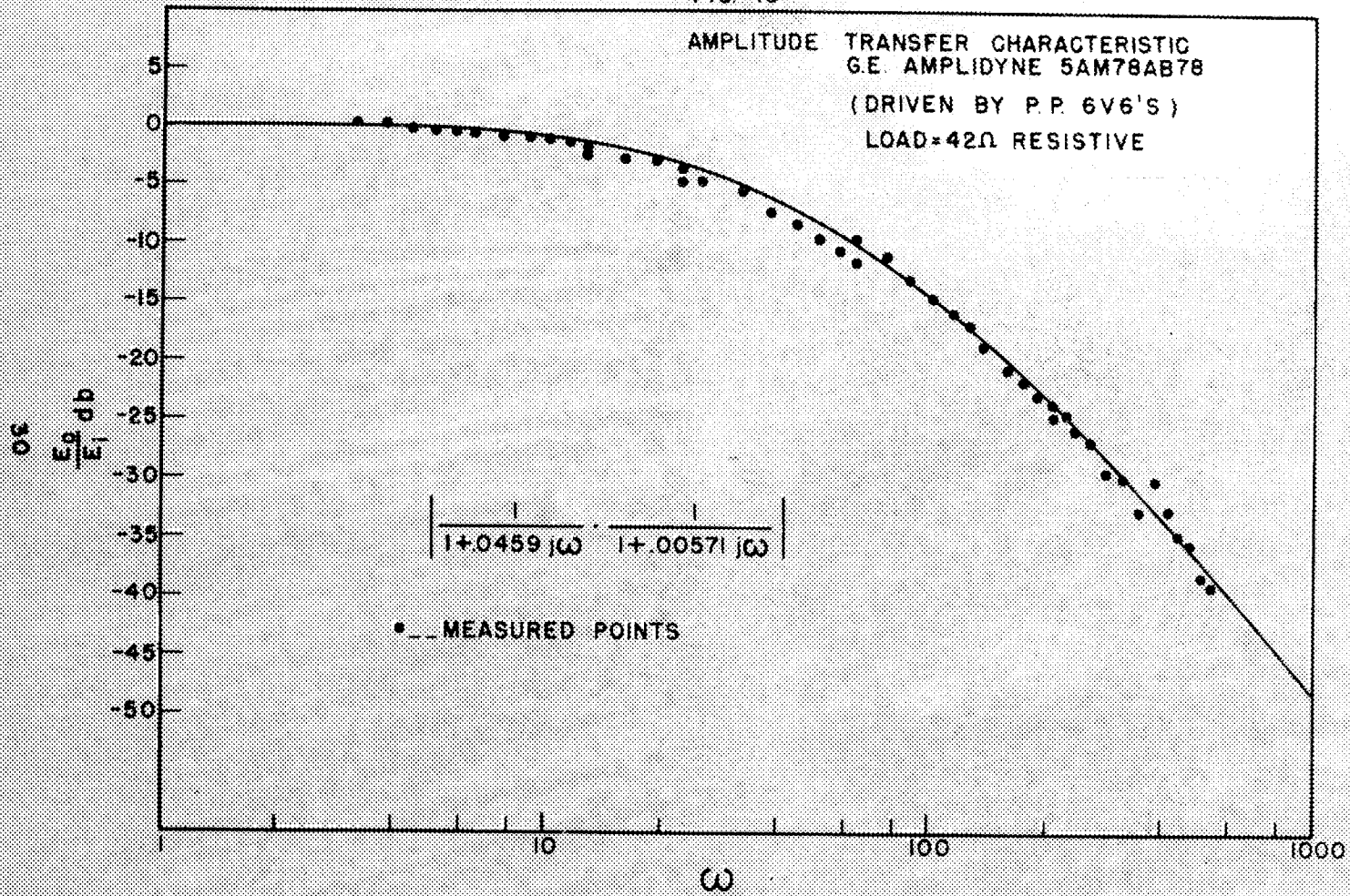
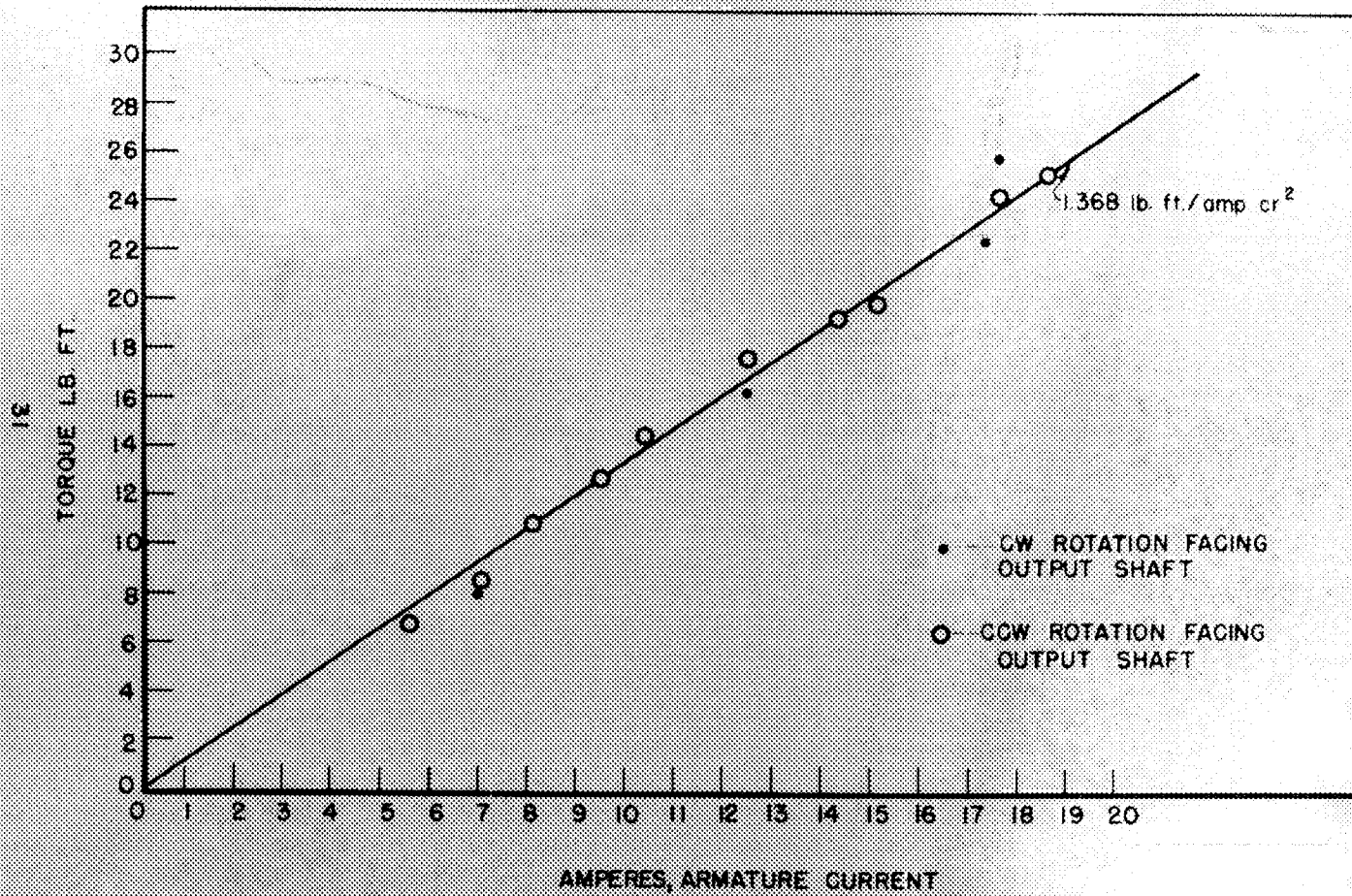
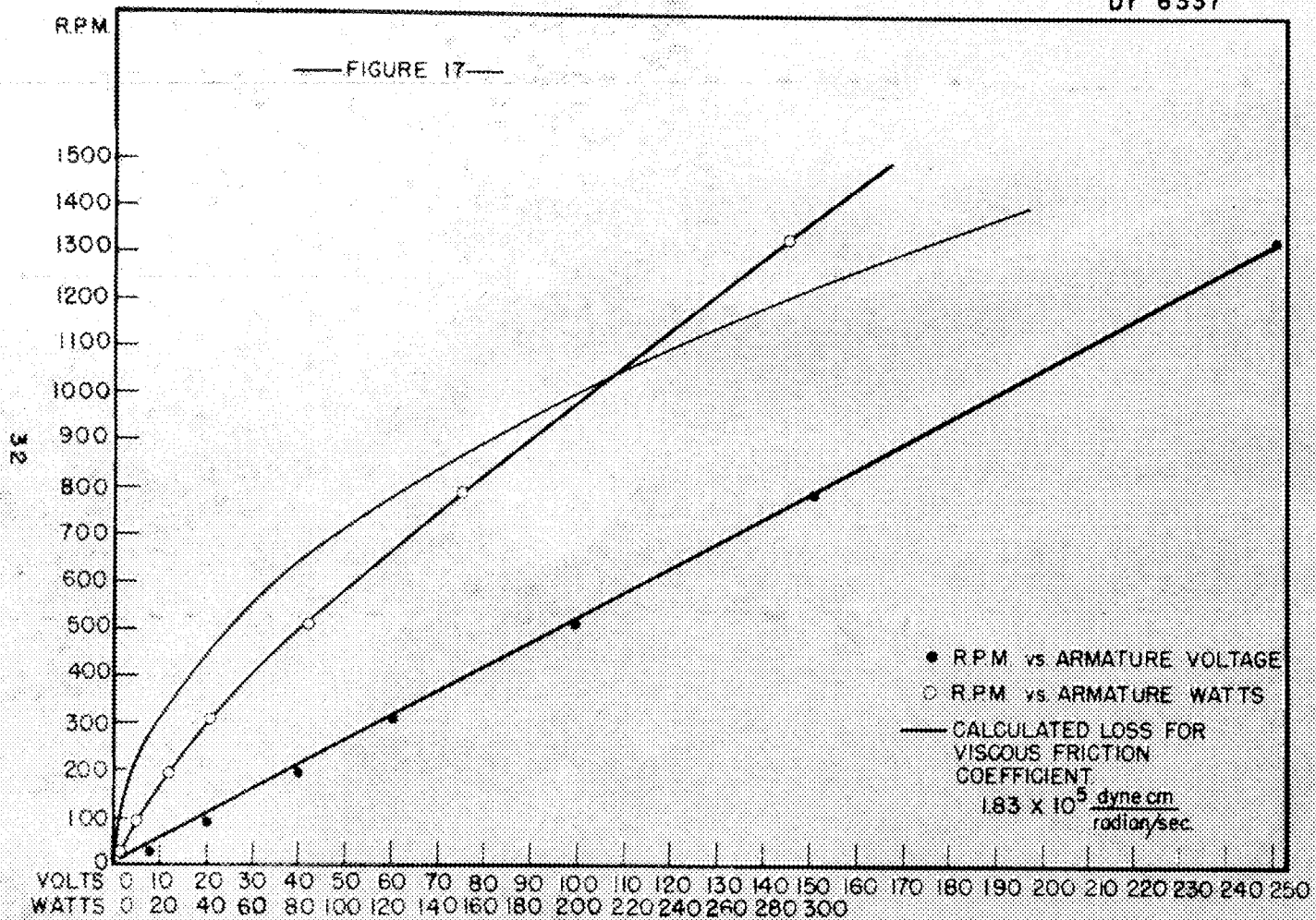


FIG. 16

NOT CLASSIFIED

TORQUE vs. ARMATURE CURRENT
FOR G.E. MOTOR 5BBY79AB7





Set

$$Y_{\text{amp}}(p) = A_0 \text{ volts/volt}$$

$$Y_{\text{fil}}(p) = Y_f(p) \text{ volts/volt}$$

$$Y_{\text{pwr amp}}(p) = A_1 \text{ milliamps/volt}$$

The product of these will yield the signal (unbalanced milliamperes) applied to the amplidyne fields per volt of error signal, ϵ , applied to the input of the amplifier.

Set

$$A_0 A_1 = A \frac{\text{milliampere}}{\text{volt}} \quad \text{Then}$$

$$Y_{\text{amp}}(p) \times Y_{\text{fil}}(p) \times Y_{\text{pwr}}(p) = A Y_f(p) \frac{\text{milliampere}}{\text{volt}}$$

Reference to Figures 12 and 13 will show that a reasonable linear approximation to the static amplidyne characteristic is 27.3 volts/milliampere. Evidently there is going to be trouble sooner or later with linear approximations being made so freely, but let's see how far we can go with them. The amplitude vs. angular frequency characteristic of the amplidyne is shown at both no load and rated D.C. load in Figures 14 and 15. Only the frequency dependence has significance in these figures; absolute magnitude is modified by the amplifier gain chosen. Fig. 14 is shown with an amplitude function superimposed on the experimental curve. This yields an approximate transfer characteristic for the amplidyne with one time delay which the simple theory of the machine does not predict. We adopt provisionally:

$$Y_{\text{amplidyne}}(j\omega) = \frac{1}{1 + j \cdot 0.040\omega} \times \frac{1}{1 + j \cdot 0.00555\omega} \times 27.3 \text{ volts/ma.}$$

Thus, the voltage applied to the motor armature per volt of error signal can be written for the steady state sinusoidal input case:

$$\frac{27.3 \times A \times Y_f(j\omega)}{(1 + j \cdot 0.040\omega)(1 + j \cdot 0.00555\omega)}$$

Fig. 17 shows motor speed at no load vs. applied voltage, and the motor speed at no load vs. input power. There is a computed curve for speed vs. input power assuming a viscous friction acting on the motor. Evidently this assumption of a viscous friction is not a very adequate description of what is going on. Actually the situation would be far better described as Coulomb friction. This regrettable fact will be disregarded for the present.

From the known armature resistance of 7.5 ohms and the speed-loss and speed-applied voltage curves of Fig. 17 one obtains the generated voltage constant of the motor, .00305 V/rps.

The manufacturer supplied the information that the moment of inertia of the motor armature is 41.2 in²-lb. This is 1.205×10^5 gm cm². In the application here contemplated the effective mass of the load is small compared to the armature inertia so the moment of inertia of the moving system will be taken as 1.2×10^5 gm cm².

One can estimate the torque constant of the motor from the shot-gun pattern of Fig. 16. The slope of the torque-current curve is given as 1.368 ft. lb/amp. In our units this is 1.35×10^7 dyne-cm/amp.

IIIb. Steady State Analysis of the Linearized System

From the elementary discussion of the amplidyne-motor system one obtains the differential equation of the motor:

$$p\theta = \frac{K}{1 + pT_{M.A.}} E_{D.A.}$$

$$K = \frac{K_T}{K_T K_v + F(R_A + R_M)}$$

with

$$T_{M.A.} = \frac{J(R_A + R_M)}{K_T K_v + F(R_A + R_M)}$$

All the quantities appearing in these recipes are known after one measures the armature resistance of the amplidyne as 3.2 Ω .

Substitution of the known quantities yields:

$$K = 6.85 \text{ rad/sec/volt}$$

$$T_{M.A.} = .061 \text{ sec.}$$

The measured tachometer voltage rate is 8.5 volts/100 rpm. This becomes 2.26×10^{-4} volts/rad/sec.

Finally one has an explicit expression for the loop gain. The loop gain is the voltage fed back to the differential per volt of error signal at the input to the amplifier in the steady oscillatory state.

$$\begin{aligned}
 AY_F(j\omega) &\times \frac{27.3}{(1 + j \cdot 0.040\omega)(1 + j \cdot 0.0055\omega)} \times \frac{6.85}{(1 + j \cdot 0.061\omega)} \times 2.26 \times 10^{-4} \\
 &= \frac{4.22 \times 10^{-2}}{(1 + j \cdot 0.040\omega)(1 + j \cdot 0.0055\omega)(1 + j \cdot 0.061\omega)} AY_F(j\omega) \quad \text{Eq. X}
 \end{aligned}$$

To see what the design problem here amounts to, this characteristic has been plotted on a Bode diagram ($|Y_m|$ db vs. $\log \omega$ and loop phase vs. $\log \omega$) in Fig. 18 with $Y_F(j\omega) = 1$. No correction is applied by a filter. The numerical factors in the numerator have been neglected since they will produce only a translation of the whole $|Y_m(j\omega)|$ curve parallel to the y axis.

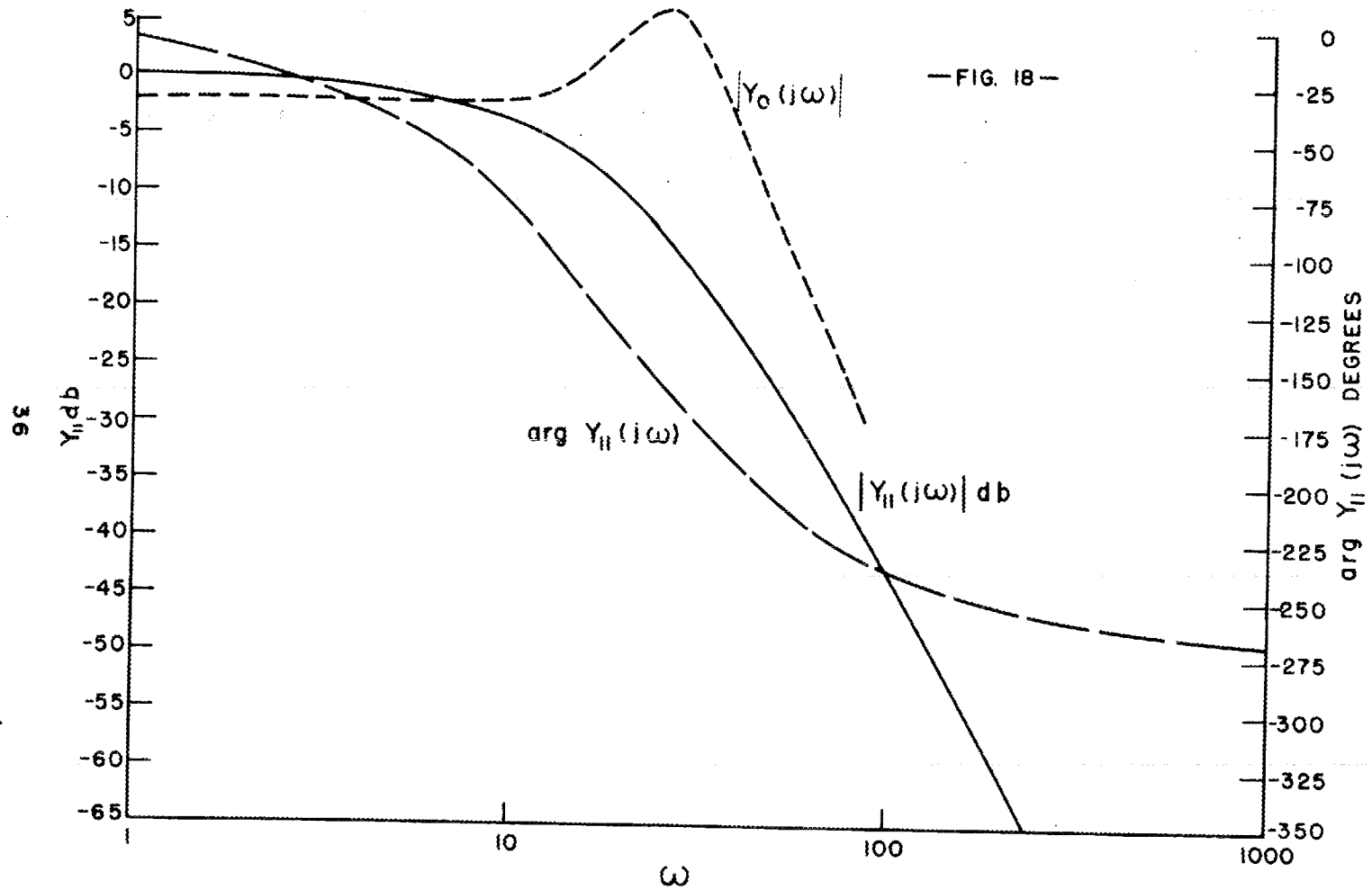
For the system to be stable it is necessary for the transfer locus to avoid the neighborhood of the mystic point $(-1, 0)$ in the Nyquist diagram. This will usually be managed satisfactorily if $\text{Arg } Y_m(j\omega)$ is less negative than -150° when the loop gain has fallen to unity, which is the zero d.b. point or "feedback cross-over." As the value of $\text{Arg } Y_m(j\omega) = -120^\circ$ at feedback cross-over, the system becomes progressively better damped and may usually be expected to be over-damped when $\text{Arg } Y_m(j\omega)$ is 60° or more positive with respect to -180° at feedback cross-over.

Take something like the limiting case: 35° phase margin at feedback cross-over. Fig. 18 shows this occurs at $\omega = 22$ radians per second. At this angular frequency one sees the $Y_m(j\omega)$ curve has fallen about 12 db. from its value at 1 radian/second. We choose this frequency for feedback cross-over and the amplifier's gain constant is then automatically set so the numerator of equation X is 12 db.

The curve y -clept $Y_G(j\omega)$ represents the over-all characteristic of the system with the amplifier just chosen and feedback cross-over at 22 radians/sec. The response level is down 2 db. at low frequencies and rises to +6 db at the resonance (larger phase margin at feedback cross-over would have reduced this resonance) in the neighborhood of 4 cycles/sec. Thus, the system will not respond to a step input signal in a monotone manner but will show a few damped oscillations.

NOT CLASSIFIED

Dr 6338

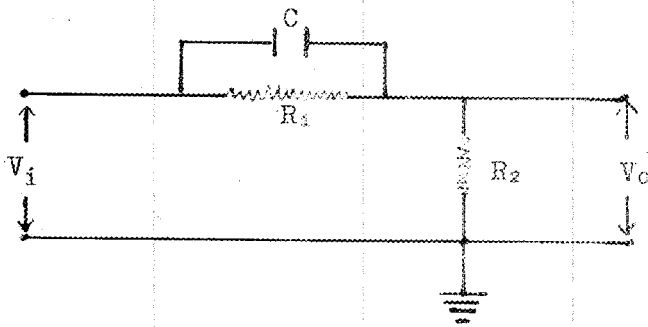


The system output velocity will build up from 1/10 to 9/10 of the final velocity in a time approximately given by

$$2 \times 6.7 T_{b.u.} = 1$$

$$T_{b.u.} = .075 \text{ sec.}$$

This performance is distinctly unimpressive. A corrective filter should be capable of improving this. What is required is a circuit which will produce a large phase advance at high frequency. A circuit which has this property is indicated below.



$$\frac{V_o}{V_i} = Y_1(p) = K_1 \frac{1 + \tau_1 p}{1 + K_1 \tau_1 p}$$

where $K_1 = \frac{R_2}{R_1 + R_2} = \text{D.C. attenuation}$

$$\tau_1 = R_1 C_1$$

This circuit will introduce a localized phase advance at the cost of low frequency attenuation. The bill in terms of low frequency attenuation gets to be pretty steep when the phase advance required becomes large. Here is a case in which division of labor really pays off. Two of these circuits will be used in cascade, with an isolating amplifier interposed. The resulting filter characteristic becomes

$$(A) \times K_1^2 \times \frac{(1 + \tau_1 p)^2}{(1 + K_1 \tau_1 p)^2}$$

In the steady harmonic-oscillation state $p = j\omega$ and one has

$$K_1^2 \frac{(1 + j\omega\tau_1)^2}{(1 + jK_1\tau_1\omega)^2}$$

This characteristic is plotted on a Bode diagram in Fig. 19 for the case $K_1 = 1/10$ and $\tau_1 = .02$. The constant multiplier is again omitted.

Fig. 20 shows the result of applying this correction to the system here being studied. The resultant phase characteristic of the loop now falls to -150° at $\omega = 210$ radians/sec instead of 23 radians/sec. Again we choose as the phase margin at feedback cross-over the value 35° . The loop phase lag reaches -145° at $\omega = 180$ radians/sec. This choice of feedback cross-over establishes the product

$$4.22 \times 10^{-4} A \times K_1^2 = A'$$

We see A' db = 37. Contrast this with 12 db allowable before.

The other curve on the figure shows the over-all frequency characteristic of the system. The resonance peak is now only 4 db. The system will show over-shoot (see Fig. 21). Again, considering that components in the frequency range where the system response is down more than 6 db, fail to contribute sensibly to the response, we find the 10% to 90% response time for a step input.

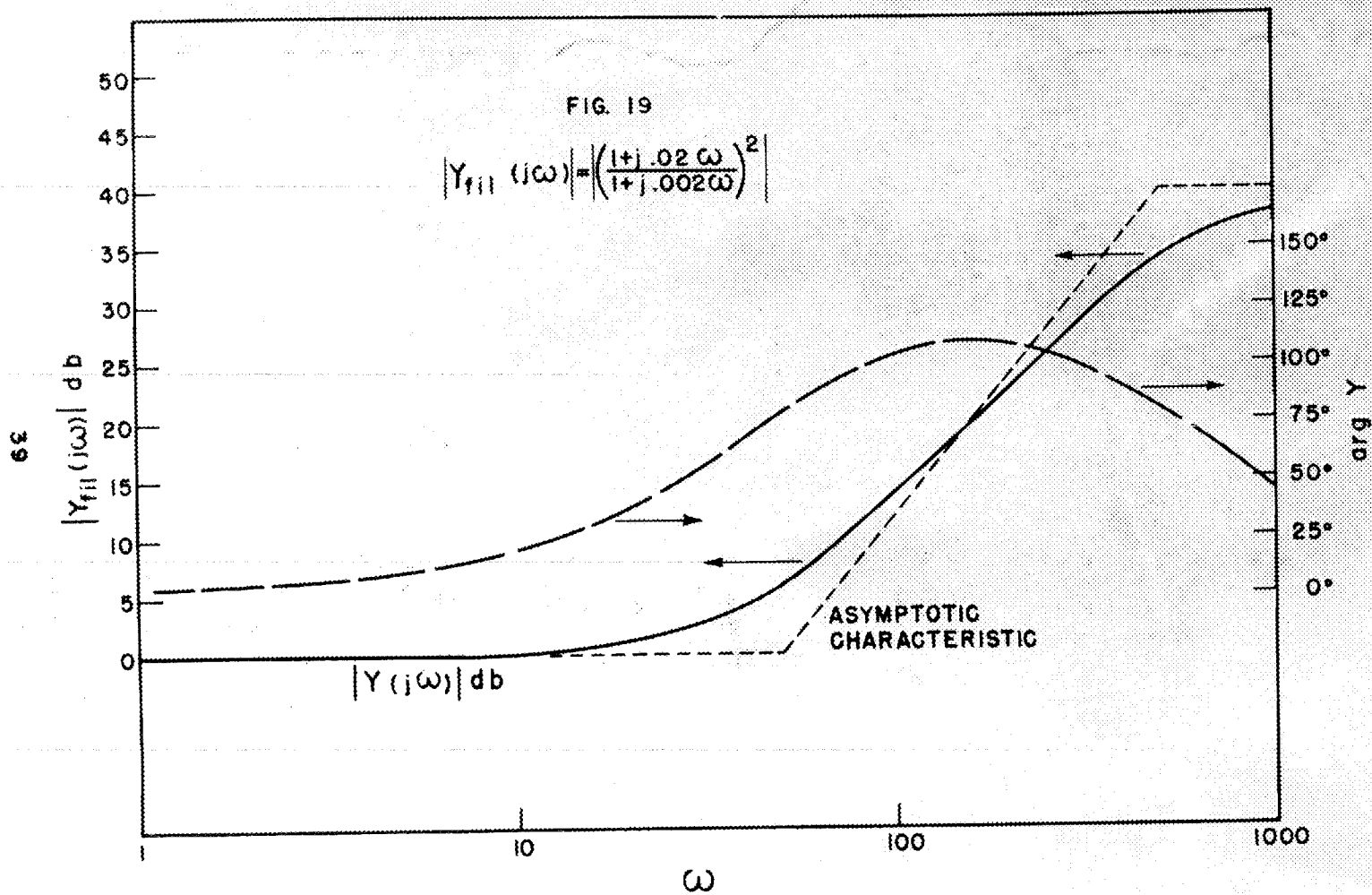
$$2 \times \frac{380}{2\pi} \times T_{b. u.} = 1$$

$$T_{b. u.} = 1/120 \times .008(3) \text{ sec.}$$

This is a reasonable improvement in speed over the uncorrected system. In addition the system is far stiffer* as well as very considerably better damped. The design problem is solved. If one had been interested in a somewhat more slowly responding system than this one, say of the order of 10 cps at feedback cutoff**, the shorter time delay in the amplidyne could have been neglected and a procedure similar to that followed in this paper up to now could have been used to design the system. This figure of 10 cps at feedback cutoff is usually considered as representing a fast system.

*The system corrects an error signal much better and prevents torques applied to the output member from producing as large an undesired output.

**Defined—the frequency at which the overall system response is down 6 db from its value at low frequencies—above which no sensible contribution to the system response can occur.



39

NOT CLASSIFIED

Dr 6340

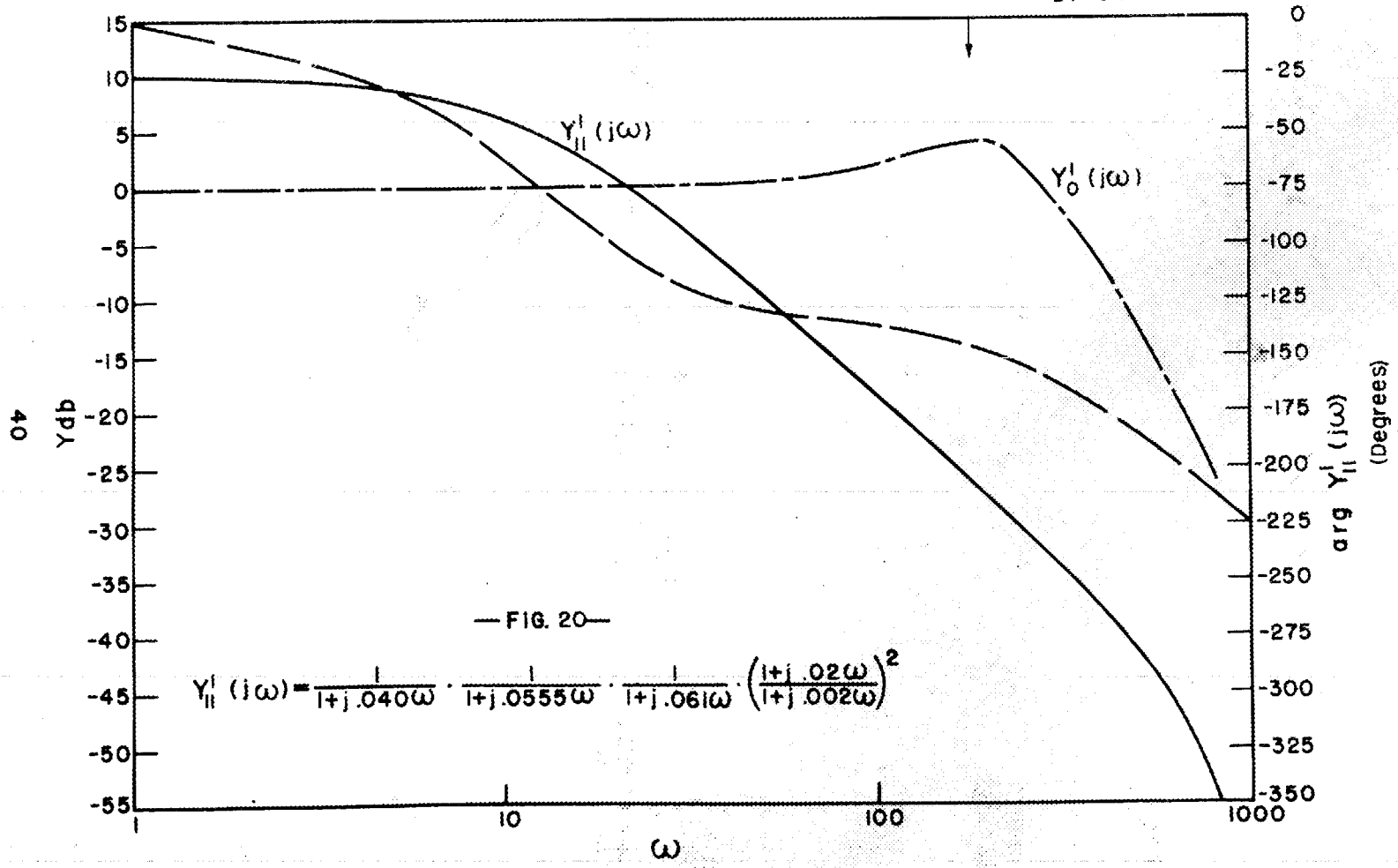
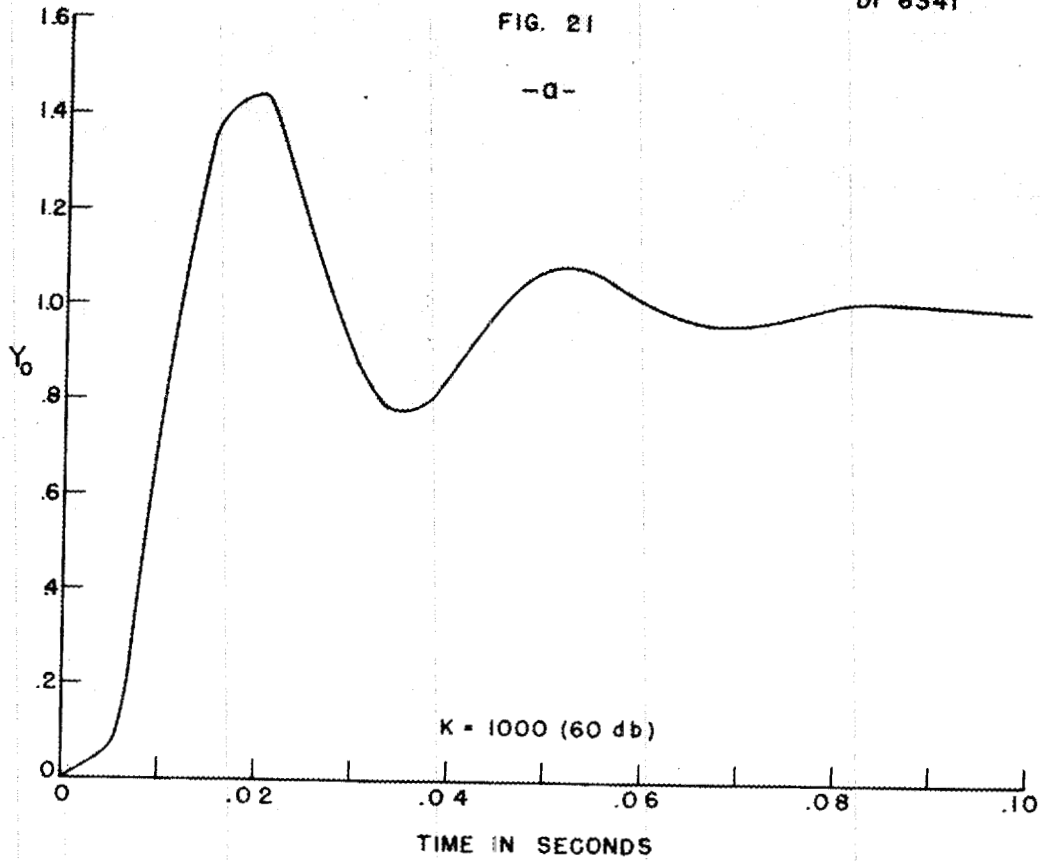
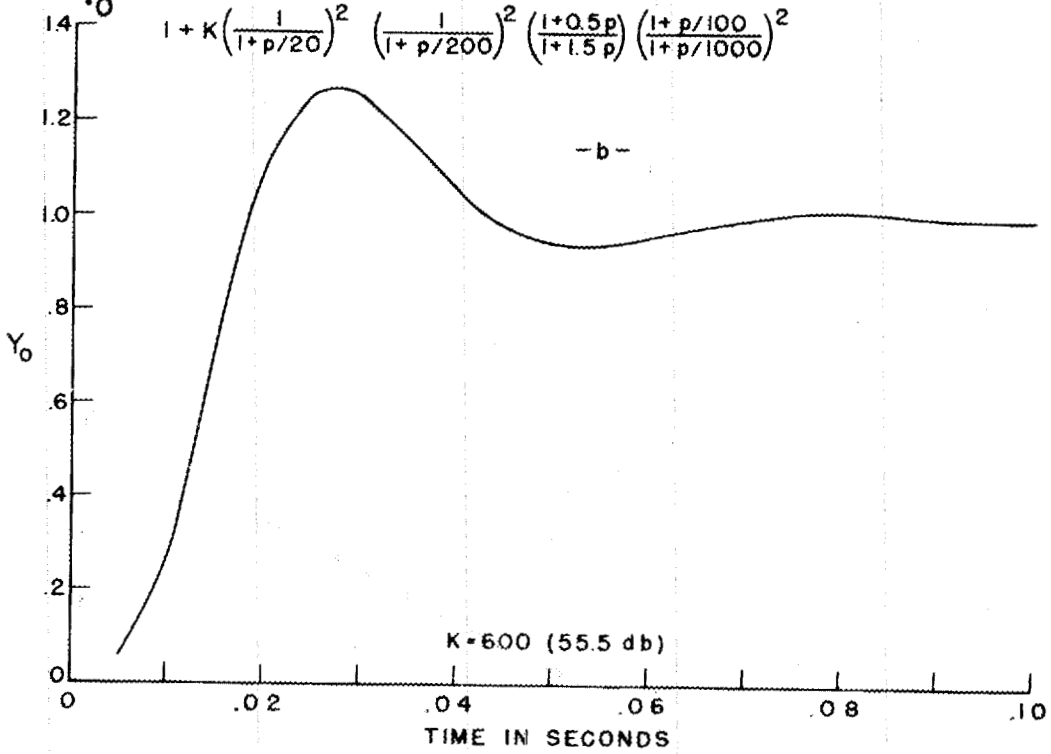


FIG. 21



$$Y_0 = \frac{K \left(\frac{1}{1+p/20}\right)^2 \left(\frac{1}{1+p/200}\right)^2 \left(\frac{1+0.5p}{1+1.5p}\right) \left(\frac{1+p/100}{1+p/1000}\right)^2}{1 + K \left(\frac{1}{1+p/20}\right)^2 \left(\frac{1}{1+p/200}\right)^2 \left(\frac{1+0.5p}{1+1.5p}\right) \left(\frac{1+p/100}{1+p/1000}\right)^2}$$



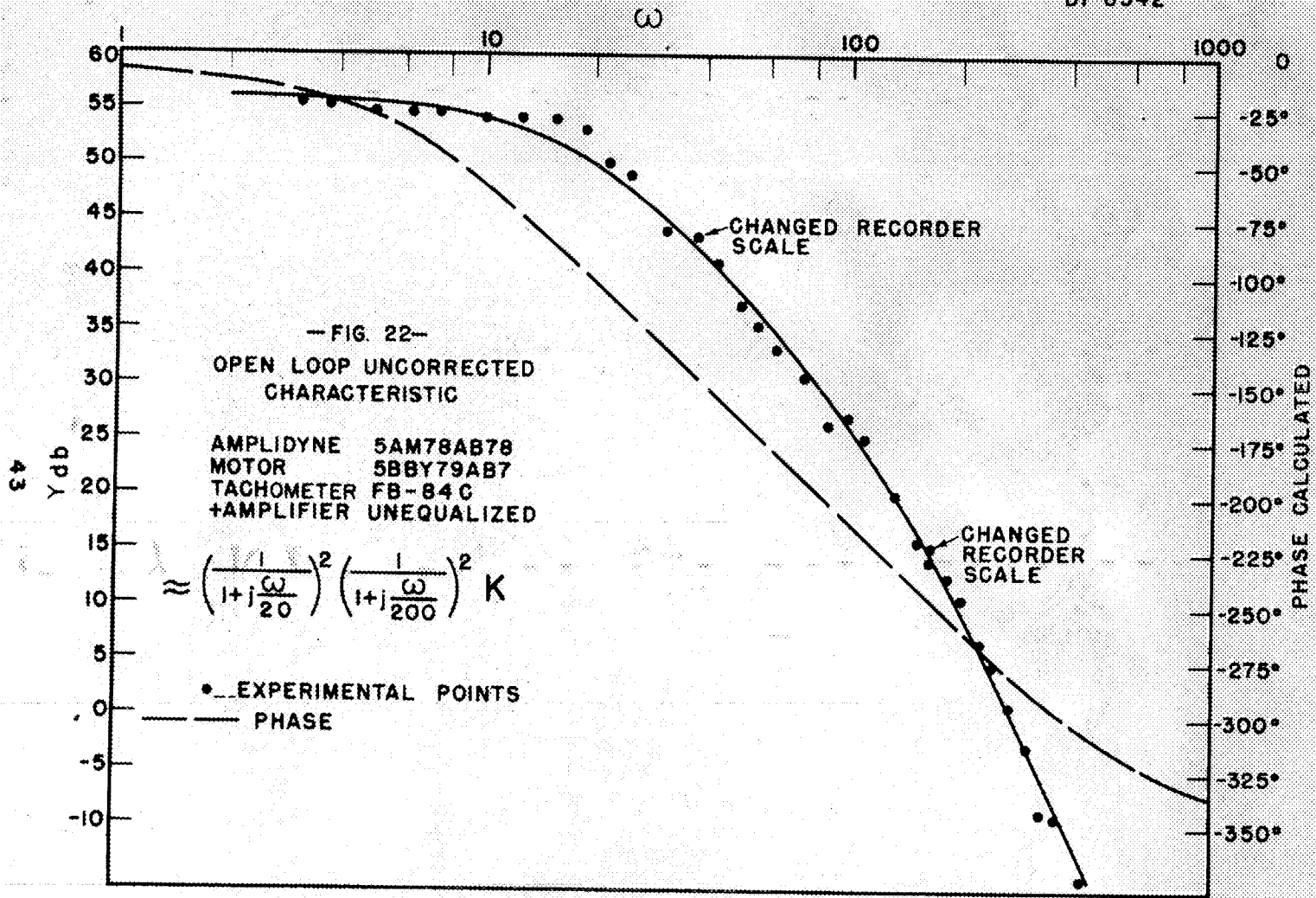
IIIc. Experimental System's Performance

There is one slight difficulty; the system does not behave as described above. Fig. 22 shows a set of experimental points carefully taken with an unequalized amplifier driving the amplidyne fields. The plotted points give the ratio of tachometer voltage to the input signal voltage at the amplifier. The absolute magnitude on the db scale is again not significant. Measurements were carried out to frequencies where the tachometer voltage readings became so small they were unreliable. A curve of the type:

$$\left[\frac{1}{1 + j\omega/20} \right]^2 \left[\frac{1}{1 + j\omega/200} \right]^2 \text{ was fitted to these points.}$$

The phase characteristic which is plotted corresponds to the above function. Here the Bode attenuation-phase shift theorem was applied, assuming no other time constants effective in the system.

Several things appear here which are at first sight a bit disconcerting. First, the time constants computed for the amplidyne-motor system have been replaced by experimental values in the transfer function. This is based on the assumption that the experimental points accurately represent the system performance, a point to be discussed in the section on experimental technique in determining the transfer function. One fits a curve to the points and does not worry too much about the failure of the fit near $\omega = 20$. It is assumed that the above function represents the transfer function for all frequencies from zero to infinity. The phase characteristic can then be directly calculated. Evidently, this cannot be exact since there is no trace of the time constant associated with the amplidyne control-field and output tube plate resistance. A computation of this time constant shows that its contribution to the phase shift at $\omega = 500$ is negligible. There is a feature of real physical significance which does enter here, **THE SYSTEM IS FUNDAMENTALLY NON-LINEAR.** This shows up in the curving characteristic of the tubes in the amplifier. This is, however, not serious since all tubes operate on a nearly linear portion of their characteristics well beyond the point at which the amplidyne characteristic becomes markedly bent. Here is one essential non-linearity of the system, saturation of the amplidyne. Also, the voltage output of the amplidyne is a hazily defined function of the control field current, depending on the past history of the machine and the

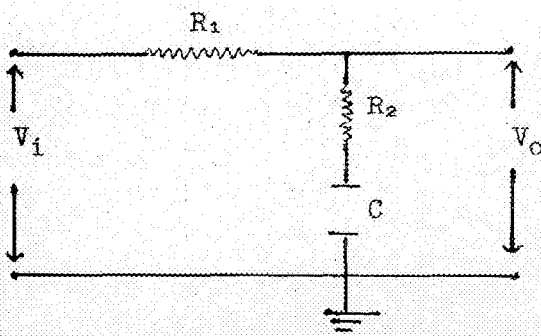


present load on it. The torque characteristic of the motor is sensibly linear far beyond the normal range of current supplied by the amplidyne. The speed-voltage characteristic is also linear. The reader probably shuddered at fitting a parabola to the speed-loss curve. This was done for the innocent purpose of obtaining an equivalent viscous friction coefficient for the machine. As mentioned earlier, Coulomb friction would represent rather better the loss function of the motor. This loss is due to the water seals on the motor shaft, and is truly scandalous. The fact must be faced that this is a large and strictly non-linear effect.

One now proceeds on the basis that the analysis of an equivalent linear system is a fiction which may yield valuable suggestions in the design but will not be too upset when he finds divergences between theory and experimental results.

One tries for a 35° phase margin at feedback cross-over. Since dual lead circuits did such wonders for the simplified case, he tries the same magic again. Fig. 23 is a Bode diagram of the transfer characteristic to be used now. It will be noted that here something new has been added in the form of an integral circuit* which costs a trifling amount of phase lag in the neighborhood where phase advance is needed, about 3°. It costs a maximum of about 64° in phase lag at low frequencies where there is phase margin to throw away. Why throw away any of the hard-bought phase margin at high frequency? The answer is a compelling one—to make the system go. Without the integral circuit (low frequency build-up) the cost of the two lead circuits, which, as has been indicated, make possible feedback cross-over at a frequency almost 10 times that attainable without equalization, would be a murderous 40 db of low frequency attenuation with respect to the high frequency amplification ahead of the amplidyne. Any attempt to make the amplifier gain high enough (in the absence of the integral circuit) for the system

*Integral Circuit.

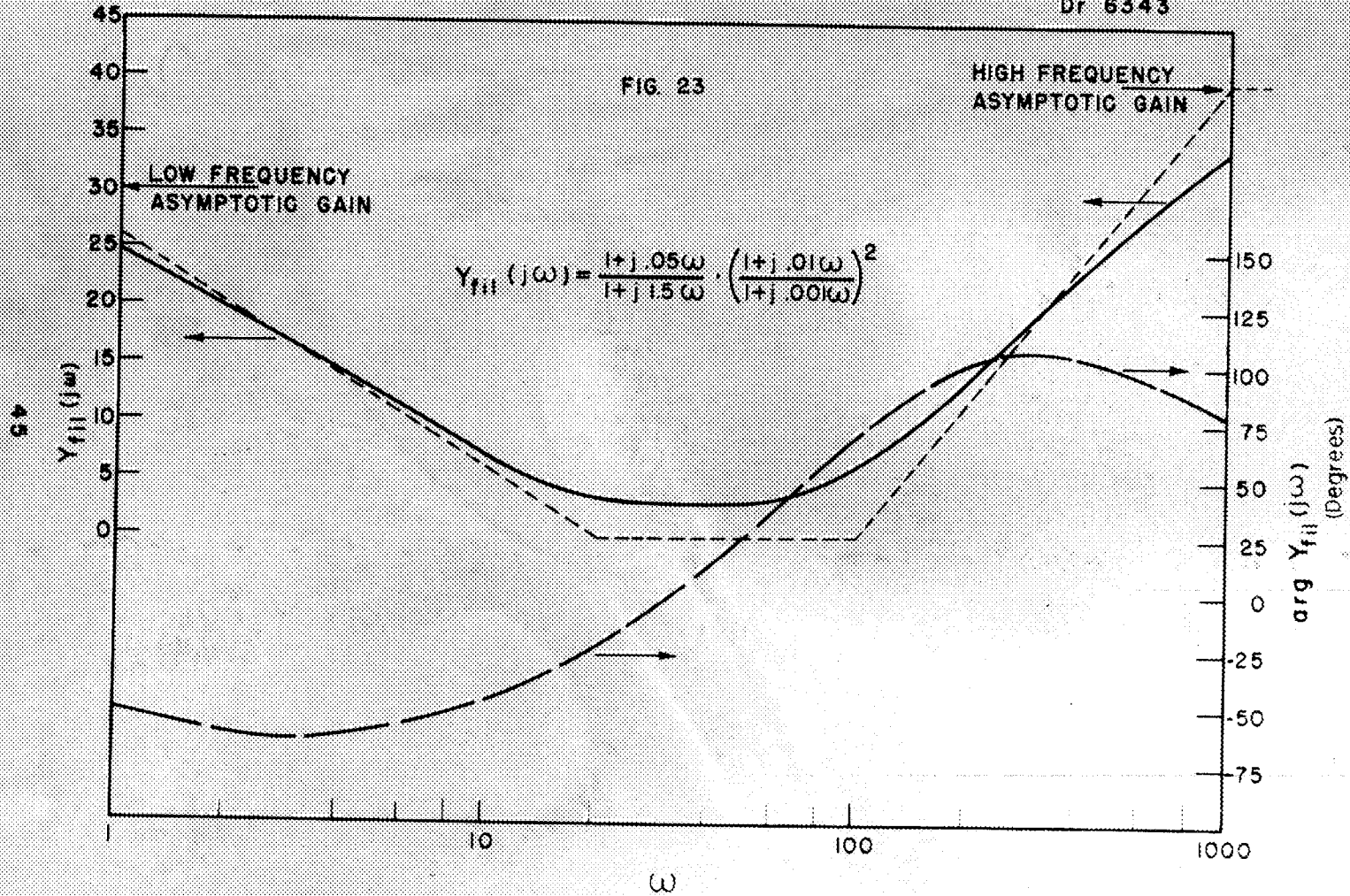


$$\frac{V_0(p)}{V_1(p)} = Y_1(p) = \frac{1 + \tau_i p}{1 + K_1 \tau_i p}$$

$$K_1 = \frac{R_1 + R_2}{R_2}$$

NOT CLASSIFIED

Dr 6343



to respond to a low frequency signal results in shutting the amplidyne down completely due to high frequency noise being amplified.

Fig. 24 shows the transfer characteristic computed for the loop associated with the differential and the associated computed phase. Y_C is the calculated value of the over-all gain of the system. The system response is down 6 db at $\omega = 280$ radians/sec. The resonant peak amounts to a little less than 6 db which is acceptable. The loop gain at $\omega = 1$ radian per second is calculated at 51 db, a little better than previously estimated.

Fig. 25 shows the experimental results obtained for the system equalized as indicated in Fig. 23. The difference in behavior at the high frequency edge of the pass band of the system from that computed is due to the setting of loop gain at a value which scamps a bit on the phase margin at feedback cut-off. Compare Fig. 26, which shows the computed over-all gain, with phase margin at feedback cut-off set at 30° and at 25° . The 25° curve agrees quite reasonably with the measured points of Fig. 25. At values of ω which are less than 20 the measured points show a lower value of $|Y_M|$ than is calculated from the uncorrected loop plus the known corrective filter characteristics, probably due to difficulties in measuring ϵ , but the measured value of $|Y_M|$ near $\omega = \text{zero}$ agrees with the computed value of 60 db.

This essentially completes the design problem from the point of view of steady state analysis. However, it is a rare and unusual condition for the system to operate in the steady sinusoidal state. The wished for normal situation is for the pile level to sit quietly at some value so the servo rate is zero. The pile may be subject to some more or less rare and more or less violent disturbances. Then the servo operates in a transient state for a short period and lapses into innocuous desuetude. Thus, although the design has been carried out by and large in terms of the steady state response, the real proof of the system lies in its transient performance. The worst type of catastrophe one can readily imagine is for the slow flux in the pile to show a step increase. The response of the servo system has been calculated for the value of Y_M corresponding to Fig. 24 and for a slightly differing value of loop gain. The computed transients are shown in Fig. 21, parts a and b.

Miscellaneous: The amplifier to be used with this system has each gain stage in the form of a long-tailed pair except the power stage which has some cathode feedback. The corrective filters are isolated by stages of amplification to make simpler the analysis of their behavior. An error measuring meter is supplied to indicate any persistent unbalance. There are terminals to facilitate

NOT CLASSIFIED

— FIG. 24 —

Dr 6344

LOOP CORRECTED BY FILTER CHARACTERISTIC OF FIGURE 23

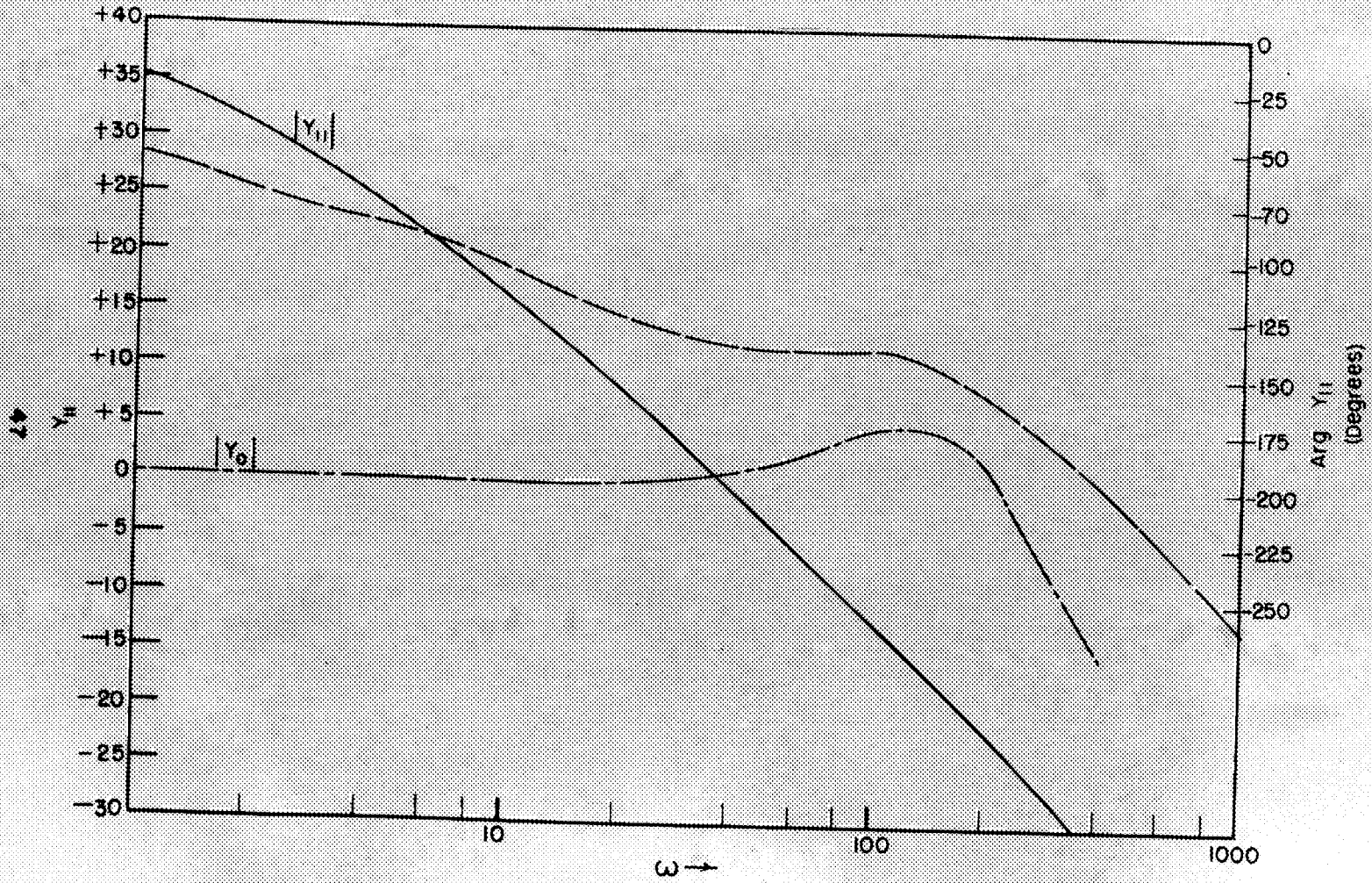
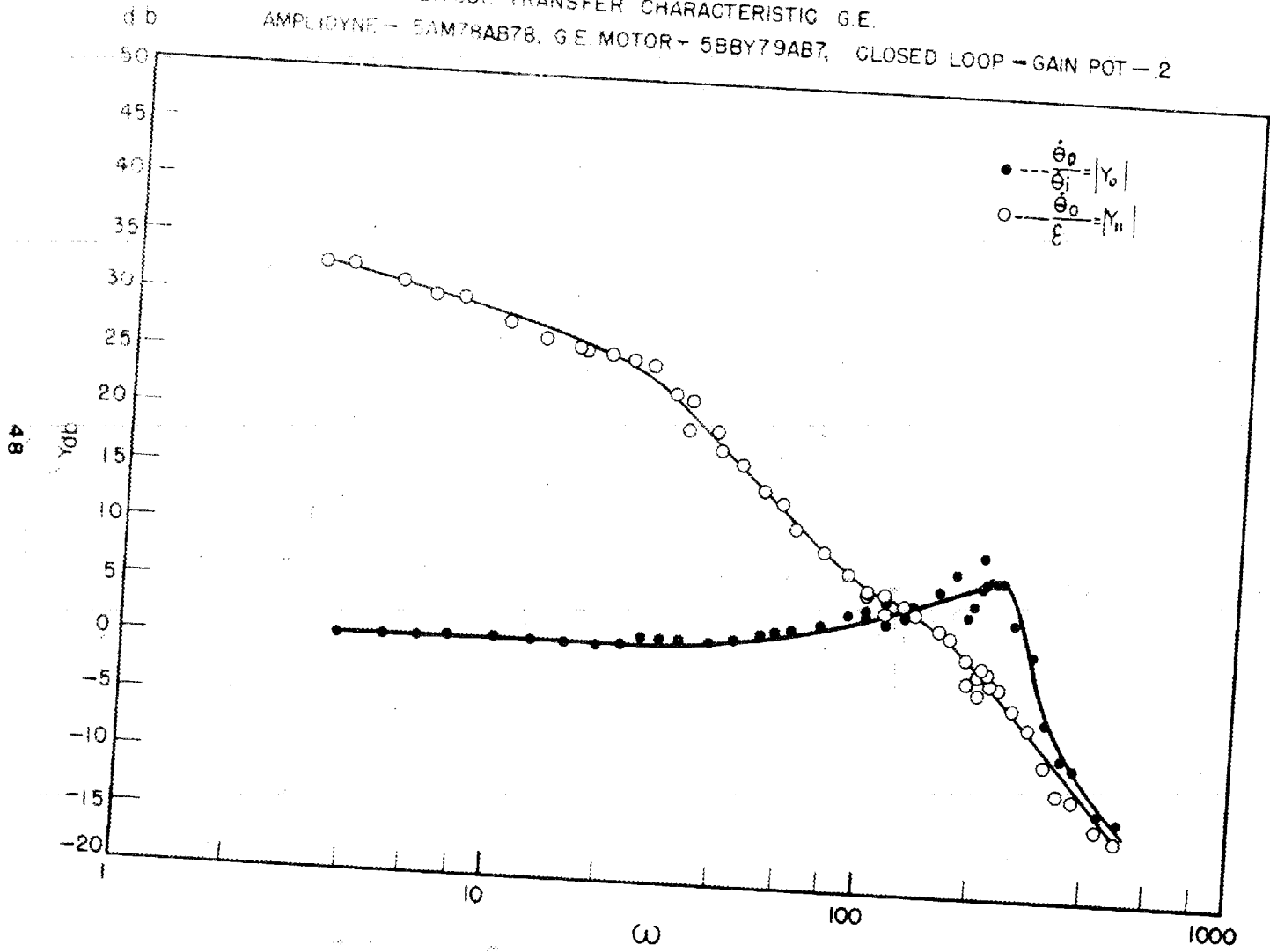
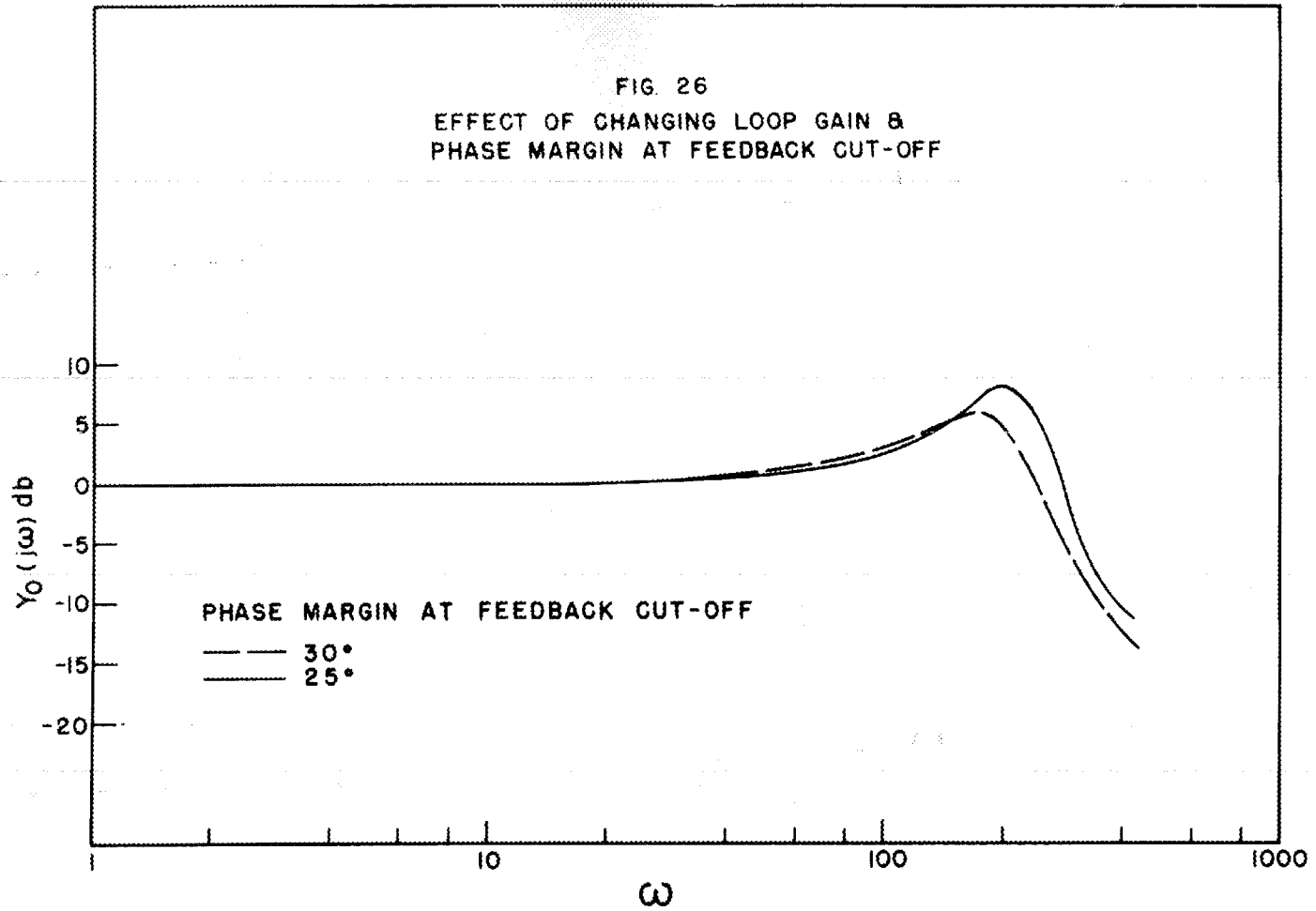


FIG 25

Dr 6345

AMPLITUDE TRANSFER CHARACTERISTIC G.E.
AMPLIDYNE - 5AM78AB78, G.E. MOTOR - 5BBY79AB7, CLOSED LOOP - GAIN POT - 2





[REDACTED]

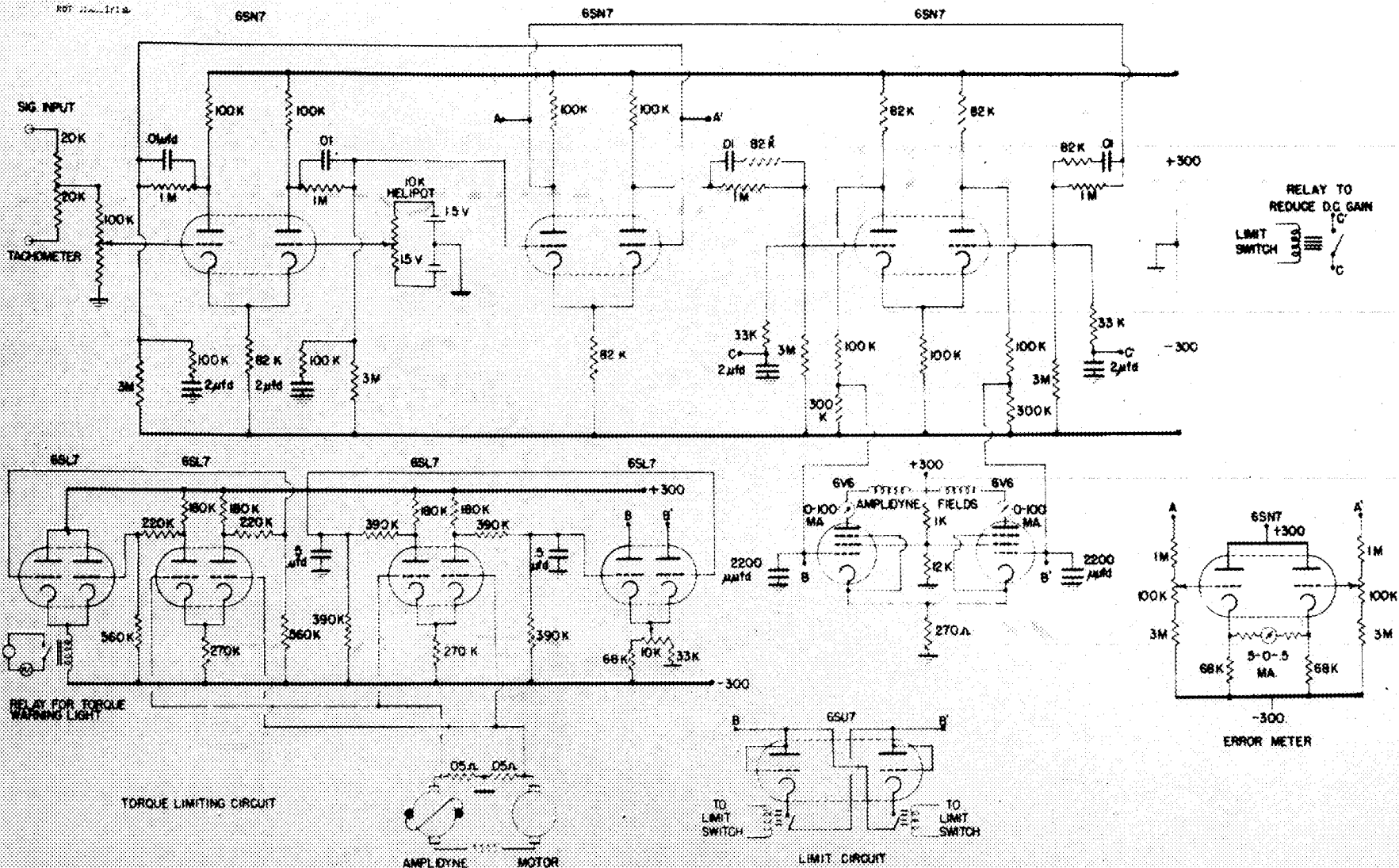
recording of the error if necessary. In addition, a time dependent torque limiter controlled by the voltage drop across a low resistance in the armature circuit of the motor supplies a degenerative feedback to the power stage when the current through the motor reaches values at which the motor torque might damage the system. This will normally not come into operation, but will probably function only in case of a mechanical interference. The servo system will have to function in conjunction with the shim rods. A relay interlock system desensitizes the amplifier at the end of the regulating rods normal stroke. This applies only to signals indicating further motion of the rod tip away from the mid-stroke position. The system maintains sensitivity for signals which tend to drive the rod tip toward the mid-stroke position. The shim rods are interlocked to the servo system so they automatically move to recenter the regulating rod tip when the regulating rod tip has reached a predetermined distance from center position. When the regulating rod has withdrawn to the end of its normal stroke, the amplidyne excitation is removed and the motor is dynamically braked by the amplidyne armature circuit. If this fails to stop the rod, mechanical shock absorbers do so. Then the regulating rod is ready for the signal to center the tip with respect to the pile. The motion of the shim automatically stops when the regulating rod has recentered. Control of the shim rods by the regulating rod will be modified as dictated by safety considerations. Fig. 27 is a schematic diagram showing the basic circuits.

Features to Be Considered in the Development of Any Servo Mechanism

There are several sources of difficulty that plague the designer of a servo system. Back-lash in gearing combined with static friction will limit the accuracy of a system. It may produce a vicious type of oscillation if it occurs between the motor and the sensing element. In the case of a high gain system, it may produce a high frequency oscillation of limited amplitude which has as one effect, the wearing out of the gear train. Friction will waste motor torque and degrade system performance even when it produces the above effects to a limited extent.

When the driven element can gain enough kinetic energy to break gear teeth on sudden stopping, irreversible gear trains are to be avoided as the plague. They rarely help system performance anyway when placed in the power train since they behave in an equivalent non-linear manner.

Elastic yield in the power gear train will introduce new frequency sensitive elements into the servo loop whose presence must be explicit in the form of the transfer characteristic. They rarely improve system performance.



They may be made more or less innocuous by raising their resonant frequencies well beyond the required response band of the system.

A very fine source of difficulty is the use of a servo so that it is essentially a sub-loop in a larger system. Process delays in the over-all system which results will normally tend to produce instability in this larger system. All such delays must be analysed to find their effect on the stability of the system.

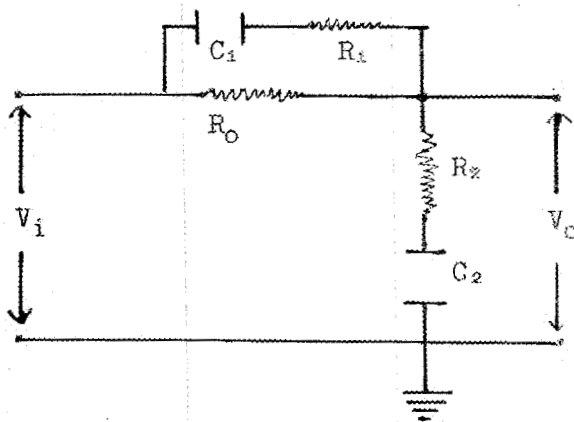
IIIId. Suggested Modifications of the Velocity Servo-Mechanism

Improving the Corrective Networks in the Amplifier

It is possible to reduce the number of stages used in the amplifier by combining the integral circuit with one of the lead circuits. The combined transfer function for these circuits isolated and cascaded is:

$$K_1 \frac{(1 + \tau_1 p)}{1 + K_1 \tau_1 p} \times \frac{1 + \tau_1 p}{1 + K_1 \tau_1 p}$$

The high frequency attenuation of the integral circuit exceeds the low frequency attenuation of the lead circuit. The circuit below has a transfer function of the type:



$$\frac{(\tau_2 p + 1)(\alpha \tau_1 p + 1)}{(\alpha \tau_1 p + 1)(\tau_2 p + 1) + \beta \tau_2 p (\tau_1 p + 1)}$$

where

$$\tau_1 = R_2 C_1$$

$$\tau_2 = R_2 C_2$$

$$\alpha = \frac{R_0 + R_1}{R_1}$$

$$\beta = \frac{R_0}{R_2}$$

The constants can be adjusted to make this function show the same functional dependence on p as does the combined characteristic above. One even has an extra variable free. This may be used to set R_0 so the impedance level is satisfactory and the condensers are of reasonable size. This is to be included in the final version of the amplifier.

The curves showing the way the pile responds to a disturbance while the servo is controlling it demonstrate that the servo is adequate at least to regulate the simulator. The following discussion will indicate a manner in which the servo performance might be improved. If the fluctuations of the pile level include components which demand continual rapid readjustments of the regulating rod, considerations of life of the mechanical elements of the system may dictate a narrowing of the band of frequencies passed by the servo. The loop transfer characteristic Y_M has been shown to approximate:

$$Y_M(p) = \left[\frac{1}{1 + .05p} \right]^2 \left[\frac{1}{1 + .005p} \right]^2 \left[\frac{1 + .05p}{1 + 1.5p} \right] \left[\frac{1 + .01p}{1 + .001p} \right]^2$$

Suppose the system is modified by making a subsidiary loop as indicated in Fig. 28. Here a subsidiary loop through the filter and 2nd differential has been included. Opening the subsidiary loop at its input to differential (2) reduces the system to the original one. To write the equations of the new system, one defines:

$$V_1 = \text{input signal} = \theta_1$$

$$\phi_0 = \text{tachometer voltage} = kp \theta_0$$

$$p\theta_0 = \text{output angular velocity at motor shaft} = \text{quantity to be controlled}$$

$$Y_A = \text{combined transfer characteristic of the voltage and power amplifier, filters in the amplifier, amplidyne and motor}$$

$$Y_F = \text{transfer characteristic of feedback filter and associated amplifier, if any}$$

$$Y_{\text{tach}} = k \text{ volts/radian per second.}$$

Then from the figure:

$$\epsilon + \phi_0 = \theta_1$$

$$\epsilon_2 + Y_F \phi_0 - \epsilon = 0$$

$$\phi_0 - kY_A \epsilon_2 = 0$$

Eliminate ϵ_2 between the last two equations and obtain

$$\frac{\phi_0}{V_1} = \frac{kY_A}{1 + kY_A Y_F}$$

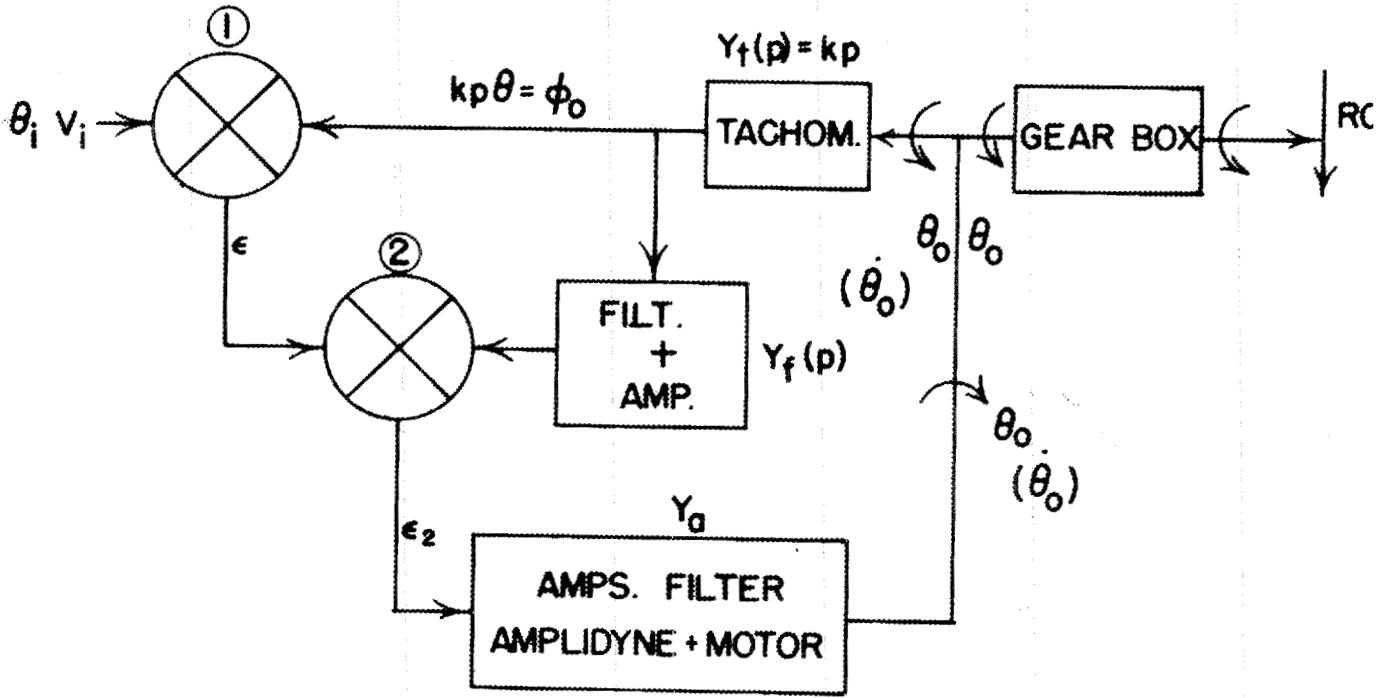


FIG. 28

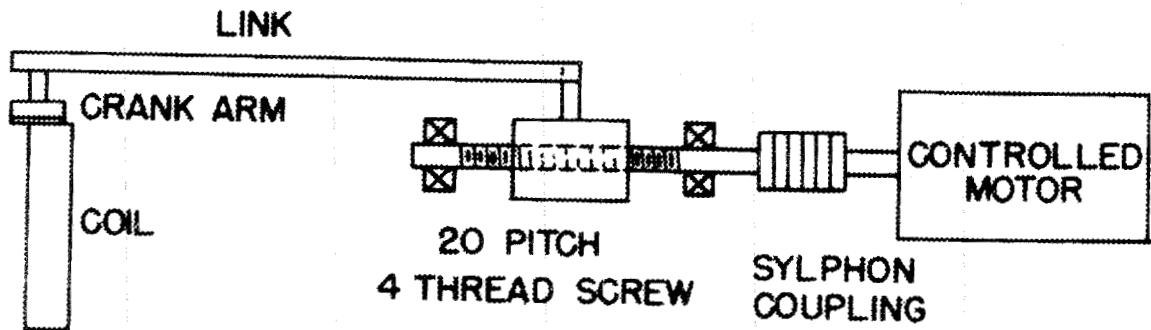


FIG. 29

In principle ϕ_o is an instantaneous measure of the velocity of the output member. The above expression is the open loop transfer characteristic of the new system in terms of the open loop transfer characteristic of the single loop system and the transfer characteristic of the feedback filter. The variable quantity in the denominator is actually the transfer characteristic of the loop associated with the second differential.

One can substitute the above expression in the first equation for the loop and obtain the over-all transfer characteristic:

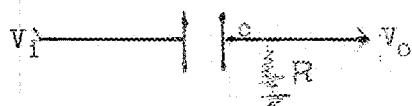
$$\frac{\phi_o}{V_i} = \frac{kY_A}{1 + kY_A + kY_A Y_F}$$

If $kY_A(1 + kY_A Y_F)^{-1}$ has no zeroes or poles in the right half-plane, one can apply the Nyquist stability criterion as readily to the 2-loop system as to the single loop system. We already know kY_A satisfies this condition. We need only study $(1 + kY_A Y_F)^{-1}$.

To study the open loop transfer characteristic it is convenient to write it:

$$\frac{1}{Y_F} \times \frac{kY_A Y_F}{1 + kY_A Y_F}$$

The latter member of the expression is most readily evaluated by the graphical methods earlier mentioned. Graphical subtraction of the log plot of Y_F from this yields the loop transfer characteristic which can then be readily converted into the closed loop function by the same graphical procedure. For example, a simple RC time delay with transfer characteristic $(1 + p\tau)^{-1}$ where $\tau = RC$, will afford extra phase margin at high frequencies to increase the speed of system response. A simple high pass filter with



transfer characteristic $p\tau(1 + p\tau)^{-1}$ in the feed-

back loop will reduce the speed of the system but afford more open loop gain at low frequency.

Reference to Fig. 30 showing the noise present in the tachometer output makes it clear that differentiating such a signal and inserting it

NOT CLASSIFIED

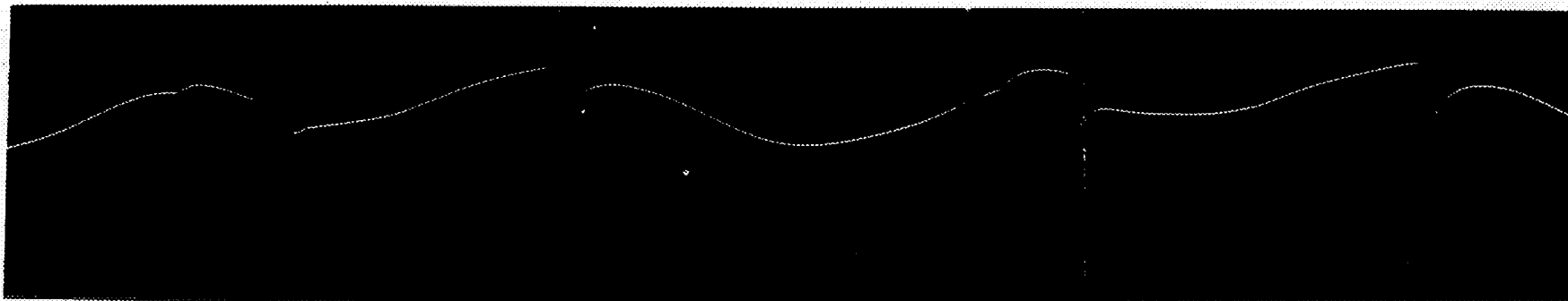


- A. D-C TACHOMETER OUTPUT - 50 VOLTS; CALIBRATION ONE VOLT PEAK TO PEAK PER MM. FILM SPEED - APPROXIMATELY 360 CM PER SECOND. APPARENT RIPPLE - APPROXIMATELY 7.5% PEAK TO PEAK.

56

FIG. 30

- B. ENLARGEMENT OF SECTION OF "A."



DT 6048

[REDACTED]

into the amplifier is not likely to produce results which are too easily predictable. To reduce these effects a tachometer, Weston Type No. 724 Special has been ordered and will be studied. It is specified to produce a good deal smaller ripple component (about 1%) in its output. As insurance, another tachometer is being studied by E.P. Epler which, taking advantage of the limited travel of the controlled element, avoids all commutator noise. This result is obtained by driving an oversize meter movement* by a mechanism of the type indicated in Fig. 29. The sylinder coupling introduces no ambiguity in the angular position of the screw with respect to the motor shaft. The screw thread is held to close tolerances and the screw is mounted in angular contact bearings which define the longitudinal position of the screw precisely. The nut is split and fitted to the screw. It is constrained against rotation. The coil rotates about a vertical axis, being driven by a radial arm whose outer end carries a bearing which is one pivot for the link which is pivoted at its other end on a precision bearing carried by the nut. The tangential error in this drive is negligible over the range of rod position encountered in normal use. Care has been taken to remove all back-lash from the drive so no spurious variations in tachometer voltage can be fed back into the system. The preliminary model of the tachometer obtains its magnetic field from an electromagnet which could be replaced by a permanent magnet field structure if the design is standardized.

IV. Performance

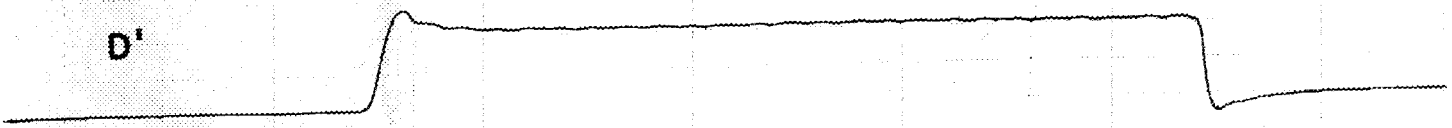
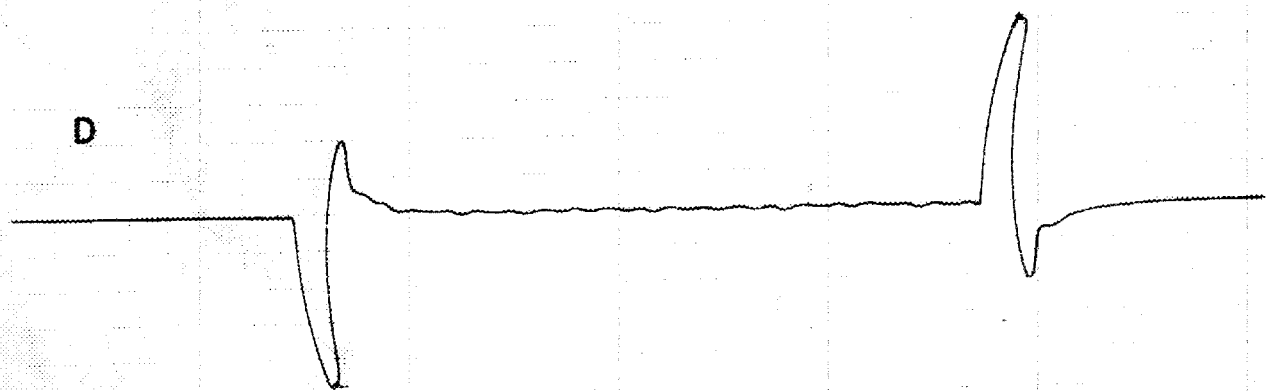
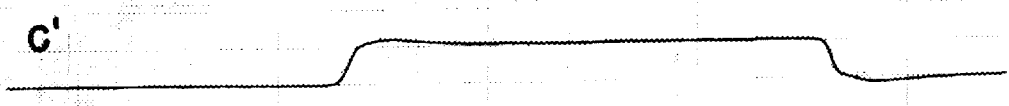
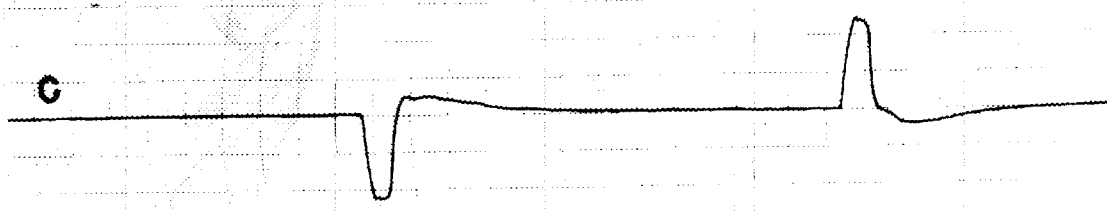
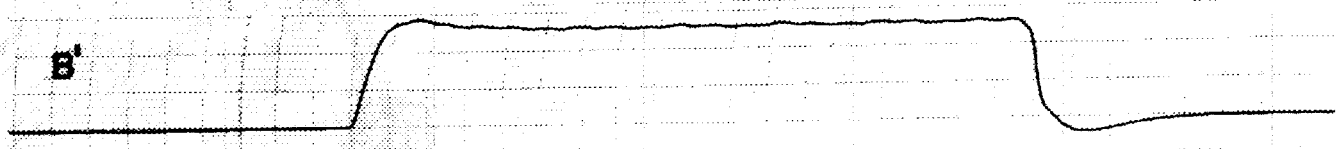
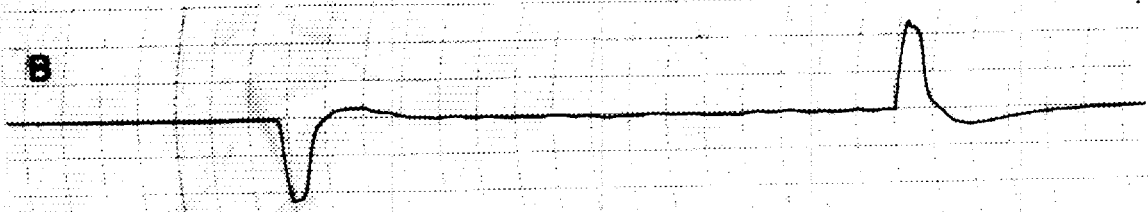
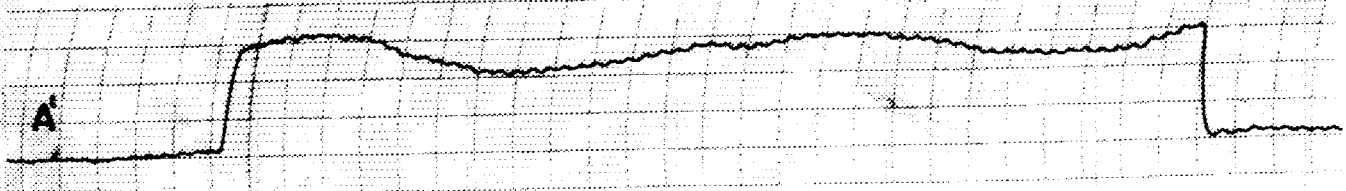
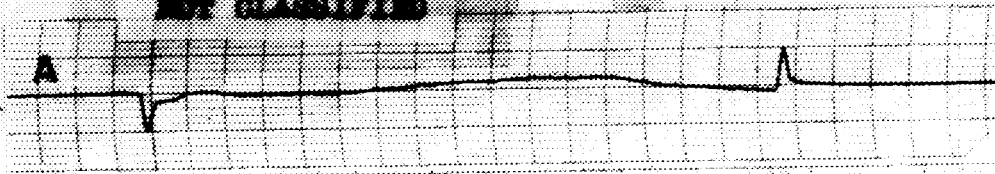
a. Notes on Performance of the Isolated Servo-Mechanism

Figures A through L show the response of the system to step inputs of different magnitudes which correspond to changes of velocity from zero to several terminal velocities and from these respective velocities to zero again. Although these transients were run with no rod driven by the gear box, they represent adequately the expected performance of the system since the reflected inertia of the rod will be small enough compared to the armature moment of inertia that the motor-amplidyne time constant will not be sensibly affected.

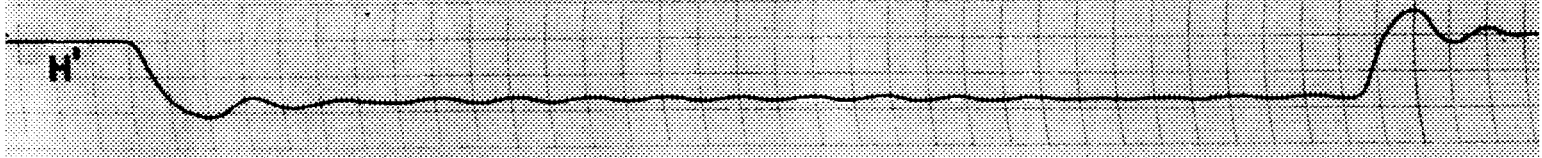
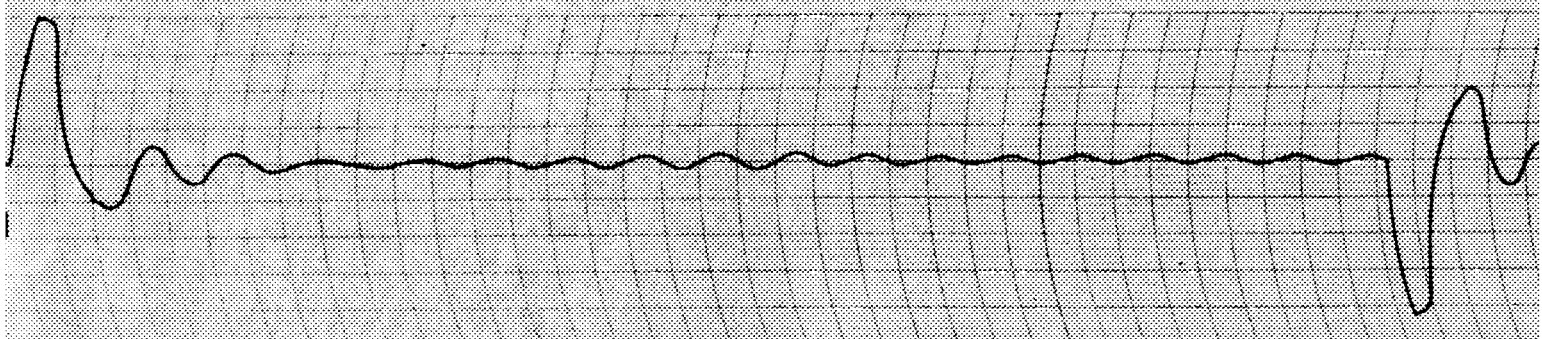
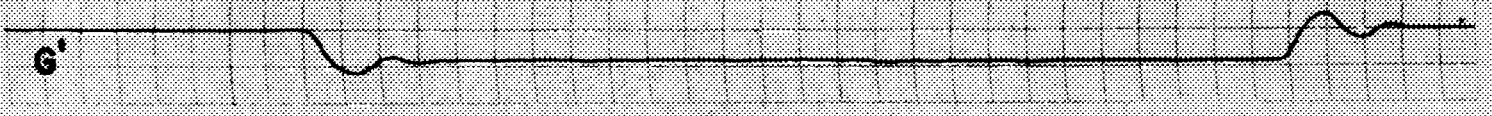
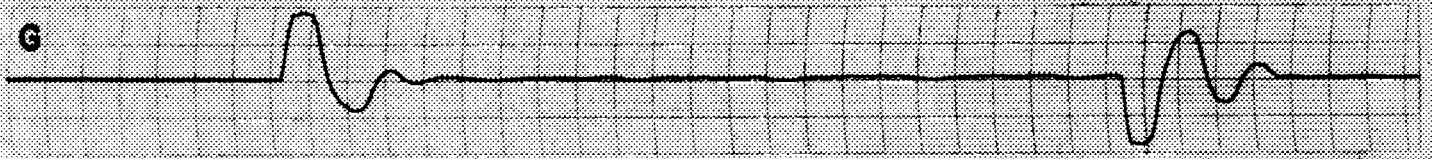
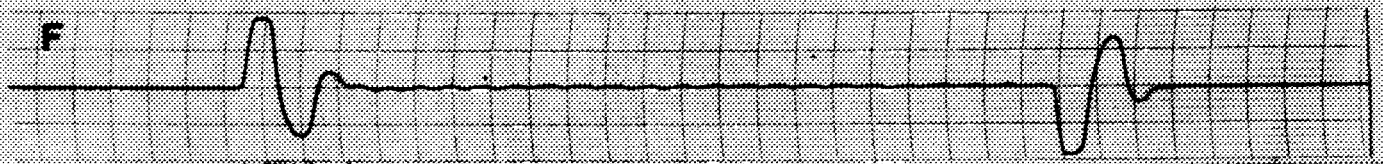
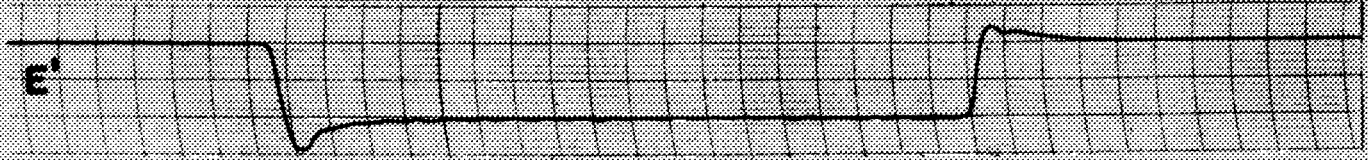
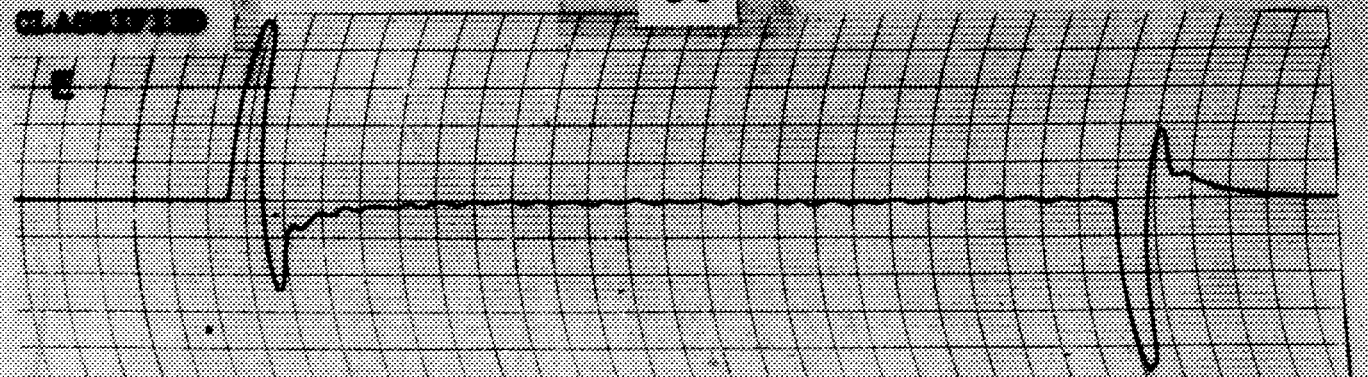
*The test model has a coil of 684 turns with a window of effective length $4\frac{1}{2}$ " long by $3\frac{5}{16}$ " wide. The coil is free to rotate through a total of approximately 120° in a radial field of about 10^4 oersteds as the rod travels 3 feet. In normal operation the full stroke of the rod is only one foot. This unit will produce at its terminals 16 volts at rated speed. The internal impedance is about 100 ohms and the signal is readily taken with respect to ground.

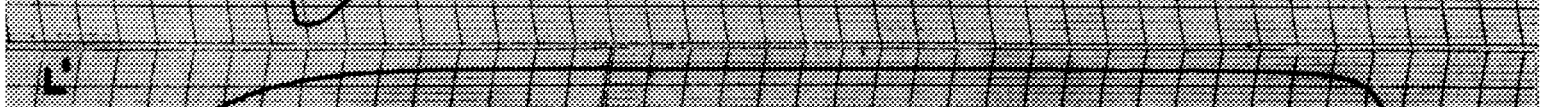
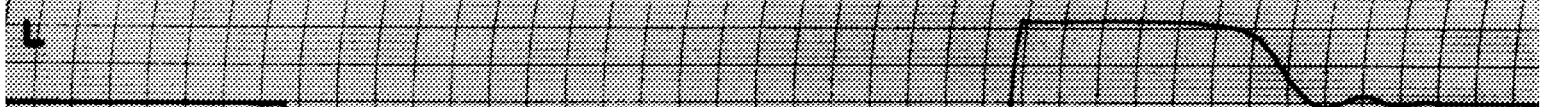
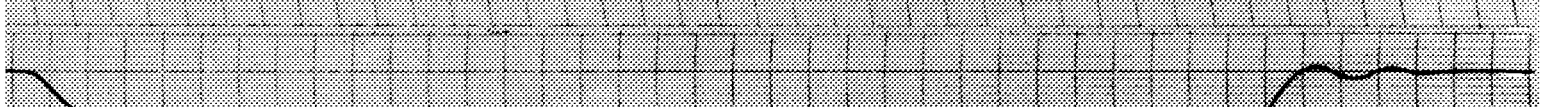
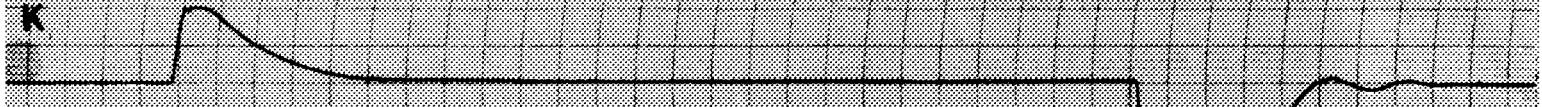
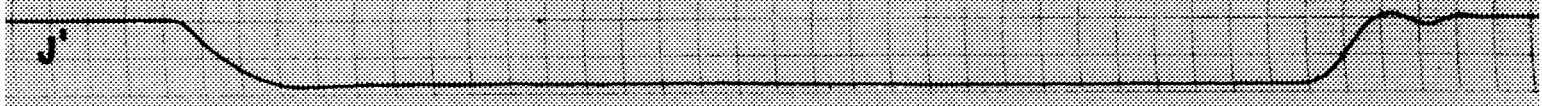
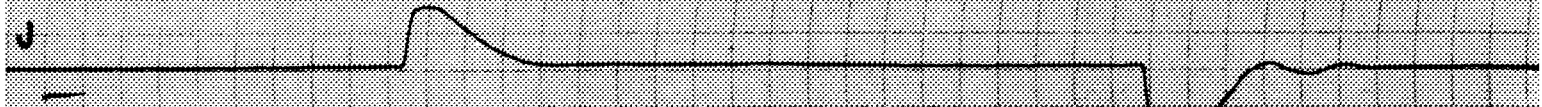
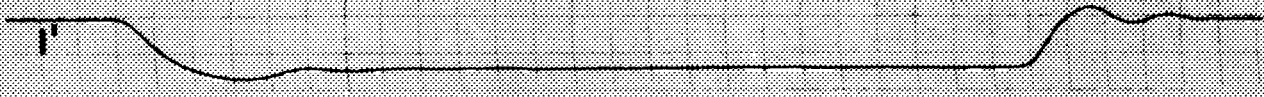
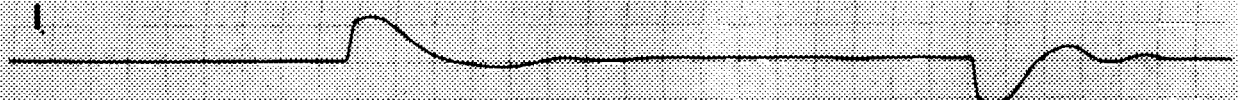
Data for Records A, A' Through L, L'
 Transient and Quasi-Steady Servo Error Signal and Output
 Chart Speed is 12.5 cm. Per Second

Record of:	Input Volts	Chart Cali. V/mm	Tachometer DC Volts (measured)
A Error/20	- 0.1	.001	
A' Output	- 0.1	.01	0.1
B Error/20	- 2.0	0.01	
B' Output	- 2.0	0.2	2.04
C Error/20	- 4.0	0.02	
C' Output	- 4.0	1.0	4.3
D Error/20	- 8.0	0.02	
D' Output	- 8.0	1.0	8.3
E Error/20	+ 8.0	0.02	
E' Output	+ 8.0	1.0	8.2
F Error/20	+ 16.0	0.1	
F' Output	+ 16.0	2.0	16.6
G Error/20	+ 32.0	0.2	
G' Output	+ 32.0	10.0	33.7
H Error/20	+ 64.0	0.2	
H' Output	+ 64.0	10.0	66
I Error/20	+100.0	1.0	
I' Output	+100.0	20.0	104
J Error/20	+136.0	1.0	
J' Output	+136.0	20.0	141
K Error/20	+173.0	1.0	
K' Output	+173.0	20.0	176
L Error/20	-208.0	1.0	
L' Output	-208.0	20.0	187



NOT CLASSIFIED





[REDACTED]

The approximate scale for the deflection of the recorder is indicated for each figure. The nominal step voltage input is recorded and the actual tachometer d.c. voltage output is indicated. All records were run at the same chart speed. The time scale is .040 sec per division. The discrepancies between the nominal values of output voltage and those derived from the recorded values are to be resolved in favor of the former since the calibration is only approximate. Since the error signal and the output voltage were recorded independently, the time base zeroes of a pair of curves for the same input signal are not related.

The measured output constant of the tachometer used in these runs is 8.8 volts per 100 rpm. In principle, the maximum value of the error signal record is a measure of the step input amplitude which reduces toward zero as the servo comes into operation. The part of the record at which the output record is essentially noise-free corresponds to the quiescent condition of the system.

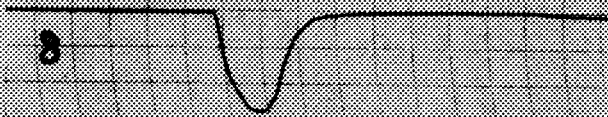
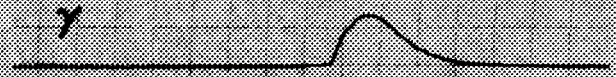
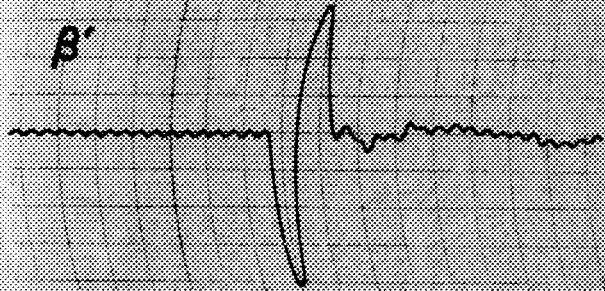
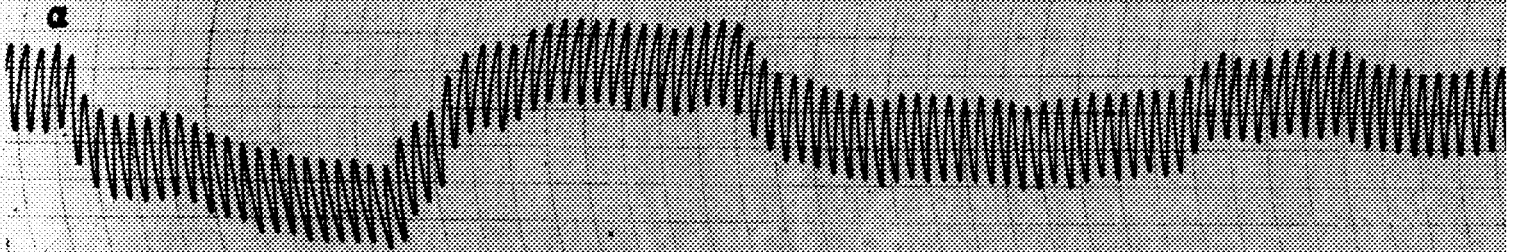
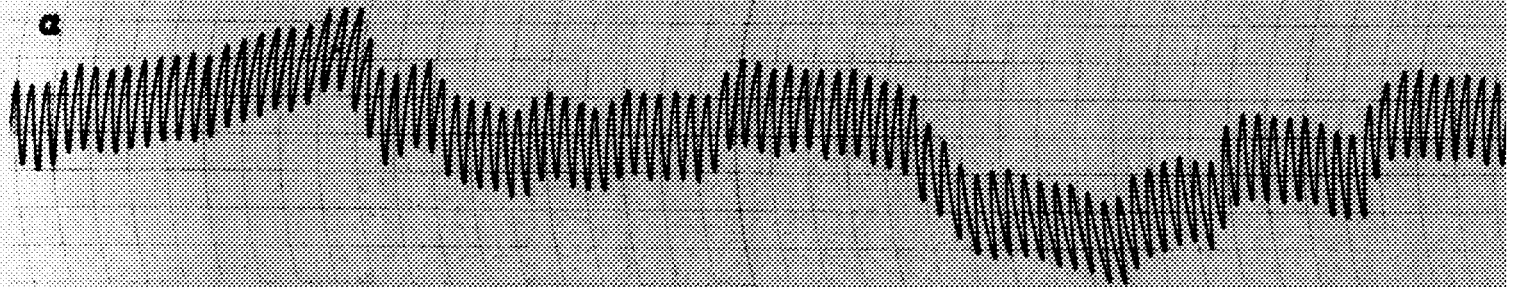
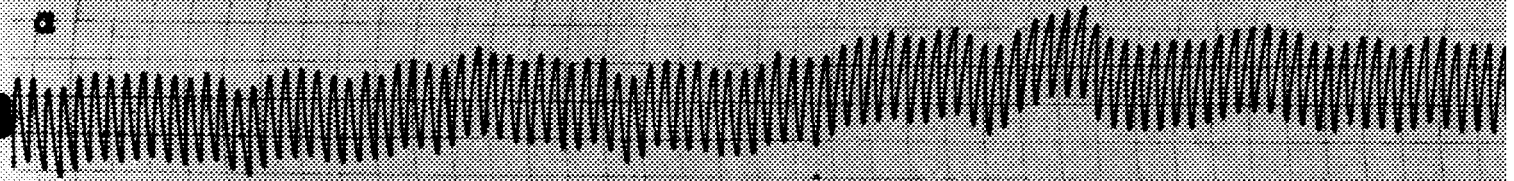
Figures D and E show the response of the system to a demand for equal step changes in velocity in opposite directions. The system is thus reasonably indifferent to the sense of the demand signal.

Corresponding to a step change of 200 rpm or more, as Figures F and those following show, the system is damped less adequately, due to saturation. Fig. I corresponds to a demand velocity step of 1200 rpm (which is the rated motor speed). The speed of response is down appreciably from its value for small signals, but is still fairly respectable. By the time that the demand speed step is 2360 rpm, the poor amplidyne has given up, as witness the very large error signal which persists in the system. The system will follow reasonably well down to motor speeds of about 1 rpm.

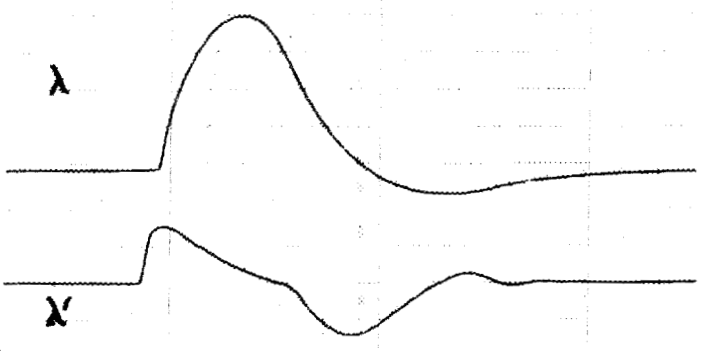
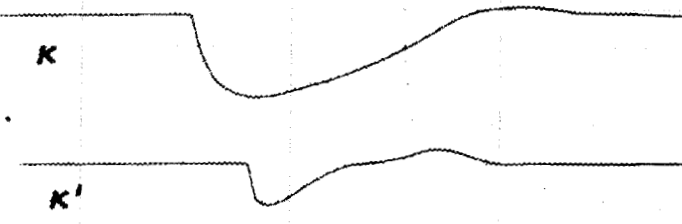
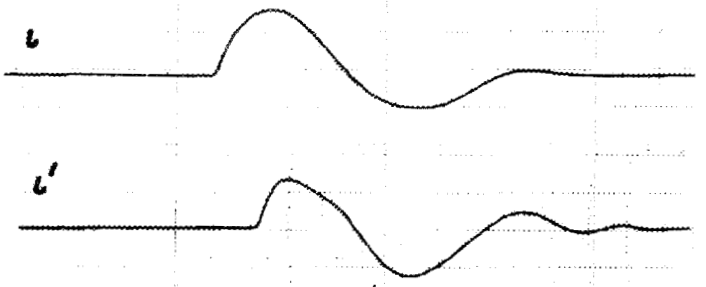
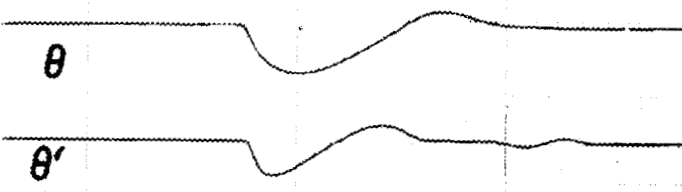
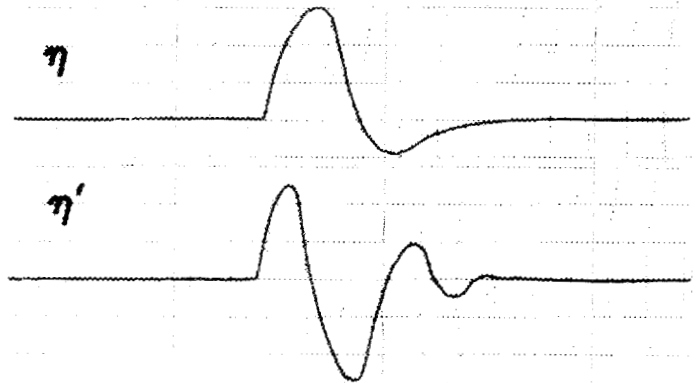
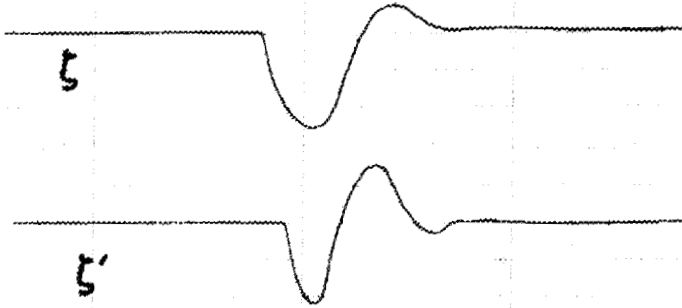
The amplifier gain is linear as a function of signal input up to signal amplitudes which badly saturate the amplidyne. On closed loop the sum of the output plate currents drop as the signal increases, due to noise from the tachometer. Corresponding to Fig. H, the sum of the plate currents has dropped from about 72 ma to about 36 ma.

IVb. The Servo System as a Regulator of the Simulator

The following set of curves, α through λ , show some of the features of the performance of the servo mechanism controlling the pile simulator. The simulated rod changes ΔK_{eff} by .6% in a stroke of 12" which is the interval of



NOT CLASSIFIED



motion in which the regulating rod acts independently of the shims in normal operation. The rod would move at a maximum terminal rate in Δk_{eff} of 2.9%/sec under extreme provocation although the rated motor speed would produce a rate of 1.6%/sec in Δk_{eff} . The gear ratio in the rod drive will be modified to make available about 2.5% Δk_{eff} /sec at about 1500 rpm.

All these traces were taken at a chart speed such that each unit on the time base represents .040 seconds. The 60 cycle ripple amounts to about 28 millivolts—peak to peak and comes from the simulator. It is not particularly significant as the servo mechanism response is down appreciably at this frequency and in addition, the condition of the gear box and the Δk_{eff} potentiometer drive at the time these data were taken were such that practically no steady state 60 cps correction would be afforded.

Traces a are records of the quantity $.75(n-N_0)$ where n is the instantaneous neutron level and N_0 the desired level (with the simulator operating at 50 volts output). The chart scale is 2 mv/mm. Thus the worst departure from the average runs about .07% of level. In the periods of best operation represented by the first curve of Fig. a the departures from desired level run about 3×10^{-4} of the desired level.

The remainder of the figures are paired. The upper figure presents the departure (multiplied by .75) of the simulator level from that desired (50v). The lower shows the error signal in the servo amplifier. Conditions for which these curves were obtained are tabulated.

Figures	Step in $\Delta k\%$	Voltage Scales (volts/mm)	
		$.75(n-N_0)$	Error/20
β & β'	-.012	.1	.02
γ & γ'	+.012	.1	.02
δ & δ'	-.025	.1	.02
ϵ & ϵ'	+.025	.1	.02
ζ & ζ'	-.05	.2	.2
η & η'	+.05	.2	.2
θ & θ'	-.13	1.	1.
i & i'	+.13	1.	1.
κ & κ'	-.23	1.	1.
λ & λ'	+.23	1.	1.

The difference between the response to positive and negative steps is primarily due to the difference in transient response of the pile; some very slight difference, showing up mainly in the overshoot, is due to the weight of the rod reacting on the servo-motor.

[REDACTED]

These represent the average responses to the above quoted step changes in reactivity. They were all obtained with the rod starting from the position with the tip at the pile's mid-height. If the rod were positioned so it had more than the half-stroke available, it could handle somewhat larger steps in Δk_{eff} without activating a shim rod and conversely smaller if there were less than the half stroke available.

Va. Experimental Methods

The steady-state study of the servo system requires a low impedance source of a.c. of controllable amplitude which can be adjusted to any frequency from the neighborhood of zero to at least 100 cycles a second. In the measurements made here a Hewlett-Packard type 202B low frequency oscillator was used. It covers the range from .5 to 1000 cps, and will supply 10V across a 1K load with less than 1% distortion from 1 to 1000 cps.

It is convenient to use a recording instrument which presents a high impedance to the system. The recorder need only be reasonably flat in response from 0 to about 100 cps. A Brush type BL201 pen writer with a Brush BL913 amplifier to drive it has been used in taking the data.

At each point the Hewlett-Packard oscillator is set at the desired frequency and, for open-loop transfer characteristic determinations, its output is applied as the amplifier input signal. The input signal is recorded. The tachometer output voltage is also recorded. In principle the tachometer voltage is a measure of the instantaneous rate of the motor driving the regulating rod. There are difficulties. There is hash from the commutator segments. There is ripple in the output of the tachometer while being driven at a constant rate due to the finite number of armature slots. Also, the tachometer armature will in general be magnetically unbalanced. Out of this mess the amplitude of the component with frequency equal to that applied by the Hewlett-Packard oscillator must be extracted and measured. At each frequency several runs must be made with different "error" amplitudes to make certain that the loop as a whole is operating in the equivalent linear part of its range. In the low frequency range Coulomb friction is an important contributor to non-linear behavior. At the high frequency end of the range the most important source of non-linearity is saturation of the amplidyne. In any case, any extra care expended in making sure of linear behavior of the system at each experimental point is well worth while; it will save much grief.

██████████

It will be noted that polynomials have been fitted to the observed transfer amplitudes, and the corresponding phase characteristics were then calculated. If a great deal of man-power is available for a system which is to go into production it might be worth-while to make detailed studies of the exact transfer characteristic, both in amplitude and phase, experimentally and theoretically, to determine the effect of expected manufacturing tolerances. Here the plan has been to describe the observed attenuation-frequency characteristic in the analytic expressions and see whether they suffice to explain the phase shift demonstrated by the maximum attainable frequency of feedback cut-off with system stability. This number-like approach is justified in this case as a net time saver in view of the difficulties in a direct determination of the phase-frequency characteristic.

One must bear in mind the large range over which the ratio of tachometer voltage to error voltage varies and that all the hash in the tachometer signal appears in the error signal when the loop is closed. A little consideration will satisfy one that experimental determination of phase of the fundamental component of the output with respect to the error signal is difficult if not utterly impossible in the neighborhood of feedback cut-off. In this region the fundamental component falls to a fairly small value, and the pursuit of the phase relations to higher frequencies is increasingly thankless since a small error in the measured quantities can completely mask the phase relations sought. The over-all reliability of a measurement of Y_m at a point frequency is about 2 db.

The system response to step inputs was determined over a wide range of step inputs and the final system gain set by adjusting for a reasonably smooth and rapid approach to demand velocity. Figures A through L' show the results of such measurements. The final test of the system is, of course, the quality of its control of pile level in the steady state and under transient conditions. The best that can be done presently in this direction is to study the pile simulator when controlled by the servo system. Figures a through λ' show records of the deviation of pile simulator level from desired level when regulated by the servo system.

Vb. Elementary Theory of the Amplidyne

Fig. 31 will indicate the essential features of the amplidyne's operation; neglecting among other things ferro-magnetic saturation. The most notable features, on first inspection, of an amplidyne are the small

NOT CLASSIFIED

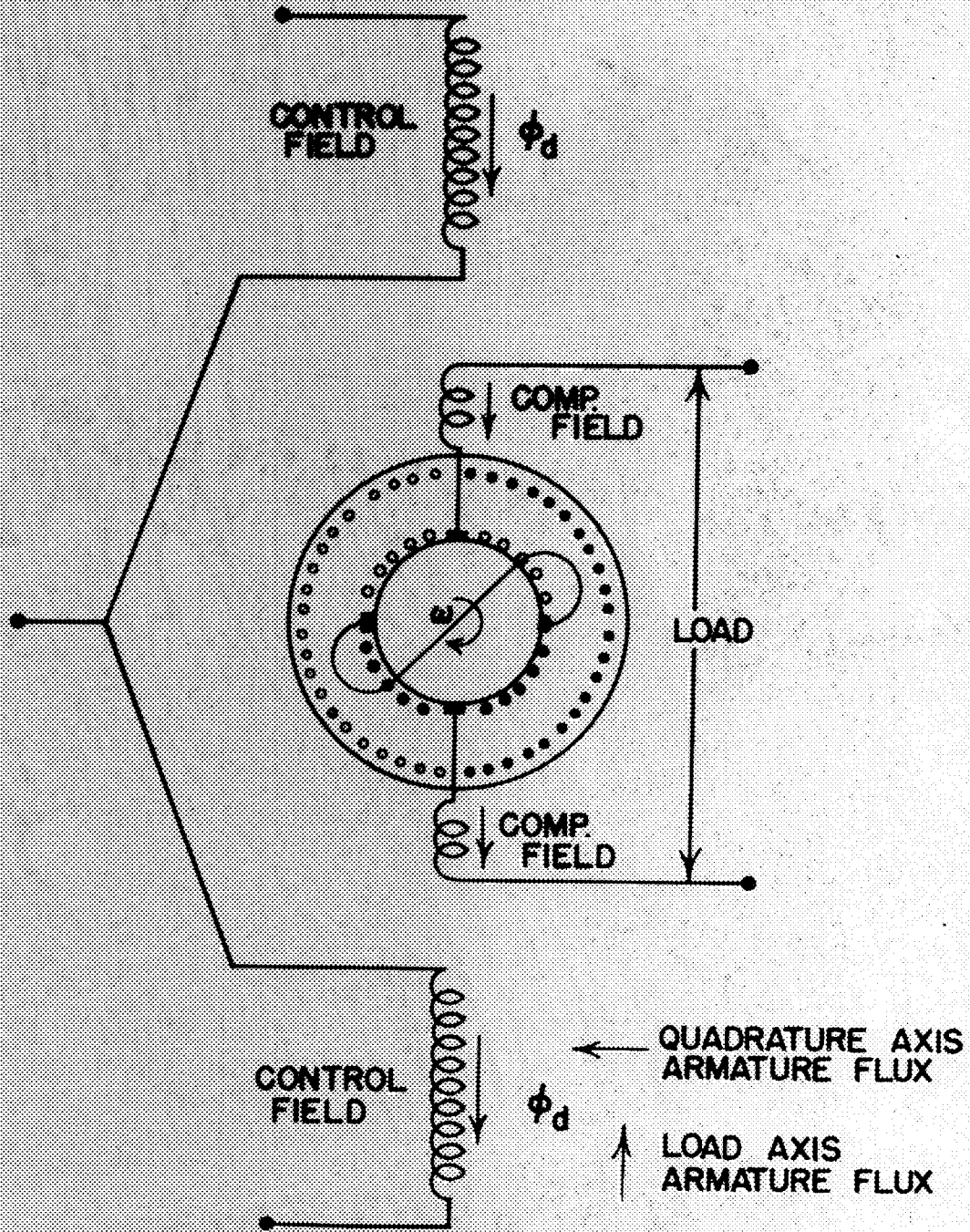


FIG. 31

excitation supplied to the control field and the short-circuit applied to the armature. The inner ring of conductors represents the current distribution in the armature due to load current. Actually the conductors are not separated as indicated here and the resultant of the two sets of currents flows in one set of armature conductors.

Suppose the control field is excited from an external source. The armature is driven at a constant rate by the associated drive motor. The short circuit in the armature results in a large circulating current which, since the short circuit brushes are fixed in space, produces the usual cross-magnetizing field of armature reaction. The effect is equivalent to a coil wound in the quadrature axis of the machine. The resultant flux $\phi_{Q.A.}$ is a direct function of the control field excitation. $\phi_{Q.A.}$ produces a current distribution, when the load circuit is completed, as shown in the sketch. The flux due to the load current is again at right angles to the field causing it. The sense of the m.m.f. is necessarily opposite to that of the control field. To reduce the malignant effects of this armature reaction, windings are placed in the stator structure so disposed that they produce an m.m.f. approximately equal to but opposing the load current m.m.f. They are connected in series with the armature so the compensation is more or less independent of load current. The charge for this improvement is an increase in both resistance and inductance of the armature circuit, the latter more than the former so the armature time constant is increased.

Assuming perfect compensation of the load current:

$$\phi_{D.A.} = K_1 \times I_f \text{ direct axis flux due to control field.}$$

No delay here except due to hysteresis (neglected).

I_f = current in control field

$$E_{Q.A.} = K_2 S \phi_{D.A.} \quad E_{Q.A.} = \text{quadrature axis generated voltage}$$

$$E_{Q.A.} = K_1 K_2 S I_f \quad S = \text{speed of machine}$$

Since the armature has resistance R and inductance L , the equation for the quadrature axis current is:

$$E_{Q.A.} = R I_{Q.A.} + L \frac{dI_{Q.A.}}{dt}$$

$$I_{Q.A.} = \frac{E_{Q.A.}}{R + pL} = \frac{\frac{K_1 K_2 S}{R}}{1 + p \frac{L}{R}} I_f$$

Thus there is a time constant L/R associated with growth of $I_{Q.A.}$ after a change in I_f . As in the control field, the only delay between $I_{Q.A.}$ and $\phi_{Q.A.}$ is due to hysteresis. We neglect it

$$\phi_{Q.A.} = K_3 I_{Q.A.} = \frac{\frac{K_1 K_2 K_3}{R}}{1 + pL/R} I_f$$

Apply the usual generator equation to this to find the generated voltage in the direct axis.

$$E_{D.A.} = K_4 S \phi_{Q.A.}$$

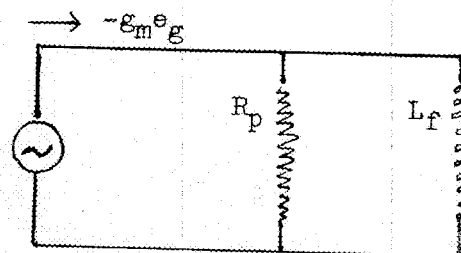
Thus

$$E_{D.A.} = \frac{K_1 K_2 K_3 K_4 S^2}{R} \frac{I_f}{1 + p L/R}$$

Thus there is a single time delay, associated with the quadrature axis, between the application of a current to the control field and the development of a voltage in the direct axis of the machine.

In machines of this type the control field inductance is of the order of 100 henries and its resistance is of the order of 1000 ohms. The control field is driven by pentodes for which $1K \ll R_p$. Thus the equivalent circuit is that shown. Then the current variation in the control field is given by

$$I_f = \frac{\varepsilon_m e_g}{1 + p \frac{L_f}{R_p}}$$



Evidently the use of a pentode reduces the time constant between the grid of the power tube and the growth of field current to something between 10^{-3} and 10^{-4} sec, much less than the value of $T_{Q.A.}$ which runs from 1/5 to approximately 1/30 sec. for most amplidynes.

The above analysis assumed perfect brush settings, no component of $\phi_{D.A.}$ in the quadrature axis and vice versa. Due to the high gain of the machine, it is very sensitive to the brush setting. Shifting the brushes off electrical center in the direction of rotation increases the gain and spoils the regulation. If the brushes are shifted too far the other way, the machine becomes regenerative and will hunt steadily. The regulation curves of the machine change slope with increasing I_f due to saturation of the pole salients. Brushes are made narrow to reduce their effective shift with wear.

Among the effects neglected above are cross talk between axes, speed regulation of the drive motor and time delays in the control system. This schematic description does, however, bring out important features of the machine.

There is another time delay which is important to consider.

R_a = resistance of amplidyne armature

R_m = resistance of motor armature circuit

$p\theta$ = motor speed

Neglect inductance of armature circuits of motor and amplidyne. Then

$$E_{D.A.} = K_v p\theta + (R_A + R_m) I_{D.A.} \quad K_T = \text{motor torque constant}$$

$$K_T I_{D.A.} = F p\theta + J p^2 \theta \quad \text{Assuming pure viscous friction with coefficient } F \\ J = \text{inertia of motor and load}$$

$$E_{D.A.} = K_v p\theta + (R_A + R_m) \left(\frac{F}{K_T} p\theta + \frac{J}{K_T} p^2 \theta \right)$$

$$= p\theta \left[K_v + \frac{F(R_A + R_m)}{K_T} + p \frac{(R_A + R_m)J}{K_T} \right]$$

Then:

$$p\theta = \frac{\frac{K_T}{K_T K_v + F(R_A + R_m)} E_{D.A.}}{1 + p \frac{J(R_A + R_m)}{K_T K_v + F(R_A + R_m)}} = \frac{K E_{D.A.}}{1 + p T_{M.A.}}$$

where:

$$K = \left[\frac{K_T}{K_T K_V + F(R_A + R_m)} \right]$$

$$T_{M.A.} = \left[\frac{J(R_A + R_m)}{K_T K_V + F(R_A + R_m)} \right]$$

K_T = motor torque const.

K_V = generated voltage const. of motor

$T_{M.A.}$ - cannot be neglected

Vc. Some Mathematical Results

Since, as shown in Section II, a servo mechanism behaves like a low pass filter, the multitude of results which have been obtained in the study of filters offers a rich field of recipes which may be applied to the study of servo mechanisms. Some of these results will be presented rather than demonstrated in this section.

The mathematical description of an N mesh linear filter is usually given as a set of integro-differential equations. These can be reduced to an equation of the type below in the output voltage E_o and the input voltage E_i .

$$L \cdot a_n \frac{d^n E_o}{dt^n} + a_{n-1} \frac{d^{n-1} E_o}{dt^{n-1}} + \dots + a_0 E_o = b_m \frac{d^m E_i}{dt^m} + b_{m-1} \frac{d^{m-1} E_i}{dt^{m-1}} + \dots + b_0 E_i$$

The a's and b's are constants and $m, n \leq 2N$ where N equals the number of independent loops including one through the source but none through the output circuit.

$E_o(t)$ depends on $E_i(t)$ and the constants in the general solution of the associated homogeneous equation. The constants of the solution are determined by the initial conditions. When the filter starts from rest as the input is initially applied, the output is termed the normal response to the specified input.

The filter output when $E_i(t)$ has become constant is the sum of $E_o = b_o/a_o E_i$ and a suitable solution of the associated homogeneous equation (transient response to the earlier history of the filter). The general solution of the associated homogeneous equation is a linear combination of the normal modes of the filter of the form:

II.
$$h_i(t) = t^l e^{p_i t}$$

l is a real constant and p_i is a general complex constant. The general form of solution is:

III.
$$E_o = c_1 h_1(t) + c_2 h_2(t) + \dots + c_n h_n(t)$$

the c_i are adjusted to the initial conditions.

If p_i is real,

$$h_i(t) = t^l e^{a_i t} \quad a_i \text{ is real.}$$

If p_i is complex, its conjugate also yields a solution of the equation and the normal mode solutions appear in pairs yielding real transient solutions of form $t^k e^{a_i t} \begin{cases} \cos \omega_1 t \\ \sin \omega_1 t \end{cases}$

If p_i has a negative real part the normal mode solution approaches zero; otherwise, the solution increases or may increase indefinitely. The filter is unstable.

As here defined, a linear filter has lumped elements constant in time and has a normal response, which, in the mathematical sense, is a linear function of the input voltage and depends only on the past history of the filter.

The Weighting Function

The normal response of a linear filter to a unit impulse at $t = 0$ is represented as $W(t)$ which is called the weighting function for reasons to be seen later. $W(t)$ may be discontinuous or may include a term $c\delta(t)$.

The normal response of a linear lumped constant filter to an impulse can be determined from the differential equation 1. After the impulse, $E_I = 0$ so $W(t)$ must be a solution of the associated homogeneous differential equation, a linear combination of normal modes of the filter. At the moment of the impulse $W(t)$ may be discontinuous and include a $\delta(t)$ if the filter has a term in the output proportional to the input.

Experimentally it is sometimes practicable to obtain the weighting function by recording the response of the filter to a suddenly applied and removed input which does not overload the system. When this is attempted, one must have $\Delta t \ll$ any natural period of the filter:

$$\Delta t \frac{dW(t)}{dt} \ll W(t)$$

The normal response of a filter to a bounded well behaved input $E_I(t)$ can be expressed in terms of its response to a unit impulse input.

$$IV. \quad E_O(t) = \int_{0^-}^t d\tau E_I(t - \tau) W(\tau)$$

Here is the normal response to an arbitrary input as an integral over past values of the input, each past value weighted by the filter response to a unit impulse.

The weighting function represents the "memory" of the filter, the extent to which the distant past affects the filter output. The filter output reproduces well inputs varying little within the memory and smoothes out changes that take much less time than the filter memory. The filter response to a sudden change comes only after a lag determined by the width of the weighting function.

The step function is defined:

$$\begin{aligned} S(t) &= 0 & t < 0 \\ S(t) &= 1 & t \geq 0 \end{aligned}$$

Normal response to unit step:

$$S(t) = \int_{0^-}^t d\tau W(\tau)$$

As the unit step is the integral of the unit impulse, so the response to a unit step is the integral of the response to a unit impulse function. The weighting function can in principle be determined experimentally as the derivative of the response to a unit step input.

In the case $E_I(t)$ and $W(t)$ are both well behaved functions with $E_I(t)$ jumping from 0 to $E_I(0)$ at $t = 0$, integration of equation IV yields:

$$E_O(t) = E_I(0) S(t) + \int_0^{t+} dt_1 E_I'(t_1) S(t - t_1)$$

the prime represents differentiation with respect to t_1 . Here we have represented the output as a sum of responses to step inputs into which the arbitrary input can be resolved, a finite step $E_I(0)$ at $t = 0$ and a continuous distribution of infinitesimal steps aggregating $E_I'(t_i)\Delta t_i$ in the interval Δt_i at t_i .

So far there has been no distinction between stable and unstable filters. This procedure has been possible because we have considered input functions differing from zero only for some finite time. A stable filter is one which produces a finite output for every bounded input. An unstable filter will produce an unbounded output for some particular bounded input.

A linear filter is stable if and only if $\int_{0^-}^{\infty} dt |W(t)|$ is finite.

The relation of this to the earlier discussion is that the weighting function of a linear filter is a linear combination of its normal mode functions

$$W(t) = c_0\delta(t) + c_1h_1(t) + c_2h_2(t) + \dots + c_n h_n(t) \quad ;$$

the h 's have been given above. Certainly $\int_0^{\infty} |h_i(t)| dt$ does not converge for any h_i for which $\alpha_i \geq 0$. Thus $\int_{0^-}^{\infty} |W(t)| dt$ will converge if and only if the

weighting function includes no normal mode functions with $\alpha_i \geq 0$. If all the α_i are negative, the filter stability is assured. The filter may be stable even when there are undamped normal modes provided they do not appear in the weighting function, i.e., they are not excited by an impulse input. As any input can be expressed in terms of impulse inputs, this means no undamped modes can be excited by any input. Thus convergence of $\int_{0^-}^{\infty} |W(t)| dt$ offers a means

of determining what normal modes of filter can be excited. We have equation IV for a bounded input $E_I(t)$ vanishing for $t < 0$. If E_I does not vanish for $t < 0$, one must extend the upper limit of integration, and if E_I began in the indefinitely distant past,

$$V. \quad E_O(t) = \int_{0^-}^{\infty} E_I(t - \tau) W(\tau) d\tau \quad .$$

For a stable filter this converges for any bounded $E_I(t)$. The integral need not converge for an unstable filter. Accordingly one can apply equation V only to stable filters and one can apply IV in general and for unstable filters in particular.

The Frequency Response Function. This is a quantity which characterizes the response of any stable filter to a pure sinusoid input.

Take as the sinusoid input to a stable filter

$$E_I(t) = Ae^{j\omega t} \quad \text{Then by equation V}$$

$$\begin{aligned} E_O(t) &= A \int_{0^-}^{\infty} d\tau e^{j\omega(t-\tau)} W(\tau) \\ &= Ae^{j\omega t} \int_{0^-}^{\infty} W(\tau) e^{-j\omega\tau} d\tau \end{aligned}$$

where $W(\tau)$ is the filter weighting function.

Define:

$$Y(j\omega) = \int_{0^-}^{\infty} W(\tau) e^{-j\omega\tau} d\tau$$

Then

$$E_O(t) = AY(j\omega)e^{j\omega t}$$

$Y(j\omega)$ does not converge for unstable filters. As a function of angular frequency $Y(j\omega)$ is called the frequency response function. It gives the amplitude ratio and phase of the output referred to the input sinusoid for a stable filter. This quantity is readily available experimentally by observations on the system in the steady state.

$$\text{If one sets } \begin{cases} E_I = e^{j\omega t} \\ E_O = Y(j\omega)e^{j\omega t} \end{cases}$$

into equation I and carries out the differentiations, he obtains:

VI.

$$Y(j\omega) = \frac{b_m(j\omega)^m + b_{m-1}(j\omega)^{m-1} + \dots + b_0}{a_n(j\omega)^n + a_{n-1}(j\omega)^{n-1} + \dots + a_0}$$

the ratio of 2 polynomials in $(j\omega)$ with coefficients that appear in the differential equation.

Since $W(\tau) = 0, \tau < 0$, one may rewrite the definition

VII.
$$Y(j\omega) = \int_{-\infty}^{\infty} d\tau e^{-j\omega\tau} W(\tau)$$

The frequency response of a stable filter is the Fourier transform of the weighting function. The integral in VII does not exist for unstable filters. The relation inverse to VII is

$$W(t) = \frac{1}{2\pi} \int_{-\infty}^{\infty} d\omega Y(j\omega) e^{j\omega t}$$

which makes possible an evaluation of $W(t)$ for a stable filter from a knowledge of $Y(j\omega)$.

The Fourier transform methods here indicated are limited in application since many functions lack Fourier transforms, e.g., the weighting function of an unstable filter, the sinusoid input, the step function, the increasing exponential.

The transfer function of a filter is the Laplace transform of its weighting function

$$Y(p) = L[W(t)] = \int_{0^-}^{\infty} W(t) e^{-pt} dt$$

The normal response of a linear filter to an input $E_I(t)$ can be written

$$E_O(t) = \int_{0^-}^{\infty} E_I(t - \tau) W(\tau) d\tau,$$

the convolution of the input and the weighting function. Thus, when the Laplace transforms exist:

$$L[E_O(t)] = Y(p) L[E_I(t)].$$

The transfer function of a filter is the ratio of the Laplace transform of any normal response and the corresponding input, a generalization of the frequency response function defined for unstable as well as stable filters and defined for general complex values of p and not only pure imaginary ones. When the frequency response function exists it can be obtained from the transfer function by replacing p by $j\omega$. The values of the frequency response function are the values of the transfer function on the imaginary axis in the p plane.

$$\text{One obtains } Y(p) = \frac{b_m p^m + b_{m-1} p^{m-1} + \dots + b_0}{a_n p^n + a_{n-1} p^{n-1} + \dots + a_0}$$

on setting up equation I and equating Laplace transforms of the two sides and setting $L[E_O(t)] = Y(p) L[E_I(t)]$.

In many problems one can deal with transfer functions and Laplace transforms of inputs and outputs exclusively, except in the final interpretation of the transform into functions of time. This reduces to a formally simpler treatment than the use of the differential equations of the system. This type of manipulation makes it simple to prove that the transfer function of 2 filters in series is the product of their individual transfer functions.

The transfer function is more generally useful in filter discussions than the frequency response function, partly because it is defined for a wider class of filters. In the case of a lumped constant filter the transfer function is rational in p with coefficients from the governing differential equation. If the numerator is of higher degree (m) than the denominator (n), the resolution into partial fractions yields terms in positive powers of p and the filter output will contain terms in derivatives of the input up to order one less than the maximum positive power of p in this resolution. Thus $W(t)$ includes derivatives of the δ -function input. Thus $\int_0^{\infty} |W(\tau)| d\tau$ does not con-

verge and the filter is unstable. This cannot happen for passive lumped constant filters, i.e., $m \leq n$ for such filters.

In case $Y(p)$ has a denominator of degree equal to or greater than that of numerator, the weighting function will include an undamped normal mode only if the resolution of $Y(p)$ into partial fractions yields a p_i , with a non-negative real part. In such case a filter may still be stable (by chance) if the factor $(p - p_i)^{n_i}$ in the denominator is canceled by an equal factor in

the numerator of $Y(p)$. A small change in the b 's, (i.e., filter constants) will ruin the stability, so don't try to use this result.

No p 's with non-negative real parts appear in the resolution of $Y(p)$ into partial fractions if and only if $Y(p)$ has no poles outside the left half plane. More generally, if $Y(p)$ is analytic in the right half plane and on the imaginary axis, the filter is stable. This does not settle the case where there are singularities other than poles on the imaginary axis. This criterion is adequate for most practical cases since filters with lumped elements have transfer functions rational and analytic except for poles.

System with Feedback

A servo system is a feedback system in which the actual output is compared with the input (i.e., desired output) and a function of the difference (error) activates the driving element. Fig. 32 shows the essential connections. The error is given by

$$(A) \quad \epsilon(t) = \theta_I(t) - \theta_O(t),$$

and controls the system through an amplifier and motor included in the box $Y(p)$ which, for a linear system, describes the system performance. In terms of Laplace transforms

$$(B) \quad \theta_O(p) = Y(p) \epsilon(p)$$

$Y(p)$ is the feedback transfer function describing the loop transmission from output of the "differential" back through the system output and into the "differential" again.

The system performance is described by an over-all transfer function $Y_O(p)$:

$$(C) \quad \theta_O(p) = Y_O(p) \theta_I(p)$$

from (A)

$$(D) \quad \epsilon(p) = \theta_I(p) - \theta_O(p)$$

from (B), (C) and (D)

$$(E) \quad Y_O(p) = Y(p) / (1 + Y(p))$$

This is one of the fundamental equations of the theory. It is valid for any system for which equation B is valid but is not valid when the servo output undergoes further filtering in the feedback loop, e.g., see Fig. 33.

NOT CLASSIFIED

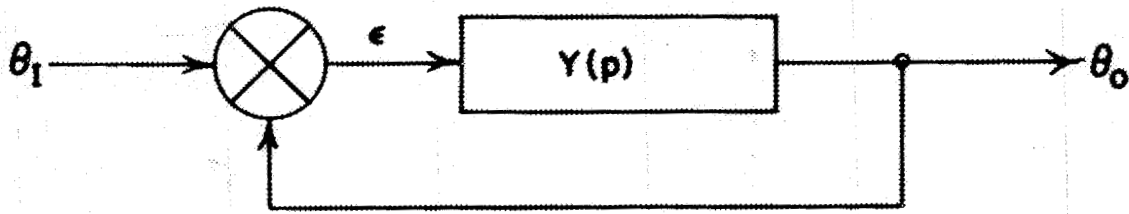


FIG. 32

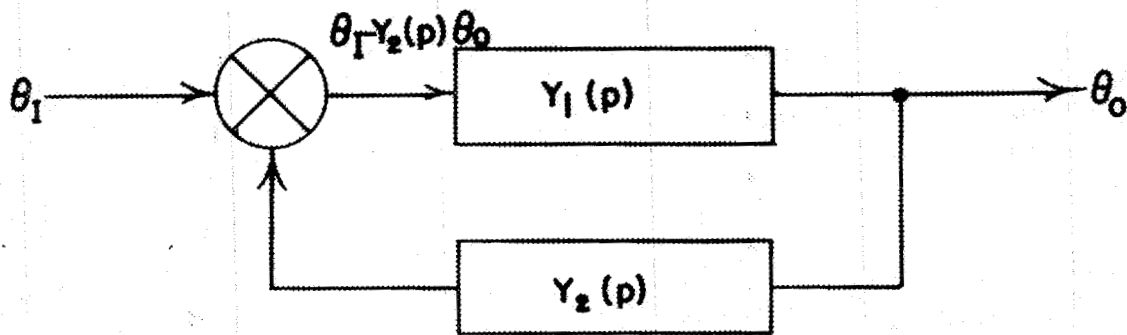


FIG. 33

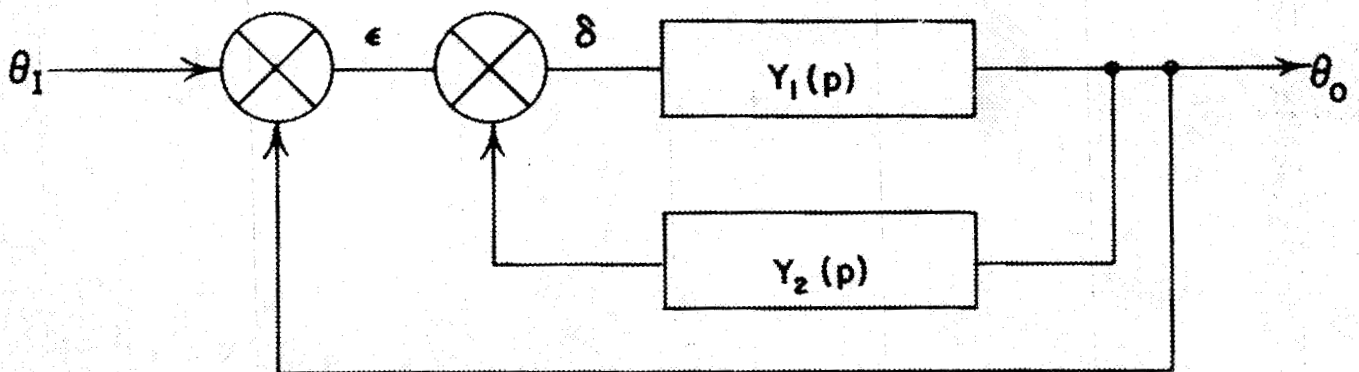


FIG. 34

Here $Y_1(p) [\theta_I(p) - Y_2(p) \theta_o(p)] = \theta_o(p)$

$$Y_o(p) = \frac{\theta_o(p)}{\theta_I(p)} = \frac{Y_1(p)}{1 + Y_1(p) Y_2(p)}$$

with the loop transfer function

$$Y_l(p) = Y_1(p) Y_2(p)$$

here equation E does not hold. But we still have the feature which is generally present that $Y_o(p)$ is expressible as a fraction with denominator equal to one plus the loop transfer function. For a system to have zero static error $Y_2(p)$ must always have the same asymptotic response to a step. This means extreme care must be taken to assure the constancy in time of $Y_2(p)$ if such an element is to be used.

Systems with several loops are commonly used, e.g., a 2 loop system, see Fig. 34. An inner loop is used to modify the characteristics of the driving element.

$$\delta = \epsilon - Y_2(p) \theta_o(p)$$

$$\theta_o(p) = Y_1(p) \delta$$

Thus defining $Y(p) = \theta_o(p)/\epsilon(p)$

$$Y(p) = \frac{Y_1(p)}{1 + Y_1(p) Y_2(p)}$$

$$\text{Thus } Y_o(p) = \frac{Y(p)}{1 + Y(p)} = \frac{Y_1(p)}{1 + Y_1(p) + Y_1(p) Y_2(p)}$$

$Y_o(p)$ is the transfer function of the servo mechanism regarded as a filter. Thus we can carry over our general results on filter stability to discussion of $Y_o(p)$. For system stability $Y_o(p)$ must have no poles on the imaginary axis or in the right half plane. Thus a servo-mechanism is stable if and only if $1 + Y(p)$ has no zeroes on the imaginary axis or in the right half of the p plane. This statement of the stability condition is valid only when $Y(p)$ is defined as in equation B. One can replace $Y(p)$ by $Y_1(p)$ in this statement only when they are related by equation E. One must re-examine the relation between the quantities in other cases.

The loop transfer function of a lumped constant servo can be written

$$Y(p) = \frac{k_1}{p^l} \frac{Q_m(p)}{P_n(p)} \quad m \leq n$$

With l an integer and k_1 a constant, Q_m and P_n are polynomials of degree m and n respectively. The coefficient of p^0 is unity in both cases. k_1 , the gain, is defined:

$$H \quad k_1 = \lim_{p \rightarrow 0} p^l Y(p)$$

l being chosen to make the limit finite and non-vanishing. The value of l is fundamental in the servo performance. From equations C and D we have

$$\epsilon(p) = \frac{1}{1 + Y(p)} \theta_I(p)$$

For a given θ_I , from equation H and the theory of Laplace transform we can find the limit of $\epsilon(t)$ as $t \rightarrow \infty$. Take $\theta_I(t) = S(t)$;

$$\theta_I(p) = 1/p. \quad \text{Then}$$

$$\begin{aligned} \lim_{t \rightarrow \infty} \epsilon(t) &= p \frac{1}{1 + Y(p)} \frac{1}{p} = \lim_{p \rightarrow 0} \frac{1}{1 + \frac{k_1 Q_m(p)}{p^l P_n(p)}} \\ &= \lim_{p \rightarrow 0} \frac{1}{1 + \frac{k_1}{p^l}} \end{aligned}$$

Thus, the servo will remove the error if and only if $l \geq 1$. For a constant velocity input, $\theta_i(p) = \frac{1}{p^2}$. By a similar computation, one obtains for the asymptotic value of $\epsilon(t)$ the value $\frac{1}{k_1}$ when l is set at 1 for the system.

The feedback transfer function describes completely the servo system. It is a complex analytic function of p . It is completely determined by its values along a curve. The imaginary axis is of special interest since $Y(j\omega)e^{j\omega t}$ is the steady state response of the feedback loop to the input $e^{j\omega t}$; $Y(j\omega)$ is available experimentally. The plot of $Y(j\omega)$ in the Y plane for all real ω is the feedback transfer locus or Nyquist diagram, which supplies a convenient way to determine the stability and performance of a servo system. Since the coefficients of the differential equation of the system are real, $Y^*(j\omega) = Y(-j\omega)$. The real part is an even function. Thus the transfer locus is symmetric with respect to the real axis, and need be plotted only for positive ω .

For a system of zero static error, the transfer function has a pole at $p = 0$. For a pole of order l , at $p = 0$, $Y(j\omega)$ becomes infinite along a line at the angle $(l\pi/2)$ to the real axis. Also as ω becomes infinite $Y(p) \rightarrow \frac{k_1}{p^{l+m-n}} \rightarrow \frac{b_m}{a_n}$ where b_m and a_n are the coefficients of the highest

order terms in the respective polynomials. The locus of $Y(p)$ approaches 0 along a line at the angle $(-\frac{\pi}{2}[l+n-m])$ to the positive real axis.

In case the feedback function has poles at other points on the imaginary axis than the origin, the transfer locus will have discontinuities as p passes through these points. Then we modify the definition of the transfer locus. Take as the contour in the p plane a path on the imaginary axis deformed to pass along a small semicircle to the right of each singular point on the axis and a semicircle in the right half plane joining large negative to large positive values of $j\omega$. The radius of the semicircle must be large enough to enclose all zeroes and poles of the rational function $Y(p)$ in the right half plane. The map of this path in the Y plane is the transfer locus $Y(p)$. This locus can be experimentally determined. The mapping of the path for non-singular points is obtained from the steady state response to sinusoidal inputs. For a pole of order k , the corresponding curve in the Y plane is essentially an arc of a circle in the counter clockwise sense traced through an angle $k \cdot \pi$, since near the pole $Y \sim \text{const}/(p - p_1)^k$. Thus it suffices to determine the order of the pole when experimentally investigating the response to input frequencies corresponding to singularities. For the large semicircle in the p plane

$$Y(p) \sim \frac{k_1 b_m}{a_n} \times \frac{1}{p^{l+n-m}} = \frac{k_1 b_m}{a_n} \times \frac{e^{-j(1+n-m)\phi}}{R^{l+n-m}}$$

and $Y(p)$ traces a circular arc of small radius through the angle $-(1+n-m)\pi$ corresponding to the large semicircle. Thus the feedback transfer function maps the closed path in the p plane into a closed path C in the Y plane. If $Y(p)$ equals minus one at any point in the right half of the p plane, C encloses $(-1,0)$. But the system is stable only if $Y(p) \neq -1$ at any point in the right half plane or on the imaginary axis. Thus the transfer locus yields a means of studying servo stability. For this purpose we need a theorem from complex variable theory.

Let $G(p)$ be a rational function of p . If p describes a closed contour k in the positive sense, the point $G(p)$ in the G plane describes a curve C in the G Plane. If k encloses, in a positive sense, Z zeroes and P poles, each counted as equal in number to its multiplicity, the curve C encircles the origin in a positive sense

$$N = (Z - P) \text{ times,} \quad \text{where} \quad \begin{cases} Z = \text{number of zeroes} \\ P = \text{number of poles} \end{cases}$$

Apply this to the function $G(p) = 1 + Y(p)$. The map of a contour in the p plane onto the Y plane is obtained by shifting to the left 1 unit the corresponding contour in the G plane. Thus the contour drawn in the positive sense in the p plane maps into the Y plane as a contour enclosing $(-1,0)$ in a positive sense $Z - P$ times. The transfer locus (a curve of this type mapping a contour in the p plane which encloses all zeroes and poles of $1 + Y(p)$ that lie in the right half of the p plane) thus encircles $(-1,0)$ a number of times equal to the difference of the number of zeroes and poles of $1 + Y(p)$ in the right half p plane. Since a system is stable only if there are no zeroes of $1 + Y(p)$ in the right half plane, this result can be used in discussing the stability of a servo system. The theorem of Nyquist applies to systems whose feedback function is that of a passive network. The presence of a motor introduces a pole at the origin. However, a large class of single loop servo systems have no poles inside the right half of the p plane. For these we have the Nyquist criterion:

The necessary and sufficient condition that a servo system be stable is that the feedback transfer function locus does not pass through or enclose the point $(-1,0)$ in the Y plane.

For multi-loop systems the feedback transfer function may include poles in the right half plane. This may occur when one of the inner loops is unstable. Then recourse must be had to the more general form of the mapping

theorem. It remains true that the system is stable if and only if $1 + Y(p)$ has no zeroes in the right half plane, but here the feedback transfer locus encircles the point $(-1,0)$ a number of times equal the number of zeroes minus the number of poles. An independent determination of the number of poles inside the right half of the p plane must be made after which the number of zeroes can be obtained from the transfer locus and reference to the mapping theorem.

Attenuation-Phase Relationships

This subject will not be treated in any detail here. See Bode's book for the clinical details. What is said here may apply to the transfer function of a corrective filter, an over-all loop transfer or a subsidiary loop transfer function. We treat the log of the function, the real part being attenuation and the imaginary part the phase. What is about to be said applies only to those transfer functions, $Y(p)$, which have no poles or zeroes in the right half of the p plane, minimum phase functions. The majority of functions used in servo theory fall into this class. They have the property that if $A(\omega)$, the real part of $\log Y(\omega)$, is known for all ω , this alone defines completely $\phi(\omega)$, the phase. The converse theorem holds also. The formula for the minimum phase associated with a given attenuation characteristic can be written:

$$\phi(\omega_0) = \frac{\pi}{12} \left(\frac{dA}{d\mu} \right)_{\omega=\omega_0} + \frac{1}{6\pi} \int_{-\infty}^{\infty} d\mu \left[\frac{dA}{d\mu} - \left(\frac{dA}{d\mu} \right)_{\omega=\omega_0} \right] \ln \coth \left| \frac{\mu}{2} \right|$$

where $\mu = \ln \omega/\omega_0$. Thus the phase in radians at frequency ω_0 is given in terms of the slope of the attenuation diagram and a weighting function. $dA/d\mu$ is the slope of the attenuation diagram in decibels per octave. The weighting function, $\ln \coth |\mu/2|$ has a total weight with respect to integration over μ equal to unity and falls off rapidly as ω departs from ω_0 . It is seen that a constant attenuation slope of 6n db. per octave is accompanied by a phase of $n\pi/2$. Also the phase changes most rapidly near changes in attenuation slope and it is appreciably affected at any frequency by changes in attenuation slope near that frequency. The formula above is too much of a mess for practical use, but it is easy to use certain procedures developed by Bode in estimating the phase corresponding to a given attenuation characteristic. Some of these methods were indicated in the course of the analysis of the simple instrument servo which was

used as a model in the discussion. It is to be emphasized that the procedures here mentioned cannot be applied blindly to given attenuation characteristics without investigation to make certain that they arise from minimum phase systems.